ENHANCED ENDOTHELIALIZATION ON SURFACE MODIFIED POLY(L-LACTIC ACID)

by

HAO XU

Presented to the Faculty of the Graduate School of

The University of Texas at Arlington in Partial Fulfillment

of the Requirements

for the Degree of

DOCTOR OF PHILOSOPHY

THE UNIVERSITY OF TEXAS AT ARLINGTON

May 2010

ACKNOWLEDGEMENTS

I would like to thank many people who gave me the guidance, help, and support to finish my doctoral research. First, I would like to thank Dr. Kytai T. Nguyen, my Ph.D. advisor, for giving me the opportunity to work in her lab. She not only gave me instructions to design and perform experiments, but more importantly, she taught me how to think independently as a scientist. This dissertation would not be possible without Dr. Nguyen's support. I would also like to thank my thesis committee members — Dr. Liping Tang, Dr. Jian Yang, Dr. Subhash Banerjee, and Dr. Cheng-Jen Chuong — for their valuable suggestion and support and for allowing me to use their labs resources.

I am grateful to all the student members of our lab. It has been a great experience to work and learned from them. Finally, I would like to give my special thanks to my wife Yue Feng, and my parents, Sheng Xu, and Lamei Wang, for their love and constant support.

April 15, 2010

ABSTRACT

ENHANCED ENDOTHELILIZATION ON SURFACE MODIFIED

POLY(L-LACTICE ACID)

Hao Xu, PhD

The University of Texas at Arlington, 2010

Supervising Professor: Kytai T. Nguyen

Current synthetic vascular grafts and polymer-coated drug-eluting stents (DES) have certain limitations, such as thrombosis and restenosis due to the incomplete recovery of vascular endothelial cells on their luminal sides. Surface modification of these materials is a viable method to enhance endothelialization. In this study, we proposed several strategies to modify poly(L-lactic acid) (PLLA), a promising material for vascular prostheses to enhance endothelialization on its surface. In the first approach, we modified the material surface with deposition of poly(vinylacetic acid) (PVAA) using plasma polymerization. PVAA films having different surface densities of –COOH groups or film thickness were created and characterized. Their effects on endothelial cell adhesion, proliferation, and function were studied. PVAA films with 9% -COOH surface density and 100 nm film thickness were found to be optimal for enhancing endothelialization. The mechanism for this enhancement might involve increased adsorption of fibronectin on its surface. In the second method, fibronectin was conjugated covalently with PVAA, which was deposited on PLLA, utilizing the rich –COOH of PVAA. Vascular Endothelial Growth Factor (VEGF) was subsequently conjugated with fibronectin for surface delivery of VEGF. Enhanced endothelial cells adhesion and proliferation was found on

this modified PLLA surface, especially when VEGF receptor-genetically modified cells were used. Lastly, we coated PLLA with poly(1,8-octanediol-*co*-citrate) (POC)/poly(lactic-co-glycolic acid) (PLGA) microparticle composite. VEGF, fibroblast growth factor (FGF), and VEGF receptor plasmids were encapsulated in the PLGA microparticles for controlled release. Fibronectin and anti-CD34 antibody were, in turn, conjugated on top of POC to capture endothelial progenitor cells (EPC). It was found that the surface-modified PLLA successfully captured EPCs in a flowing condition, and rendered quick endothelialization on the surface. Using these strategies, enhanced endothelialization can be achieved on polymers such as PLLA, which naturally do not support endothelial cell growth, in order to reduce thrombosis and restenosis on vascular prostheses.

TABLE OF CONTENTS

LIST OF ILLUSTRATIONS

LIST OF TABLES

CHAPTER 1

INTRODUCTION

1.1 Cardiovascular Disease

Cardiovascular disease (CVD) is the No. 1 cause of death in the United States and many other countries in the world. More than eight million deaths (34.2 percent of all deaths), or 1 of every 2.9 deaths were claimed due to CVD in 2006 in the United States alone according to Centers for Disease Control (CDC) statistics [1]. Among CVD, coronary heart disease (CHD) is the major cause of death. An estimated 1.2 million Americans will have a new or recurrent heart attack in 2010, with a total cost of 165 billion U.S. dollars [1].

The main cause of CHD is atherosclerosis, a buildup of cholesterol plaques on the arterial wall. Though not completely understood, scientists have found atherosclerosis is a chronic inflammation and its formation involves several complicated processes. In patients with hypercholesterolemia, excess low-density lipoprotein (LDL) infiltrates the innermost layer of the artery and is retained in the intima, particularly at sites of hemodynamic stress. These LDL are oxidized and modified by enzymes, leading to the release of inflammatory phospholipids that induce endothelial cells to express leukocyte-adhesion molecules such as vascular cell adhesion molecule 1 (VCAM-1) [2]. Monocytes, which carry receptors for VCAM-1, attach to the activated endothelial cells, migrate into the subendothelial space, and differentiate to macrophages, under the cytokines produced in the inflamed intima. Through several specific receptors, such as scavenger receptors expressed on the cell membrane, these macrophages uptake the oxidized LDL and gradually become “foam cells”. Increasing numbers of foam cells accumulated in the subendothelial layer form the “fatty streaks” ─ the initial form of atherosclerosis. Additionally, these cells release various cytokines that stimulate the vascular smooth muscle cells (VSMC) in the artery wall to migrate towards the atherosclerotic core,

which is made of foam cells and extracellular lipid droplets. These cells also proliferate and produce excess extracellular matrix, e.g. collagen, which eventually form fibrous tissues that overlay the lipid core like a cap [3, 4]. With continuous growth, the plaque gradually narrows the luminal space of the artery and restricts blood flow. A heart attack will happen when complete occlusion of a coronary artery occurs due to the atherosclerotic plaque rupture and sudden blood clot formation.

1.2 Vascular Stents and Grafts

Various treatments can be used once a heart attack happens. Thrombolytic therapy can be administrated in a short time period after myocardial infarction. Tissue plasminogen activator (tPA), urokinase, and streptokinase are the common fibrinolytic drugs used to dissolve the clots and reopen the arteries. In some cases, invasive treatments such as angioplasty, vascular stenting, or coronary artery bypass graft (CABG) surgery are used to reopen or bypass the blocked arteries. In CABG surgery, the patient's own saphenous vein or internal mammary artery is used as an autologous graft to bypass the blocked artery. In cases when patients do not have appropriate autologous vascular grafts, synthetic vascular grafts usually made of polymers can be used for CABG. Common materials to make vascular grafts include expanded polytetrafluoroethylene (ePTFE), polyethylene terephthalate (PET, Dacron®), and polyurethane (PU) [5]. Though these polymers are good for large artificial vascular grafts, they are often problematic, prone to thrombosis, and lose their graft patency for vascular grafts of a smaller size (< 6 mm in diameter), such as those used for coronary arteries [6].

An alternative of CABG is angioplasty, which is a technique of expanding a balloon under high pressure (6-20 atmospheres) to reopen the obstructed artery mechanically. Angioplasty is often combined with the implantation of a vascular stent, which is a mesh-like tube, often made of stainless steel or nickel titanium (nitinol) to support the expanded artery. Within the last few years, angioplasty and vascular stenting have increasingly become popular

to treat acute heart attacks in the U.S. due to its procedural ease and minimal injury compared to CABG. However, angioplasty and vascular stenting still cause injuries on the treated arteries, resulting in inflammation, thrombosis, and neointimal thickening that eventually cause re-narrowing of the arteries. This is called in-stent restenosis [7]. For patients receiving bare metal stents, the restenosis rate within 3-6 months is 20-30% [8]. To reduce restenosis, drug-eluting stent (DES) was developed to inhibit the overgrowth of neointima. Antiproliferative drugs such as sirolimius and paclitaxel are incorporated in a thin polymer coating on the struts of DES, and delivered gradually over a period of time to introduce a locally-high concentration of drugs. Current F.D.A.-approved DES include CYPHER™ sirolimus-eluting stent, TAXUS™ paclitaxel-eluting stent, and ENDEAVOR™ everolimus-eluting stent. DES effectively reduces post-angioplasty restenosis mainly by inhibiting the proliferation of the vascular smooth muscle cells [9]. However, the use of DES have been shown to be associated with increased rates of late thrombosis, a life-threatening complication that occurs after one year or more of stent implantation [10-13]. It is postulated that delayed healing, an incomplete endothelial recovery on the luminal side of the DES, could be the major cause contributing to late thrombosis [14].

1.3 Endothelialization on Vascular Prostheses

Under normal physiological conditions, the entire luminal side of blood vessels are covered with endothelial cells (EC), which have natural antithrombotic properties by producing a number of antithrombotic factors, such as nitric oxides, prostacyclin (PGI_2), plasminogen [15], and thrombomodulin [16]. In contrast, ECs do not fully cover the surface of synthetic vascular grafts or DES, and a higher rate of late thrombosis is found [17]. Therefore, it is generally believed that recovery of functional EC layer on the luminal side of vascular grafts or stents could help to prevent late thrombosis and inhibit restenosis.

Unfortunately, many synthetic materials for making vascular grafts or stents do not have natural affinities for endothelial cells to adhere and grow on their surfaces, and therefore they

need to be modified with either bulk modification or surface modification to help endothelial cells grow on their surfaces. For bulk modification, new co-polymers are usually synthesized by incorporating hydrophilic segments or cell-friendly molecules, such as poly(L-lysine) [18] and malic acid [19, 20]. Another way of bulk modification is blending the original hydrophobic polymer with other hydrophilic materials. For examples, dextran [21], hydroxyapapite [22], or chitosan [23] are mixed with PLLA to enhance PLLA's affinities for the cells. However, modifying the polymer chain creates the risk of changing the polymer's mechanical properties, which are critical for their applications in vascular stents or vascular grafts. An alternative of bulk modification is to modify the material surface. Therefore, surface modification appears to be a better route to achieve improved EC-material interaction without changing the structure and properties of these vascular prostheses.

1.4 Plasma Polymerization

A number of methods have been used to modify material surface characteristics, such as hydrophilicity, surface energy, electric charge, and roughness. These modification methods include hydrolysis [24], chemical grafting [25], radiation-induced grafting [26], photoinitiated grafting [27], and layer-by-layer (LBL) polyelectrolyte coating [28], among others. Radio frequency glow discharge (RFGD), also identified as plasma enhanced chemical vapor deposition (PECVD), or plasma polymerization, has some unique features compared to other surface modification techniques. First, it is easy to control the coating with desired chemical groups, such as –COOH, $–NH_2$, or –OH groups, by choosing from a wide range of different monomers. Secondly, the processing is comparatively easy and rapid. Also, the surface density of the functional groups can be precisely controlled by adjusting the processing mode and time [29]. Another important feature of RFGD is that it can be used to coat irregular surfaces or even porous scaffolds. Previous studies found that surface modification with certain functional groups such amine ($–NH_2$) [30, 31], imine (=NH) [32], hydroxyl (–OH) [33-35], ester (–COOC–) [36, 37],

and carboxyl groups (–COOH) [38-40], can enhance cell attachment. Among these functional groups, –COOH groups have been found to promote the best cell attachment and growth [41-43].

1.5 Poly(L-lactic acid)

The current vascular prostheses made of metals (e.g., stainless steel or nitinol) or non-degradable polymers (e.g., ePTFE or Dacron) have serious limitations in terms of their permanence when used in children and young patients whose vasculatures are still growing. These materials might also trigger life-long immune responses due to their permanent presence. Additionally, metal stents can interfere with vasculature remodeling due to their rigidity and permanence [44]. Other limitations of metal vascular stents include thrombogenecity and possible erosion [45]. To overcome these limitations, biodegradable polymers have been increasingly investigated as alternative materials to form vascular stents and grafts. In light of the inherent degradation of such materials, they could overcome the problems noted above, particularly those involving pediatric care.

Poly(L-lactic acid) (PLLA), a material which has received F.D.A. approval for implants, is one of the most promising biodegradable synthetic polymers identified to date. For example, its use extends to a wide variety of implantable medical devices including sutures, dental devices, and orthopedic plates and screws [46-49]. The safety and feasibility of a PLLA stent was first reported by Tamai and his colleagues early in 2000 [50], and more recently, the IGAKI-TAMAI® bioabsorbable PLLA stent received approval for use by the European Union in 2007. In the U.S., clinical studies of Abbott Vascular Inc. using PLLA-based everolimus-eluting stents found minimal intrastent neointimal hyperplasia after one year of implantation [51]. These studies suggest that PLLA is a promising material for use as biodegradable vascular prostheses.

Despite the promising results noted above, concerns remain with respect to the biocompatibility of PLLA as vascular grafts and stents, especially with its endothelialization following implantation. PLLA has a very low affinity for endothelial cells, due to its relatively high hydrophobicity and lack of active functional groups on its surface [52]. As a result, PLLA needs to be surface-modified to enhance its affinity to encourage more adherence and growth of endothelial cells.

1.6 Endothelial Progenitor Cells

A traditional method of endothelialization is to seed endothelial cells on the luminal side of vascular grafts or stents before their implantation [53]. Recently, endothelial progenitor cells (EPCs), a class of mononuclear hemangioblasts (a common precursor of endothelial cells and hematopoietic stem cells derived from bone marrow and other sources), has been suggested to be a promising autologous cell source involved in repairing or generating new vasculatures [54-56]. Infusion of circulating EPCs into the lumens of denuded rabbit carotid arteries has shown improved vascular functions, suggesting infused EPCs integrated in the arteries [57]. EPCs are mobilized from bone marrow, circulated in peripheral blood, anchored on vasculatures, and differentiated to mature endothelial cells [58]. Low-density lipoprotein (LDL) uptake, lectin binding, and expression of stem cell and endothelial cell markers are generally used to characterize EPC [59]. The two major hematopoietic stem cell surface markers of EPCs are CD34 and CD133 while endothelial cell markers include vascular endothelial growth factor receptor (VEGFR), von Willebrand factor (vWF), endothelial NO synthase (eNOS), VE-cadherin, CD31, and Tie-2 [60-62].

Autologous EPCs can be used for endothelialization on vascular prostheses. It has been found that EPC grown on vascular stent surfaces can retain partially after implantation, and promote endothelium recovery on both the stent struts and the denuded vessel surface [63, 64]. The generation of endothelium by EPC seeding can inhibit thrombus formation on these

prostheses [65-67]. However, seeding EPC on vascular stents and grafts prior to implantation requires extensive culture time to get enough cells for seeding, and there is a potential loss of seeded cells during the implantation process.

To overcome these limitations, a new strategy of seeding endothelial cells on implanted vascular prostheses, called "*in vivo* endothelialization" or "autoseeding" was invented. Autoseeding of EPCs is a new concept to provide endothelial cell coverage on vascular prostheses, by capturing the EPCs circulating in the blood stream via specific molecules such as anti-CD34 antibodies and P-selectin, which are immobilized on vascular implant surfaces. In order to differentiate EPCs to mature ECs, varieties of growth factors such as VEGF and FGF are needed [68, 69]. In fact, VEGF and FGF are two ingredients of the supplement of the EGM-2 Microvascular Endothelial Cell Growth Medium, which is widely used for EPC culture and differentiation. VEGF and FGF also contribute to EPC mobilization from the bone marrow [70, 71].

Because VEGF and FGF are costly growth factors, and using them in high dosages might bring unwanted side effects, a controlled local delivery of these growth factors in a lower but effective dosage by vascular grafts and stents has been extensively investigated. However, because VEGF and FGF are both hydrophilic, they cannot simply be mixed with hydrophobic materials and used as the coating for drug-eluting stents or making synthetic vascular grafts. Therefore, a better strategy for delivering these hydrophilic growth factors is needed to help EPC proliferation and differentiation to mature endothelial cells.

1.7 Overview of Research Project

Quick endothelialization on vascular stents and grafts is in great demand, especially for pediatric patients. The use of patient's autologous EPCs represents the future trend of endothelializing vascular prostheses to inhibit thrombosis and restenosis. The objective of this research was to develop a strategy to enhance the endothelialization on PLLA, using surface

modification techniques, combined with EPC capture, and controlled release of growth factors and plasmids.

To achieve this goal, three aims were pursued as following:

- Aim 1: Determine the effects of surface modification with poly(vinylacetic acid) (PVAA) on endothelial cell adhesion and proliferation.
- Aim 2: Investigate the effects of surface modification of PLLA using PVAA deposition, fibronectin conjugation, and VEGF delivery on endothelialization.
- Aim 3: Enhance endothelialization on PLLA using surface modification with POC/PLGA microparticle composites and EPC autoseeding. Growth factors VEGF, FGF, and VEGFR plasmids will be encapsulated in PLGA microparticles for controlled delivery.

The innovative aspect of this research is that it combines EPC autoseeding with surface modification of PLLA. On one hand, autoseeding allows using patients own EPCs, which could prevent immune responses. It also overcomes problems such as lengthy cell expansion and cell detaching after implantation. On the other hand, surface modification of PLLA provides necessary factors to aid EPC adhesion, proliferation, and differentiation to mature endothelial cells. A successful outcome of this research would represent a feasible strategy to enhance endothelialization on materials which have good physical and chemical properties to be used for vascular stents or grafts.

CHAPTER 2

EFFECTS OF SURFACE DEPOSITION OF POLY(VINYLACETIC ACID) ON ENDOTHELIALIZATION

2.1 Introduction

Surface modifications are commonly used to improve cell adhesion and accelerate cell proliferation on biomaterials, which have low affinities to endothelial cells. Plasma polymerization is an attractive coating technique due to its convenience, uniform coating, and versatility of coating on irregular shapes or porous structures. In plasma polymerization, the reactive species created by high-energy electrons and ions bind with the substrate to be coated, forming an ultra-thin film strongly attached to the substrate surface.

Previous researches found –COOH groups show the best effects for endothelial cell adhesion on materials. Therefore, in the present study, we used vinylacetic acid (CH_2=CH-CH_2-COOH) as the monomer for plasma polymerization, utilizing its abundant –COOH groups. In order to study the effects of different surface densities of –COOH groups and polymerized film thicknesses on endothelial cells, pulsed plasma discharge was employed in addition to the conventional continuous-wave (CW) operational mode. PVAA films achieved at different conditions were characterized using Fourier transform spectroscopy (FTIR spectroscopy), X-Ray Photoelectron Spectroscopy (XPS), Atomic Force Microscopy (AFM), and water contact angle measurements. Cell adhesion and proliferation on PVAA films were studied using Picogreen DNA assays. In addition, the expression of vWF on endothelial cells grown on PVAA, as a biomarker, was studied using immunofluorescence staining. The adsorption of fibronectin on deposited PVAA films was also studied to explore the mechanism of enhanced cell growth on PVAA.

2.2 Materials and Methods

2.2.1 Deposition of Poly(vinylacetic acid) Film by RFGD Plasma Polymerization

Vinylacetic acid (VAA) was purchased from Sigma-Aldrich, St. Louis, MO and had a stated purity of 97%. The monomer was repeatedly freeze-thawed to remove any dissolved gases prior to use. Monomer vapor was subjected to RFGD at room temperature, in a bell-shaped reactor chamber, as described elsewhere [72]. After the substrates were placed inside the reactor, the system was evacuated to a background pressure of 4 mtorr. Monomer vapor was introduced into the chamber and an RF plasma glow discharge ignited. Three different power input conditions were employed, namely, pulsed discharges at duty cycles of 2/30 and 10/30 (time on/time off, ms), plus runs using the CW operational mode. All samples were prepared using a 150 W peak power input. Although all runs were carried out at a 150 W peak power, it is important to note that the average power input differs significantly in contrasting the pulsed and CW depositions. The average power was computed from the plasma duty cycle (ratio of on time to the sum of the on plus off time) multiplied by the peak power. Thus the average power inputs were 9.4 and 37.5 W for the 2/30 and 10/30 runs, respectively, compared to the 150 W for the CW experiments. Monomer pressure of 160 mtorr was employed for the 2/30 duty cycle polymerizations and 40 mtorr for the 10/30 duty cycle and CW runs. Deposition times were adjusted to deposit ~ 100 nm thick films for each set of plasma conditions employed. In the second set of experiments involving PVAA film thickness variation, a single duty cycle (2/30) pulsed plasma was employed to polymerize VAA, and the deposition time was varied accordingly to obtain different film thicknesses ranging from 25 nm to 200 nm.

PVAA was deposited on KBr disks for FTIR spectroscopy. Polished silicon wafers were used as substrates for XPS, AFM and water contact angle measurements. All silicon wafers were treated with acetone, methanol and hexane to clean the wafer surface prior to use. For cell adhesion and proliferation studies, TCP was used as substrate for the plasma-deposited PVAA films.

2.2.2 Characterization of PVAA Films

To characterize the PVAA films, FTIR spectroscopy, XPS, AFM, and water contact angle measurements were used. The FTIR spectral analyses were carried out using a Bruker Vector-22 FTIR spectrophotometer operated at 4 cm^{-1} resolution. XPS spectra were obtained using a Perkin-Elmer PSI 5000 series instrument equipped with a monochromator and 8.95 eV pass energy. A neutralizer was used on these measurements since the samples were non-conductive. The high resolution XPS spectra were analyzed using Casa XPS software. The binding energy of the carbon atoms not directly bonded to any heteroatoms was centered at 284.6 eV.

Surface roughness of the deposited films was determined using an AFM-SPM Nanoscope from Veeco. A phosphorus (n) doped silicon tip (RTESP from Veeco Probes) was used to scan the surfaces under tapping mode operation. Rame-Hart sessile drop goniometer was used to measure the instant static water contact angle of the polymeric films. PVAA film thickness was measured using Tencor Alpha step 200 profilometer. In brief, a metal tipped pen was employed to scratch a thin line in the polymer films deposited on polished silicon wafers. The thickness of the films reported is an average of three measurements taken for each sample. A Rame-Hart sessile drop goniometer was used to measure the static water contact angle of the polymeric films.

2.2.3 Cell Preparation

Human Aorta Endothelial cells (HAEC) were purchased from Cascade Biologics Inc., OR. The cells were cultured with Medium 199 (Invitrogen Inc., CA) supplemented with 5% Fetal Bovine Serum (Hyclone Inc., UT), Endothelial Growth Supplement (Cascade Biologics Inc., OR), and 1% penicillin-streptomycin (Invitrogen Inc., CA) at 37ºC. Cells between passage 5 and 10 were used for all the experiments.

2.2.4 Cell Adhesion and Proliferation

All of the PVAA deposited substrates employed in this study were subjected to overnight vacuum oven exposure at 40°C prior to the spectral analyses and cell culture studies. This vacuum oven treatment was carried out to eliminate any monomer molecules or oligomers which may have been incorporated in the films during the plasma polymerization depositions. This was taken as a precautionary step in order to minimize the cytotoxicity of the plasma-deposited PVAA films. Substrates were washed twice with sterile PBS before seeding of endothelial cells.

HAECs were seeded at a density of 5×10^3 cells/cm² on the PVAA deposited 12-well TCPs for all cell adhesion and proliferation studies. Untreated TCPs were used in the control groups. Cells were incubated for 6 hours or 3 days for adhesion or proliferation study, respectively, on PVAA which had varying –COOH surface densities (3.6%, 6.2%, and 9%). In another study, HAECs were seeded on PVAA with the same 9% -COOH surface densities, but having different film thicknesses (25-200 nm). Cells were incubated up to seven days for their effects on cell proliferation. In all experiments, cell culture mediums were changed every 48 hours. At the predetermined time, cells grown on the substrates were lysed with 1% Triton X-100 (MP Biomedicals Inc., OH). The total cell DNA in the collected cell lysis was analyzed using PicoGreen dsDNA kit (Invitrogen Inc., CA) following the manufacturer's instruction. The cell numbers were obtained by calculation based on the cell DNA, using a calibration curve of the total cell DNA versus known numbers of cells.

2.2.5 Immunofluorescence Staining of HAEC

HAECs were seeded at 5×10^3 cells/cm² on 35 mm diameter polystyrene petri dishes with or without PVAA deposition. After culturing for 24 hours, cells were fixed with 4% cold formaldehyde for 30 minutes and treated with 0.02% Triton X-100 for 5 minutes for increasing membrane permeability prior to staining. Rabbit anti-human von Willebrand Factor (vWF) IgG

and bovine anti-rabbit IgG-FITC, (both from Santa Cruz Biotechnology Inc.,CA) were used as the primary and secondary antibody, respectively, for immunofluorescence staining of the cells. After staining, the cells were mounted with UltraCruz™ mounting medium (Santa Cruz Biotechnology Inc., CA) containing 1.5 µg/ml 4',6-diamidino-2-phenylindole (DAPI) for DNA counterstaining. The cells were observed with the Zeiss fluorescent microscope at magnification of 200 X.

2.2.6 Quantification of Fibronectin Adsorption on PVAA

One milliliter fibronectin/PBS solution (33 µg/ml) was added on top of the PVAA deposited 12-well TCP. Same as in the cell adhesion and proliferation study, these PVAA films were either in 100 nm thicknesses with different –COOH surface densities (3.6%, 6.2% or 9%), or with 9% –COOH surface density but in varying film thicknesses (25, 50, 100 and 200 nm). Untreated TCPs were used as controls. The fibronectin solutions were incubated on these substrates for 2 hours at 37 ºC and the substrate surfaces were gently rinse with PBS to remove any loosely attached fibronectin. To detach the adsorbed fibronectin, 400 µl SDS solution (1% w/v) was added on the substrates and incubated for 1 hour with constant shaking. The fibronectin concentration in the collected SDS solution was measured using the BCA protein assay (Pierce Biotechnology Inc, IL) following the manufacturer's instruction.

2.2.7 Statistical Analysis

Data were obtained at least in triplicates and presented as mean ± standard error of the mean. One-way ANOVA at a significance level of $p < 0.05$ was performed using StatView 5.0 software (SAS Institute).

2.3 Results and Discussion

2.3.1 Characterization of PVAA Films

FTIR spectra of the plasma polymerized VAA films, although relatively qualitative in nature, show progressive changes in film composition with variations in the RF duty cycles employed during the film deposition process. Figure 2.1 shows a plot of FTIR transmission spectra of the PVAA films deposited at pulsed discharges at 2/30 and 10/30 (on/off, ms), or under CW conditions, reading from top to bottom. These spectra revealed a progressive increase in the retention of the monomer's -COOH content with decreasing RF duty cycle (plasma on / off time) employed during the deposition. This increase can be easily noted by comparing the relative intensities of the C=O stretching frequency for – COOH (1706 cm^{-1}) and the characteristic H-bonded –OH stretch for COOH (broad region from 3300 cm^{-1} to 2500 cm^{-1}). Additionally, there was a progressive increase in the intensity of the C-O stretching vibration (~1100 cm^{-1}) with decreasing RF duty cycle, which was consistent with the increasing amount of –COOH in the films. These spectra revealed that the extent of C=O retention was proportional to -OH retention in the film which would be consistent with the increasing presence of intact -COOH functional groups. It can also be noted that the intensities of the C-H (~2900 cm^{-1}) absorptions, relative to the C-O containing moieties, increased with the increasing RF duty cycles. This was consistent with the decreased retention of –COOH functionality, as the plasma duty cycle increased.

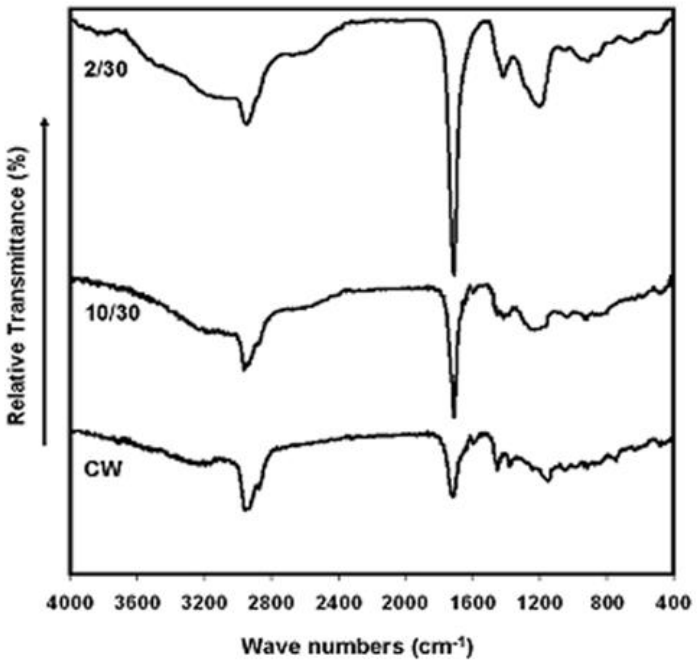

Figure 2.1 FTIR spectra for PVAA films deposited under pulsed (2/30 and 10/30) and CW plasma conditions.

High resolution C(1s) XPS spectra are shown in Figure 2.2, along with accompanying peak assignments. The peaks centered at 284.6 eV represents C-C and C-H groups, i.e. carbons not bonded directly to any oxygen atoms. The other peaks were fitted using the following assignments: a β-shifted carbon bonded to carboxylic acid (C-COOH) at 285.3 eV, alcohol/ether (C-OH/C-O-C) at 286.3 eV, carbonyl (C=O) at 287.5 eV and carboxylic acid (COOH) at 288.9 eV. These peak assignments are in accord with many prior analyses of this type [73]. Clearly, there was a progressive decrease in the number of carbon atoms present as –COOH, when the plasma on time increased in the order of duty cycles 2/30, 10/30 to CW mode. Table 2.1 provides a quantitative measure of the percent surface carbon functionalities obtained from integration of the deconvoluted XPS high resolution C(1s) peaks. As these data showed, there was a steady decrease in the surface density of -COOH functionality from ~9% to ~3.6%, expressed as a percent of total surface carbons, as the deposition condition switched from pulsed plasma (duty cycle, 2/30 ms) to CW plasma operating mode. The progressive

increase in the peak at 284.6 eV, i.e., an increase in the C–C and C–H groups compared to other functional groups, was indicative of the increase in polymer crosslinking with increasing average power input as the plasma duty cycle is increased. It should be noted that films containing up to 20% -COOH can be obtained when polymerizing vinylacetic acid at even lower average power inputs. However, we observed that PVAA containing more than 9% -COOH were relatively unstable in cell culture media, reflecting the lower degree of crosslinking. For this reason, we limited the present study to films having a maximum –COOH surface density of 9%.

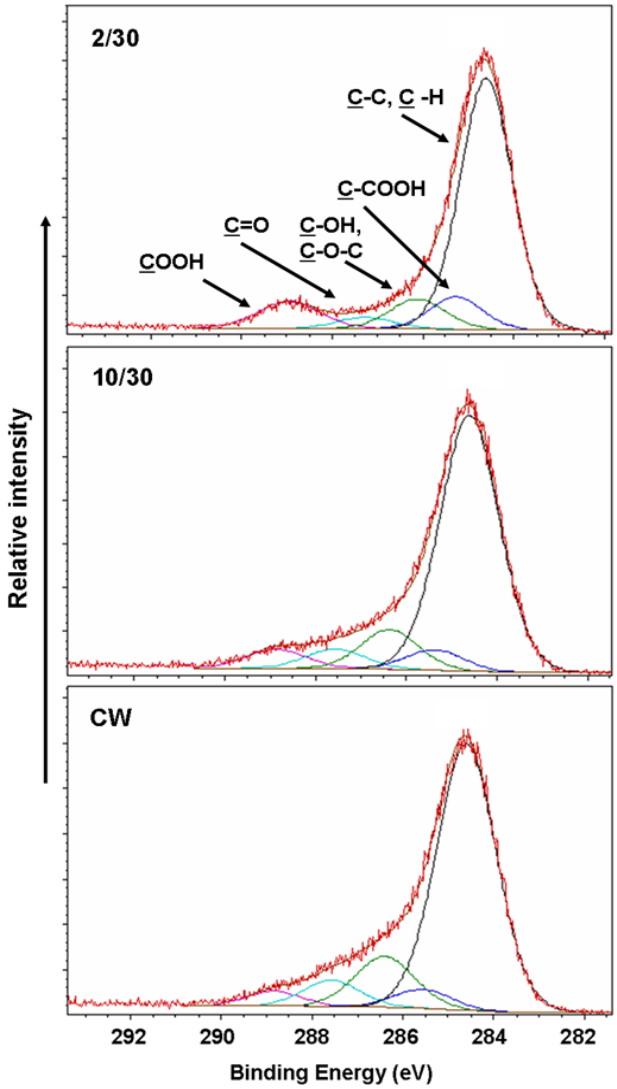

Figure 2.2 High resolution C(1s) X-ray photoelectron spectra for PVAA films deposited under pulsed (2/30 and 10/30) and CW plasma conditions.

Table 2.1 Percent surface functional groups of the plasma polymerized vinylacetic acid films deposited under pulsed (2/30 and 10/30) or CW plasma conditions.

Plasma conditions (on/off, ms)	Avg. power input (Walts)	O/C Ratio	C-C, C-H 284.6 eV	C-COOH 285.3 eV	C-OH, C-O-C 286.3 eV	C=O 287.5 eV	COOH 288.9 eV
2/30	9.4	0.24	70.2	9.0	8.5	3.3	9.0
10/30	37.5	0.22	71.2	6.2	10.8	5.6	6.2
CW	150	0.19	72.6	3.6	13.6	6.6	3.6

High resolution C(1s) XPS spectra were also obtained for a series of films ranging in thicknesses from 25 nm to 200 nm, all deposited using the 2ms on / 30 ms off pulsed plasma. Each of these films exhibited the same XPS spectrum as that shown in the top spectrum of Figure 2.2, thus revealing no measurable changes in the polymer composition with increasing film thicknesses.

Prior studies have demonstrated that surface roughness can affect cellular behavior on surfaces. In particular, changes in the surface roughness in the micron range have been shown to affect cell attachment and morphology [74-76]. For that reason, we examined the surface roughness of the PVAA films in the present study. The surface roughness of PVAA films, deposited at conditions of 2/30 or 10/30 duty cycles, or CW mode, having film thicknesses of 100nm, as well as the films of different thicknesses (25 nm, 100 nm, 200 nm) deposited at the 2/30 duty cycle, were examined by AFM (Figure 2.3). The mean roughness values (RMS) were shown in Table 2.2. As tabulated in Table 2.2, relatively small changes, on the order of 0.15 nm, were observed in the root mean square roughness of the PVAA films. Little change in surface roughness was noted with variation of the film thickness produced at the constant 2/30 duty cycle. Surface roughness did not vary more than ± 0.1 nm as the thickness of PVAA film increased from 25 nm to 200 nm. Given the fact that the surface roughness of these PVAA films was less than one nanometer and not significantly different from each other (0.4-0.6 nm shown

in Table 2.2), we can assume that roughness of PVAA films would be the cause of any variations in cell adhesion or proliferation on PVAA films.

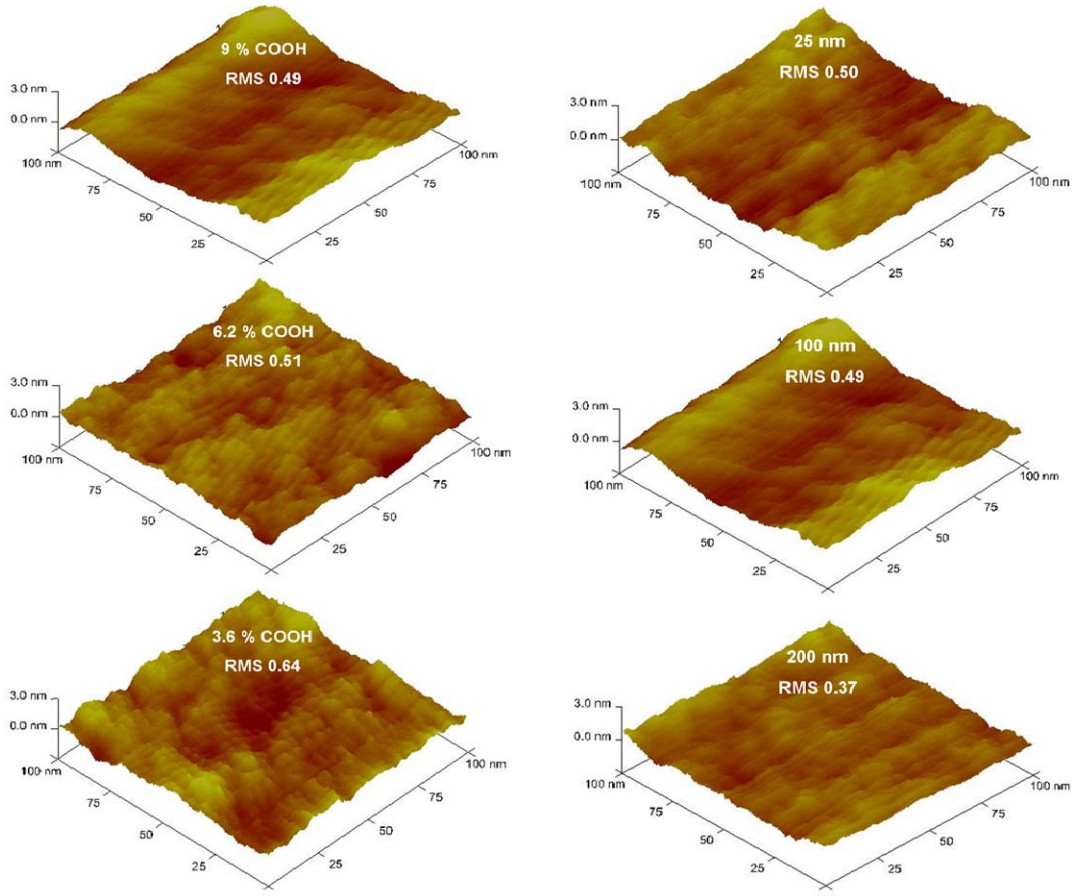

Figure 2.3 AFM images of PVAA film surfaces. Left colum: 100 nm thick PVAA films having different -COOH surface densities; Right column: PVAA films with constant 9% -COOH surface density but different film thicknesses.

Table 2.2 AFM mean roughness values for PVAA films with different –COOH surface densities or film thicknesses (average of three different regions on each sample)

Plasma condition (on/off ms, thickness)	Average power input (Walts)	-COOH retention (%)	Roughness (RMS)
CW, 100 nm	150	3.6	0.64 ± 0.1 nm
10/30, 100 nm	37.5	6.2	0.51 ± 0.1 nm
2/30, 25 nm	9.4	8.9	0.50 ± 0.01 nm
2/30, 100 nm	9.4	9.0	0.49 ± 0.01 nm
2/30, 200 nm	9.4	8.8	0.37 ± 0.01 nm

The sessile water contact angles on PVAA films were summarized in Table 2.3. The contact angles shown represent the average of at least three measurements of each film. The measurements show a slight decrease in the water contact angles with increasing –COOH surface densities on the PVAA films. This result is in accordance with the spectroscopic data shown in Figures 2.1 and 2.2. The obtained contact angles ranging from around 38° to 60°, are in the range reported to be ideal for enhanced cell adhesion on polymer surfaces [43, 77].

Table 2.3 Instant sessile drop water contact angles on PVAA films having different –COOH surface densities and film thicknesses.

-COOH surface density (%)	Film thickness (nm)	Water contact angle after deposition (°)
3.6	100 nm	60 ± 1
6.2	100 nm	48 ± 3
9	100 nm	38 ± 2
9	25 nm	39 ± 1
9	50 nm	38 ± 2
9	200 nm	39 ± 2

2.3.2 Endothelial Cell Adhesion and Proliferation on PVAA Films Having Different –COOH Surface Densities

To study the effects of different –COOH surface densities on HAEC adhesion and proliferation, 100 nm thick PVAA films having 3.6%, 6.2%, or 9% –COOH surface densities were used as the substrates. Untreated TCPs were used as controls. As shown in Figure 2.4, six hours after cell seeding, significantly higher cell adhesion (~ 180%) was found on PVAA having 9% –COOH surface density, compared to untreated TCP ($p<0.05$). While on PVAA having lower –COOH surface density (3.6% or 6.2%), similar levels of cell adhesion were found as to that attached on untreated TCP. Three days of culture resulted in noticeable cell proliferation on all the substrates in this test. Significantly higher amounts (~140%) of HAECs were found on PVAA films having 9% –COOH compared to those on untreated TCP. In contrast, cell proliferation on PVAA films having lower –COOH surface density (3.6% or 6.2%) was less than on untreated TCP. Clearly, these data indicate the cell sensitivity to the –COOH surface density, i.e., 9% –COOH provided a suitable surface for HAEC adhesion and proliferation than the other surfaces in this test.

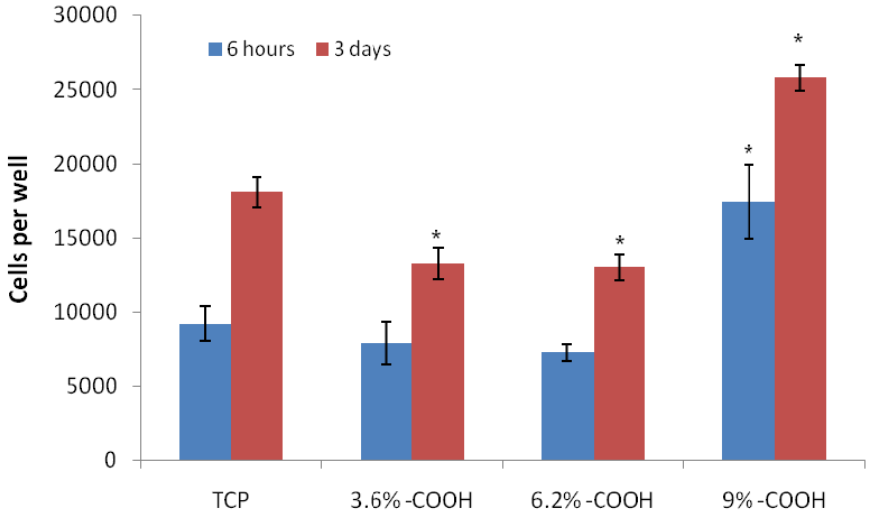

Figure 2.4 HAEC adhesion (6 hours after seeding) and proliferation (3 days after seeding) on PVAA films having 3.6%, 6.2% or 9% –COOH surface densities. All the PVAA films were 100 nm thick. N=4, *: $P<0.05$ compared to TCP (control) at the same time point.

2.3.3 Endothelial Cell Adhesion and Proliferation on PVAA Films Having Different Thicknesses

The effects of plasma polymerized film thicknesses on cell growth have never been reported before. Therefore, it was our interest to see whether different thicknesses of PVAA film would affect HAEC adhesion and proliferation. The PVAA films with 9% –COOH surface density (the optimal –COOH concentration for HAEC growth), and varying film thickness (25, 50, 100 and 200 nm) were tested in this study. Additionally, cell proliferation time was elongated to 7 days for a better observation.

The results show that compared to the cell adhesion on untreated TCP control, significantly higher HAEC adhesion was found on 100 nm-thick PVAA films but not on PVAA films with 25 nm, 50 nm, or 200 nm thicknesses (Figure 2.5). The cells grown on the 100 nm thick PVAA films performed better than those on the other substrates 1 day after cell seeding. However, when cell growth continued to day 7, relatively small differences were found on all the PVAA films, although cell growth on these films remained measurably higher than those on the untreated TCP.

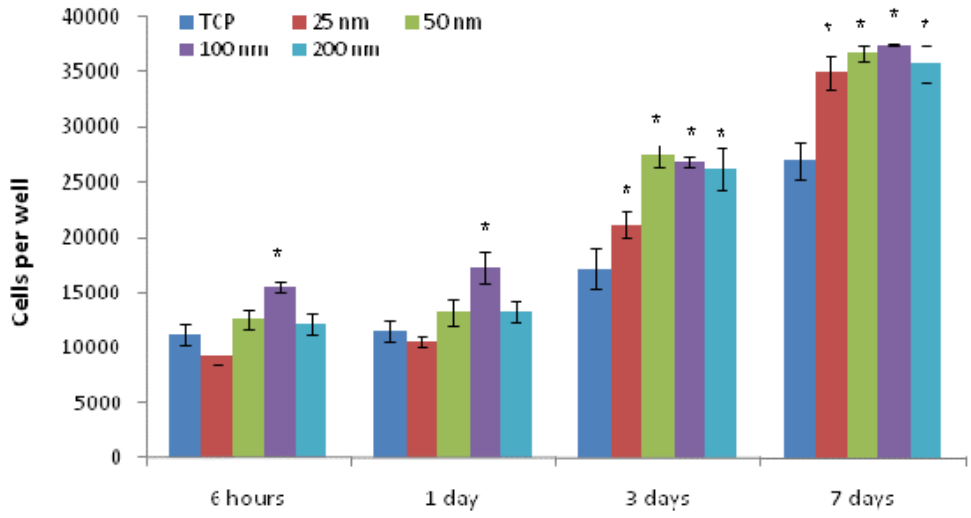

Figure 2.5 HAEC adhesion (6 hours after seeding) and proliferation (1, 3, 7 days after seeding) on PVAA films having the same 9% –COOH surface density but different thickness (25-200 nm). N=4, * : P<0.05 compared to cells grown on untreated TCP at the same time point.

The magnitude of enhanced cell adhesion and proliferation observed in the present study is quite significant. It is interesting to compare the present results with prior reports involving cell growth on –COOH functionalized surfaces, which denoted unchanged, increased, or decreased cell adhesion and growth on –COOH modified surfaces [39, 40, 78, 79]. However, few previous researchers have studied the effects of different surface densities of –COOH, nor the thickness of the PVAA films to the cell adhesion and growth. It is possible that the decreased growth reported by Tidwell et al. using –COOH terminated SAMs [78] was because of the thickness effect, since in the SAMs work, the actual width of the –COOH containing portion of the surface would have been much smaller than the lowest film thickness (25 nm) employed in the present study.

2.3.4 Immunofluorescence Staining of vWF on HAEC

von Willebrand Factor (vWF) is a type of glycoprotein synthesized by vascular endothelial cells. Therefore, it is often used as a biomarker for vascular endothelial cells and to evaluate the cell function [80]. The purpose of this study was to see whether PVAA would affect HAEC function by examining the vWF expression on the cells grown on PVAA films. As shown in Figure 2.6, HAECs grown on PVAA having 9% –COOH and 100 nm film thickness had similar vWF expression as the cells grown on untreated TCP. All cells presented normal EC morphologies. These results imply that PVAA films having 9% -COOH and 100 nm thickness are compatible for HAEC growth, not only supporting their adhesion and proliferation, but also maintaining the cell function well.

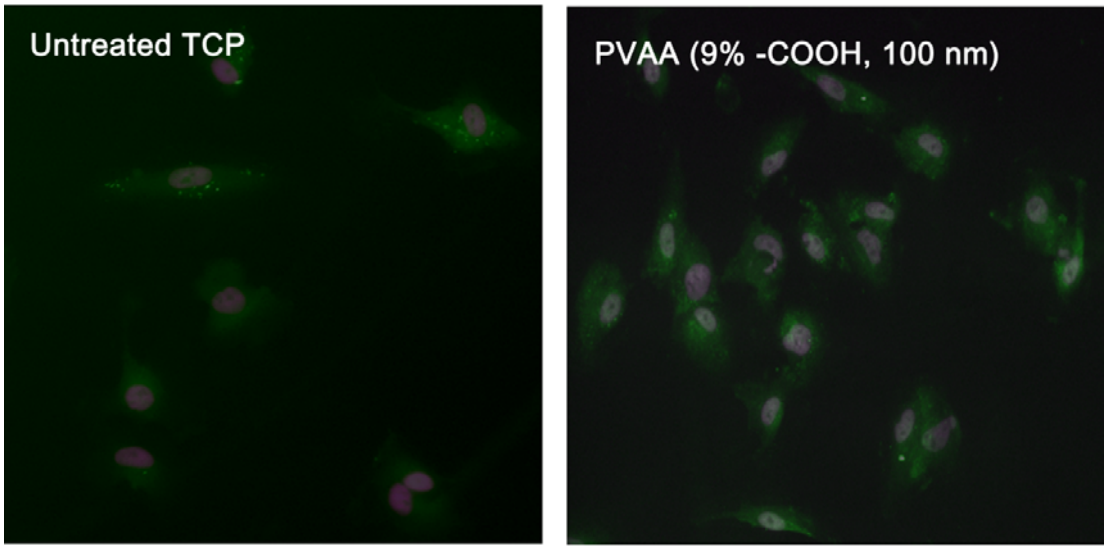

Figure 2.6 Immunofluorence staining of von Willebrand Factor (vWF) on HAEC grown on untreated TCP, or PVAA films having 9% –COOH surface density and 100 nm thickness. Magnification: 200 X.

2.3.5 Fibronectin Adsorption on PVAA Film

Cell adhesion and proliferation are all regulated by cell-extracellular matrix (ECM) interactions. Fibronectin is one of the most important ECM proteins involved in cell adhesion, migration, and proliferation by binding to intergrins on cell membranes [81]. Since fibronectin is one of the major ECM proteins existing in the cell culture medium containing FBS and it has been shown to play an important role in cell adhesion, we hypothesized that the difference in cell adhesion on PVAA films might be caused by the variance of fibronectin adsorption on the substrates. Therefore, the amount of passively adsorbed fibronectin on the PVAA films was quantified. As shown in Figure 2.7a, PVAA having 9% –COOH exhibited more than twice as much fibronectin adsorption as on untreaed TCP, or PVAA films having 3.6% or 6.2% –COOH. Additionally, the thickness of the PVAA films also affected fibronectin adsorption, as observed on PVAA films having 9% –COOH and 25 – 200 nm thickness. As shown in Figure 2.7b, the 100 nm-thick PVAA films had the highest fibronectin adsorption, while the untreated TCP had the least amounts of fibronectin adsorbed on its surfaces. Thus, increased adsorption of

fibronectin might play a major role in the enhanced cell adhesion and proliferation on surface-modified PVAA films.

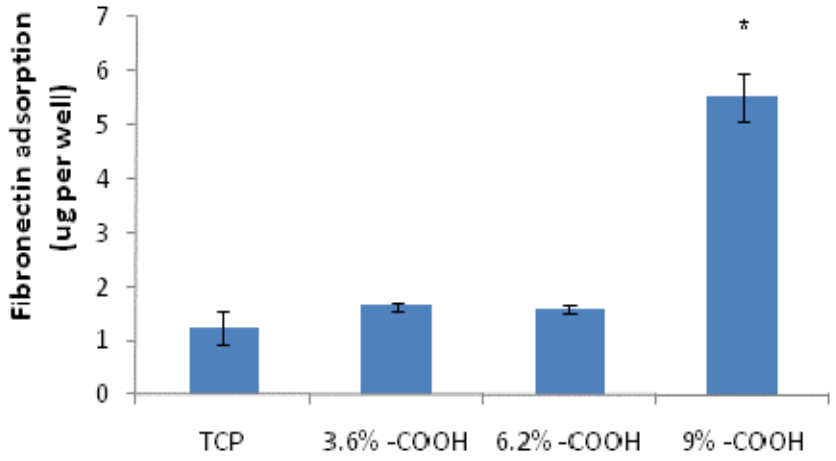

(a)

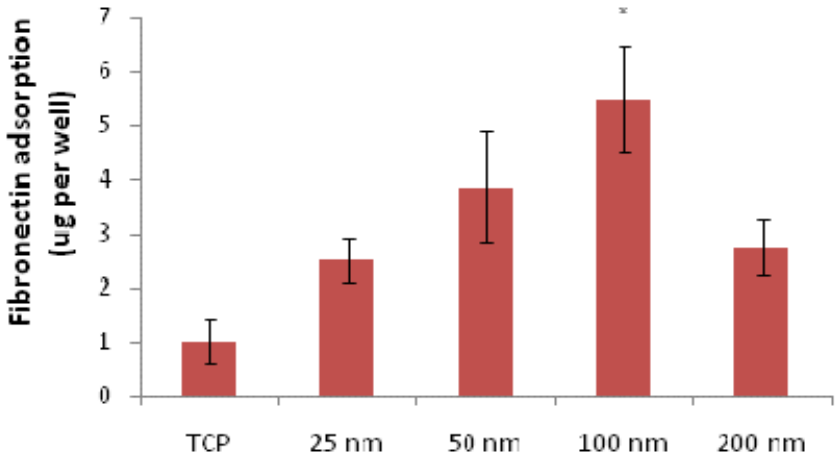

(b)

Figure 2.7 Fibronectin adsorption on PVAA films having different –COOH surface densities or different film thickness. (a) Fibronectin adsorption on 100 nm thick PVAA films having 3.6%, 6.2%, or 9% –COOH surface density; (b) Fibronectin adsorption on PVAA film having 9% –COOH, but different thickness (25-200 nm). N=4, * : $P<0.05$ compared to untreated TCP.

2.4 Conclusion

The adherence and proliferation of HAEC was found to be dependent on the -COOH surface density and film thickness of PVAA deposited on TCP under plasma polymerization. PVAA having 9% –COOH surface density and 100 nm film thickness was optimal for supporting the best HAEC adhesion and proliferation. The ECs grown on PVAA also preserved normal vWF expression, indicating they maintained normal cell function. One of the possible mechanisms accounting for the enhanced EC growth on PVAA might be the enhanced fibronectin adsorption on the surface.

CHAPTER 3

SURFACE MODIFICATION OF POLY(L-LACTIC ACID) USING PVAA DEPOSITION, FIBRONECTIN CONJUGATION, AND VEGF SURFACE DELIVERY FOR ENHANCED ENDOTHELIALIZATION

3.1 Introduction

In the previous chapter, we demonstrated that surface deposition of PVAA, particularly with 9% -COOH surface density and 100 nm film thickness, using plasma polymerization of vinylacetic acid is an effective and convenient method to modify material surfaces for the purpose of enhanced endothelialization. The increased cell adhesion and proliferation might due to the increased adsorption of extracellular matrix (ECM) proteins on PVAA. Coating of ECM proteins, e.g., collagen or fibronectin, has been widely used as a surface modification method. However, physical adsorption of the ECM proteins is generally fairly weak and they can be quickly displaced by other proteins. Additionally, the adsorbed molecules are poorly resistant to the fluidic shear stress presented in arteries, therefore they are easily washed away from the material surface.

In principle, covalent binding of ECM proteins to the material surface would represent a sufficiently strong interaction to resist desorption and thus retain the ECM molecules. However, a difficulty encountered with respect to covalent attachment of molecules to PLLA is the absence of reactive surface groups. Thus in order to increase its covalent binding capacity for ECM proteins, the PLLA substrates must be modified to provide more active groups on their surfaces for this purpose.

Therefore, in order to increase the covalent binding capacity for ECM proteins, the PLLA substrates must be initially surface-modified to provide more active groups for this purpose. In the present study, the feasibility of a strategic surface modification to achieve

improved endothelialization on PLLA substrates was explored. For this purpose, PVAA was first deposited on top of PLLA under plasma to introduce –COOH groups on the substrate surface, as introduced in the previous chapter. Subsequent molecular tailoring of these surfaces included covalent coupling of fibronectin to the plasma deposited –COOH groups, followed by attachment of growth factor VEGF to promote EC surface adhesion and growth. VEGF is a well-known angiogenic growth factor stimulating EC proliferation [82, 83], which exerts its function mainly through binding to VEGF receptor-2 (also called KDR) on human ECs. We hypothesize that gene-transfected ECs over expressing KDR would also promote higher proliferation of ECs and thus would enhance endothelialization of PLLA. As detailed below, this surface tailoring approach, particularly when coupled with KDR transfected ECs, provides a very large increase in cell growth as studied with the use of pig aorta ECs.

3.2 Materials and Methods

3.2.1 Materials

PLLA (L210 Resomer, MW=130,000 g/mol) was purchased from Boehringer Ingelheim Inc., Germany. Human fibronectin was purchased from Chemicom Inc., CA. Vinylacetic acid, 2-(N-Morpholino) ethanesulfonic acid (MES) and 1-[3-(Dimethylamino) propyl]-3-ethylcarbodiimide (EDC) were purchased from Sigma Inc., MO. Rabbit anti-human fibronectin polyclonal antibody, and bovine anti-rabbit IgG-FITC antibody were purchased from Santa Cruz Biotechnology Inc., CA. $VEGF_{165}$, Human VEGF Enzyme-Linked ImmunoSorbent Assay (ELISA) kit, and Picogreen DNA assay were purchased from Invitrogen Inc., OR. CellTiter 96® AQ_{ueous} One Solution MTS Cell Proliferation Assay was obtained from Promega Inc., WI. Mouse anti-human VEGF receptor-2 IgG antibody was purchased from Zymed Invitogen Inc. CA. Goat anti-mouse IgG-FITC antibody was a product of Jackson ImmunoResearch Laboratories Inc., PA. All the other chemicals are from Sigma-Aldrich Inc., MO.

3.2.2 PLLA Film Preparation

PLLA powder was dissolved in chloroform to make 2.5% (w/v) solution, then cast into 12 cm in diameter Teflon Petri dishes and allowed to dry completely. PLLA film was cut into round discs (1.5 cm in diameter), glued on round glass cover slips with medical grade UV glue, and placed in a 24-well TCP. The films were washed with ethanol, de-ionized water, and sterilized under UV before use. For cell retention studies, PLLA films were cast on glass slides.

3.2.3 Deposition of PVAA on PLLA Film

PVAA film with 100 nm-thickness and 9% -COOH surface density was polymerized on top of PLLA using RFGD plasma polymerization at 2/30 duty cycle, as described in the previous chapter.

3.2.4 Characterization of PVAA Film by FTIR Spectroscopy, XPS, and Contact Angle

FTIR spectra of the plasma-deposited PVAA films were obtained using a Brucker Model Vector 22, with spectra recorded using 4 cm^{-1} resolution. The XPS spectra were acquired using a Kratos, model Axis, ultra DLD instrument equipped with a monochromator operated at a pass energy of 10.0 eV. A neutralizer was used in these measurements since the samples were non-conductive. The neutralizer was operated at a current of 1.7A and charge balance of 3.4V. The high resolution XPS spectra were analyzed (deconvoluted) using Casa XPS software. The binding energy of the carbon atoms not directly bonded to any heteroatoms was centered at 284.6 eV. XPS data were acquired for the various samples starting with the unmodified PLLA films and continuing though the sequence of surface modifications involving the plasma depositions and attachment of fibronectin.

3.2.5 Conjugation of Fibronectin

Fluorescence labeling studies were also employed to characterize the extent of covalent coupling of human fibronectin to plasma modified PLLA substrates. In detail, human fibronectin was conjugated to PLLA substrates using two methods, passive adsorption and covalent coupling. For passive adsorption, 500 µl fibronectin (33 µg/ml) was added on top of each PLLA film with or without PVAA deposition, and incubated for 4 hours at room temperature. For covalent coupling, PLLA films with or without PVAA depostion were treated with 10 mg/ml EDC in 0.1 M MES buffer for 20 minutes to activate the –COOH groups on the film surface, followed by incubation with 500 µl fibronectin (33 µg/ml) for 4 hours at room temperature with gentle agitation, a two-step method used by Bang's Lab [84]. After conjugation, the films were rinsed gently with PBS buffer to remove any loosely attached proteins.

To quantify the amount of fibronectin coated on these surfaces, control and surface-modified films were incubated with rabbit anti-human fibronectin polyclonal antibodies as the primary antibody, followed by bovine anti-rabbit IgG-FITC antibodies as the secondary antibody. After removal of unbound antibodies by thorough rinsing with PBS, the PLLA films were treated with 2% Sodium dodecyl sulfate (SDS) for 2 hours with constant agitation, to strip off the antibodies. The fluorescence intensity of antibodies, which correlates with the amount of surface bound fibronectin was measured using Versafluor™ fluorometer (Bio-Rad).

3.2.6 Conjugation and Release of VEGF

After conjugation with fibronectin, as described above, PLLA films were washed with ice-cold binding buffer (containing 25 mM HEPES and 0.1% BSA, pH 5.5), then incubated with 250 ng $VEGF_{165}$ for 2.5 hour at 4 °C in the same buffer. Following incubation, the PLLA films were gently washed with PBS to remove loosely attached VEGF.

To quantify the release of surface-conjugated VEGF, the films were incubated with 1 ml of PBS at 37 °C for up to 5 days with constant agitation. At preset time (1, 2, 3, and 5 days), 0.5

ml PBS containing released VEGF were collected and replaced with 0.5 ml fresh PBS. VEGF Human ELISA Kit was used to measure the VEGF concentration in the releasing medium following the manufacturer's instruction. The cumulative VEGF released was plotted as a function with incubation time.

3.2.7 PAE and KDR-PAE Cell Proliferation on Surface-Modified PLLA

Pig Aorta Endothelial Cell (PAE) and KDR transfected PAE (KDR-PAE) were generous gifts from Dr. Rolf Brekken from University of Texas Southwestern Medical Center. Cells were cultured using F-12 cell culture medium supplemented with 10% FBS and 1% penicillin-streptomycin. Cells between passages 10 and 13 were used in all experiments. For the cell proliferation study, three substrate groups were tested, namely: (1) untreated PLLA film; (2) PLLA film deposited with PVAA, then covalently conjugated with fibronectin via EDC [PLLA-PVAA-(EDC)-FN]; and (3) PLLA deposited with PVAA, covalently conjugated with fibronectin via EDC, followed by VEGF incorporation [PLLA-PVAA-(EDC)-FN-VEGF]. PAE or KDR-PAE cells were seeded on these substrates at a density of 5,000 cells per well and cultured in 37^0C incubator for up to 5 days. At preset time of 1, 3, and 5 days, cell adhesion and proliferation was assessed using CellTiter 96® AQ_{ueous} One Solution MTS assay following the manufacturer's instruction.

3.2.8 Immunofluorescence Staining of KDR on EC

PAE and KDR-PAE cells were grown on PLLA-PVAA-(EDC)-FN-VEGF films or untreated PLLA films for 3 days. For immunofluorescence staining, the cells were fixed with 2% formaldehyde, treated with mouse anti-human KDR antibody as the primary antibody, followed by goat anti-mouse IgG-FITC antibody as the secondary antibody. After staining, the cells were mounted with UltraCruz™ Mounting Medium containing 1.5 μg/ml DAPI for DNA

counterstaining. The cells were observed with a Zeiss fluorescent microscope at magnification of 200 X.

3.2.9 SEM of ECs Grown on Surface-Modified PLLA

To observe the cell morphology, PAE grown on untreated PLLA films, or KDR-PAE grown on PLLA-PVAA-(EDC)-FN-VEGF films for 5 days were fixed with 1.5% gluteraldehyde for 20 minutes, post-fixed with 1% osmium tetroxide for 1 hour, then dehydrated with alcohol (50%, 75%, 90%, and 100% in sequence). After completely drying, the samples were sputter-coated with silver and then examined with a scanning electron microscope (SEM, Hitachi S-3000N).

3.2.10 Cell Retention under Fluid Shear Stress

An *in vitro* parallel flow system was used to assess the cell retention under fluidic shear stress [85]. The PAE and KDR-PAE cells were grown on PLLA-PVAA-(EDC)-FN-VEGF films or untreated PLLA films for 5 days. The cells were then exposed to the cell culture medium flowing over the cells with a shear stress of 15 dyn/cm² for 30 minutes. Following this flow exposure, the cells remaining on the films were lysed with 1% Triton X-100. The total amount of cell DNA was measured with PicoGreen DNA assays. Cells not exposed to flow were also analyzed as static controls. The cell numbers were obtained by calculation using a calibration curve of the total cell DNA versus known numbers of cells.

3.2.11 Statistical Analysis

Results are shown as mean ± standard deviation. Analysis of the results was performed using one sample t-test. $P < 0.05$ was regarded as significant differences existing between two groups.

3.3 Results and Discussion

3.3.1 Spectroscopic Characterization of Surfaces Employed

The thickness of PLLA films was approximately 500 μm, and its surface was fairly smooth, as observed with SEM. An FTIR spectrum of the synthesized PLLA films employed, along with a spectrum of the plasma generated PVAA film are shown in Figure 3.1. The PVAA was deposited on a KBr substrate. These spectra are important with respect to presence and absence of –COOH groups in these films. As shown in PLLA spectrum (Figure 3.1a), there was virtually no absorption in the spectral region extending from around 3400 to 3000 cm^{-1}. In contrast, the PVAA film exhibited a very broad band, extending from approximately 3400 to 2600 cm^{-1} (Figure 3.1b). This broad band is uniquely associated with the presence of –COOH groups [86]. The absorbance bands around 3000 to 2850 cm^{-1} are those associated with C-H stretching vibrations, as expected from the presence of C-H bonds in each film. The additional bands, including particularly the strong absorptions at ~1750 cm^{-1} characteristic of C=O from carboxyl groups, are in accord with the expected film compositions. Thus, the IR data confirmed the absence of –COOH in the PLLA and the presence of such groups in the PVAA-modified PLLA films.

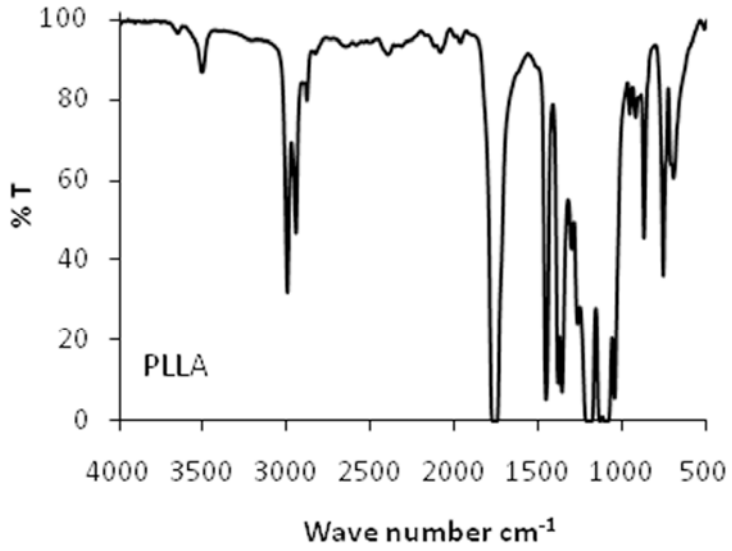

(a)

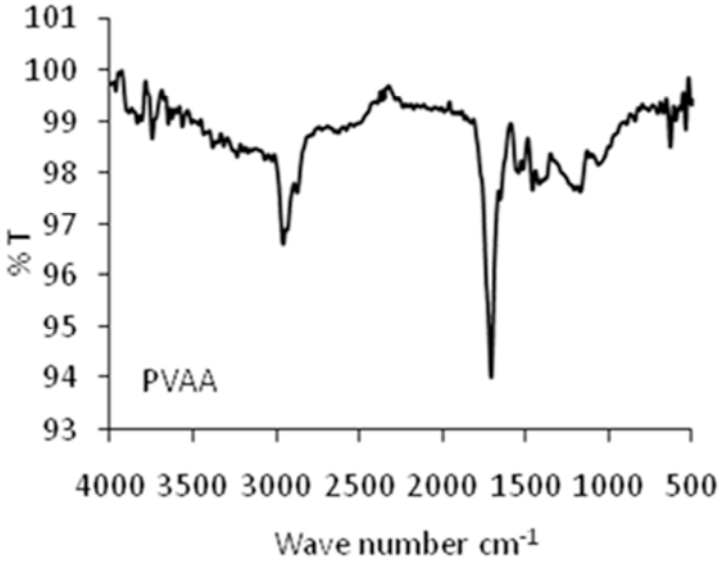

(b)

Figure 3.1 FTIR absorption spectra of PLLA (a) and PVAA (b) films.

XPS spectra of the various surfaces employed in this study are shown in Figures 3.2 and 3.3. The high resolution C(1s) spectra obtained from the pure PLLA (Figure 3.2a), PVAA-modified PLLA (Figure 3.2b), and fibronectin-bound PVAA-modified PLLA (Figure 3.2c) are

presented. The XPS of the pure PLLA film is in excellent accord with the accepted spectrum for this polymer [87]. The 3 peaks shown in its C(1s) spectrum correspond to the presence of saturated C atoms not directly bonded to O atoms (binding energy 284.6 eV); C atoms singly bonded to O atoms of a carboxyl group, i.e., –C-O-C(=O) (B.E. 286.5 eV); and C atoms of the carboxyl group –C-O-C(=O) (288.5 eV). Deposition of the PVAA film on the PLLA dramatically changes the C(1s) spectrum, as shown in Figure 3.2b. The much enhanced peak at 284.6 eV, relative to the other peaks, is consistent with the higher content of saturated C atoms not bonded to O atoms in the VAA monomer to that of lactic acid. The C(1s) peaks at the intermediate binding energies of 285.5 and 287 eV can be assigned to –OH and carbonyl groups produced from partial fragmentation or rearrangement of the VAA during plasma exposure, as generally observed in plasma polymerizations [88]. The peak at 288.5 eV, representing 9% of the total carbon content, is that of the carboxyl groups of the starting VAA which are retained in the plasma film. A further change in the C(1s) spectrum was easily observed after attachment of the fibronectin as shown in Figure 3.2c. Most notable are the increases in the high binding energy peak at ~288 eV and the intermediate binding energy peak around ~286.5 eV. The relative increased prominence of these peaks, compared to PVAA, is consistent with presence of –COOH and amide groups corresponding to the presence of the fibronectin. Since this protein is presumably present as a monolayer, it is important to recognize that photoelectrons from the underlying PVAA film undoubtedly contribute to this spectrum under the 70^0 take-off angle employed, thus complicating more quantitative discussion.

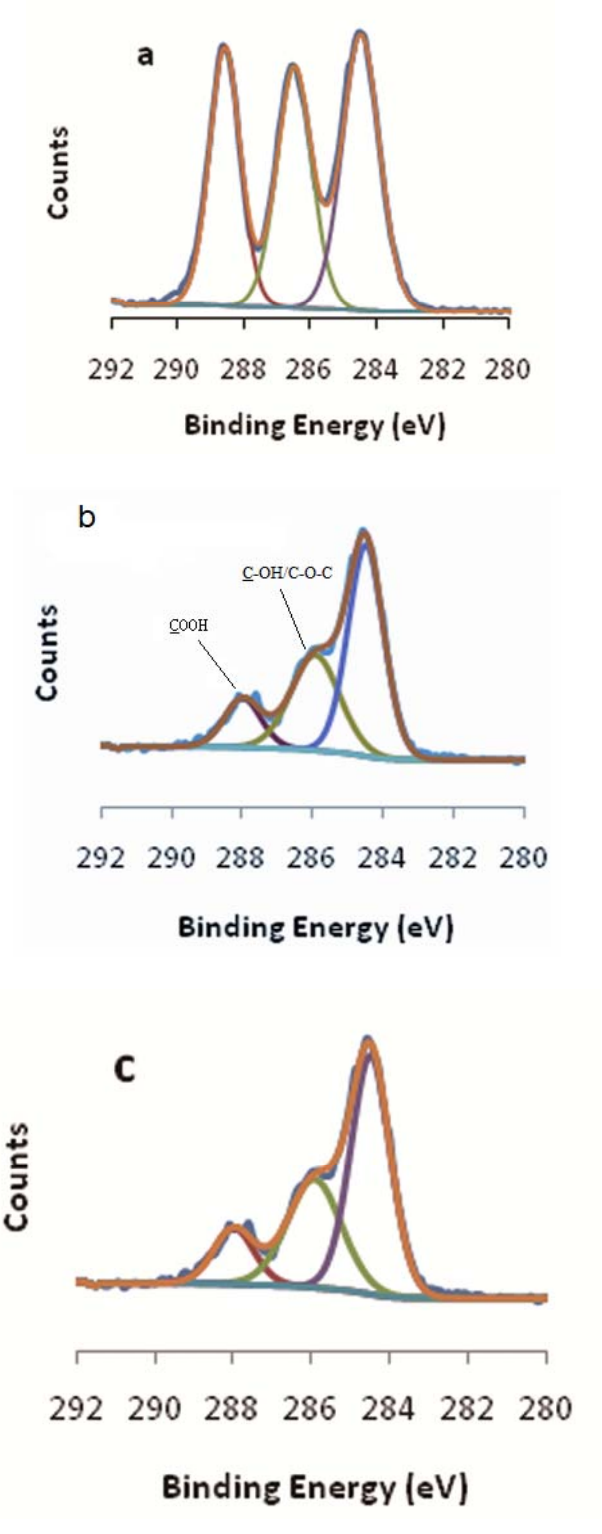

Figure 3.2 High resolution XPS C (1s) spectra of PLLA (a); PVAA (b); and PLLA-PVAA-(EDC)-FN (c)

Additional evidence of successful conjugation of fibronectin to PVAA surfaces was documented by survey XPS survey scans as shown in Figure 3.3. This figure showed the comparison of results from a spectrum of fibronectin covalently bonded to the surface, PLLA-PVAA-(EDC)-FN (Figure 3.3a) compared to that of fibronectin simply adsorbed on the PLLA, PLLA-FN (Figure 3.3b). The important distinction between these two spectra is the prominent N(1s) peak at 400 eV in Figure 3.3a compared to the trace quantity in the Figure 3.3b spectrum. In both cases the samples were subjected to thorough rinsing before the XPS were taken. The nitrogen atom content of the covalently coupled fibronectin was 8.8% as compared to only 2.3% for the physically adsorbed fibronectin.

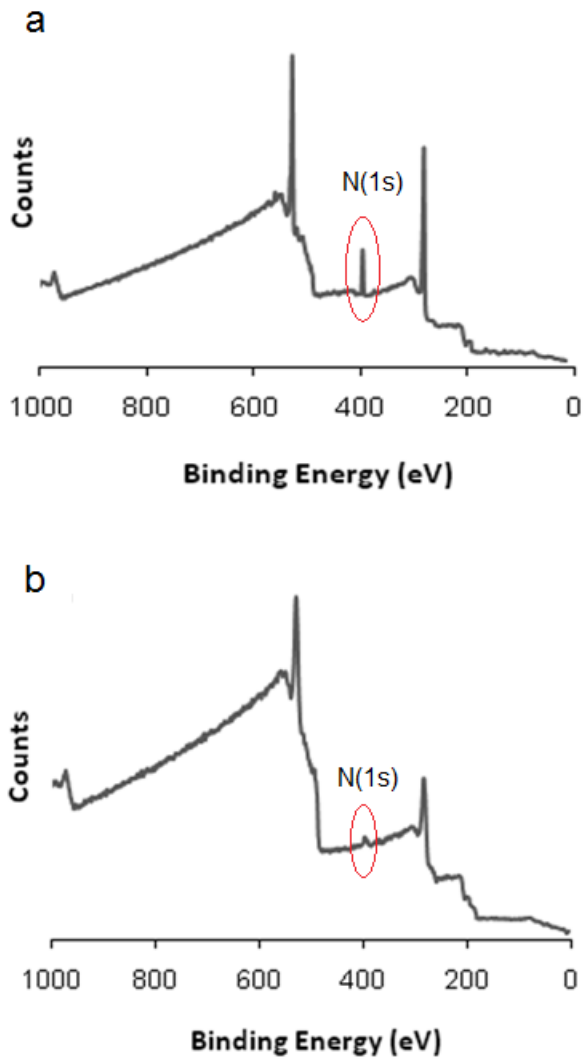

Figure 3.3 XPS survey scan of PLLA-PVAA-(EDC)-FN (a) and PLAA-FN (b).

Covalent conjugation of fibronectin on the PVAA deposited PLLA films was also documented by fluorescence measurement of FITC labeled antibodies. As shown in Figure 3.4, the amount of fibronectin passively adsorbed on untreated PLLA or PLLA deposited with fibronectin (PLLA-PVAA) was essentially same. In contrast, a marked increase of covalently coupled fibronectin, in excess of 100%, was observed on the PLLA-PVAA sample compared to other control samples. The control samples included unmodified PLLA, PLLA exposed to EDC and fibronectin but not plasma-treated, and PLLA-PVAA exposed to fibronectin in the absence

of EDC exposure. These results demonstrated a much higher surface coverage of fibronectin attachment on the plasma modified PLLA surface using covalent coupling method, which is attributed to the sufficient –COOH groups on the PVAA-modified PLLA surfaces.

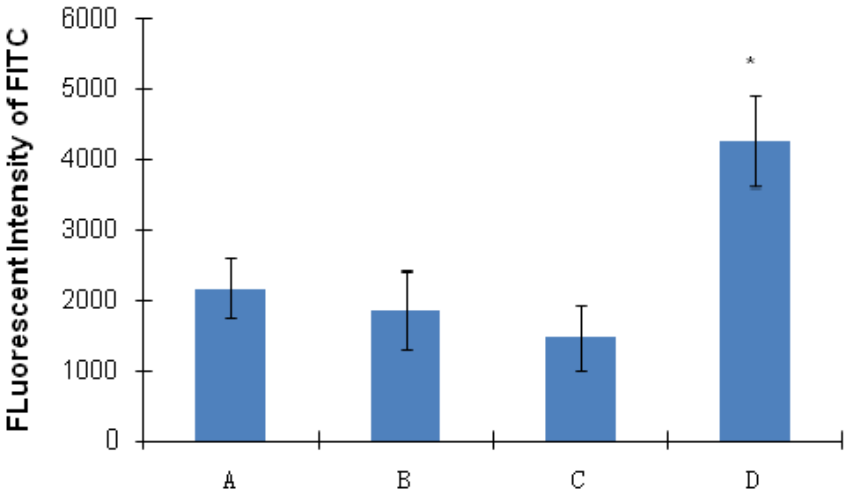

Figure 3.4 Fluorescent intensity measurement of fibronectin coated on original PLLA or PVAA deposited PLLA, with or without EDC coupling, as shown. A): PLLA-FN; B): PLLA-PVAA-FN; C): PLLA-(EDC)-FN; D): PLLA-PVAA-(EDC)-FN. N=4, *: $p<0.05$ compared to all the other groups.

3.3.2 VEGF Surface Conjugation and Release

Previously studies have shown that VEGF can bind to fibronectin through specific binding domains [89], and their binding is enhanced in an acidic (pH 5.5 – 7.0) environment [90]. In the present study, slightly acidic buffer was used for the conjugation of VEGF to fibronectin on PLLA films. The release of VEGF from PLLA films to the surrounding medium was measured for up to 5 days, and was plotted as cumulative release curves, as shown in Figure 3.5. VEGF conjugated on all four groups showed an initial quick release at the first day, followed by a comparatively slower release thereafter. A plateau was shown on the release curve after day 3, indicating most VEGF was released within the first three days. Four sample types employed in the fibronectin studies were used in the VEGF release experiment. As shown in Figure 3.5, the PLLA coated with PVAA and covalently conjugated with fibronectin using EDC coupling [PLLA-

PVAA-(EDC)-FN] had the highest amount of VEGF conjugation on its surface and subsequent VEGF release. This trend is similar to that of fibronectin conjugation on PLLA (shown in Figure 3.4).

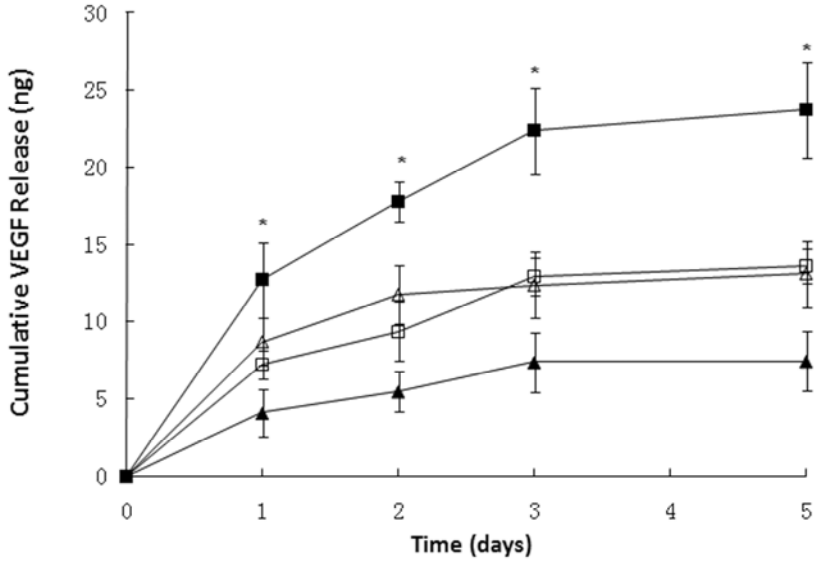

Figure 3.5 Cumulative release of VEGF from PLLA or PVAA deposited PLLA. Fibronectin (FN) was coated on these substrates by either covalent coupling via EDC or by passive adsorption. ■: PLLA-PVAA-(EDC)-FN-VEGF; △: PLLA-FN-VEGF; □: PLLA-PVAA-FN-VEGF; ▲: PLLA-(EDC)-FN-VEGF. N=4. *: $p<0.05$ compared to all the other groups at the same time point

Surface-conjugated fibronectin makes possible the subsequent incorporation of VEGF onto the PLLA surfaces. ECM proteins such as fibronectin [89], fibrin [91], vitronectin [92], and tenascin [93] posses specific binding domains for VEGF. In this study, a substantially increased amount of VEGF was present on the PLLA films with the increased amount of fibronectin on the surface. Although the effective concentration of VEGF to enhance EC proliferation is low (1-6 ng/ml) [94], high dosages are required for systemic delivery, considering its distribution into the whole body. These high dosages of VEGF are not only costly, but lead to certain undesired side effects, such as increasing the permeability of blood vessels [95, 96]. Therefore, localized

delivery of VEGF to the adjacent cells or tissues is favorable since it requires relatively small amounts to reach the effective concentration at the targeted site.

3.3.3 PAE and KDR-PAE Cell Adhesion and Proliferation on Surface-Modified PLLA

In these experiments, cell adhesion after 1 day incubation, and cell proliferation after 3 or 5 days incubation on surface-modified PLLA were compared with the cell growth on untreated PLLA. As shown in Figure 3.6, PLLA films modified with PVAA and fibronectin [PLLA-PVAA-(EDC)-FN] significantly enhanced both PAE and KDR-PAE cell adhesion. At day 3 and 5, both PAE and KDR-PAE cells in contact with untreated PLLA exhibited a discernible decline in surface density, suggesting cells were dying on the untreated PLLA films. In contrast, both PAE and KDR-PAE cells exposed to surface-modified PLLA films, exhibited fast proliferation, especially on the PLLA-PVAA-(EDC)-FN-VEGF films. The cell proliferation of KDR-PAE cells appeared to be slightly better than that of the PAE cells, particularly on PLLA-PVAA-(EDC)-FN-VEGF films, which deliver VEGF.

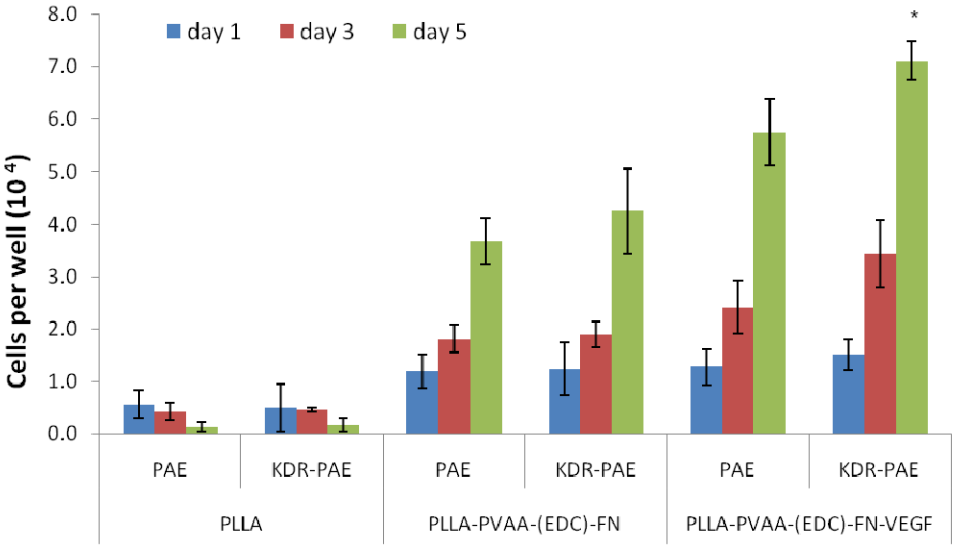

Figure 3.6 PAE or KDR-PAE cell adhesion and proliferation on untreated PLLA, PLLA-PVAA-(EDC)-FN, or PLLA-PVAA-(EDC)-FN-VEGF. N=4, *: $p<0.05$ compared to PAE cells grown on the same film at the same time point.

These results indicate the PLLA film modified with PVAA, fibronectin, and VEGF are a suitable surface supporting EC adhesion and growth. In this study, greater cell proliferation was observed with only nano-gram quantities of VEGF released from the PLLA films. It should also be noted that although the surface delivery of VEGF was clearly effective in stimulating EC growth, the release appeared to last only a short time, approximately 3 days. Some studies have shown that the period of VEGF release can be extended. For example, fibrin was used to deliver growth factors in a proteolysis-triggered manner [97, 98]. Three-dimensional scaffolds, hydrogels, and nano- or micro- particles are also used to increase the growth factors loading capacity and extend its delivery period depending on the applications [99-101].

KDR has been reported to act as the principal signaling receptor for VEGF to exert its biological activities on ECs [102]. Up-regulation and activation of KDR has been observed in enhanced EC proliferation and angiogenesis [103, 104], while impaired expression of KDR has been related to the ineffectiveness of VEGF for angiogenesis [105, 106]. In the present study, KDR-transfected PAE cells demonstrated a higher cell proliferating activity than untransfected PAE cells on surface-modified PLLA delivering VEGF. This result is reasonable since the genetically modified ECs which overexpress KDR might able to use the VEGF better in stimulating EC growth. This also implies that transfection of KDR could be potentially useful to enhance endothelialization.

3.3.4 Immunofluorescence staining of KDR on EC

KDR is a large multimeric glycoprotein produced constitutively in vascular endothelial cells, and is often used as an EC marker to assess EC function. As shown in Figure 3.7, both PAE and KDR-PAE cells preserved KDR well, indicating that they both retained proper EC functions. Additionally, it is noted that the cells exhibited poor surface coverage and uneven spreading on untreated PLLA films, while on the surface-modified PLLA films, the cells were evenly spread and exhibited a far better coverage.

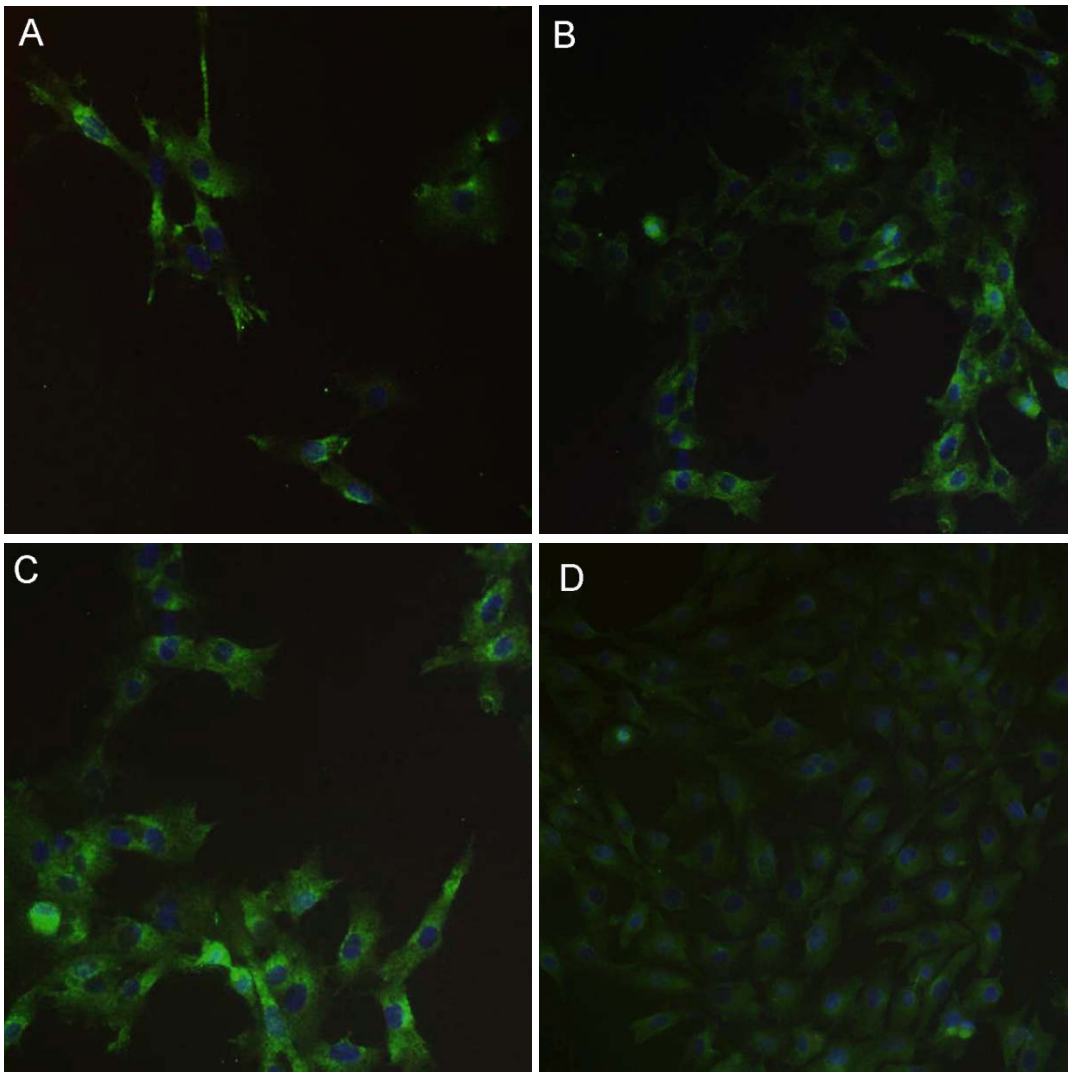

Figure 3.7 KDR immunofluorescence staining of PAE or KDR-PAE cells grown on untreated PLLA or surface-modified PLLA film. A): PAE cells grown on untreated PLLA; B): PAE cells grown on PLLA-PVAA-(EDC)-FN-VEGF; C): KDR-PAE cells grown on untreated PLLA; D): KDR-PAE cells grown on PLLA-PVAA-(EDC)-FN-VEGF.

3.3.5 SEM of EC Grown on Surface-Modified PLLA

SEM studies were employed to provide morphological information of cell growth on the different surfaces. Specifically, KDR-PAE cells grown on PLLA-PVAA-(EDC)-FN-VEGF surfaces were compared to that of PAE cells grown on untreated PLLA film. As shown in Figure 3.8A, KDR-PAE cells grown on surface-modified PLLA had nearly full coverage of the available surface, with the cells exhibiting a contiguous, flatter morphology. In contrast, the PAE cells

covered only a small portion of the untreated PLLA film, were sporadically located and exhibited abnormally bumpy, tortuous morphology (Figure 3.8B). The results further supported that surface-modified PLLA is better for EC growth.

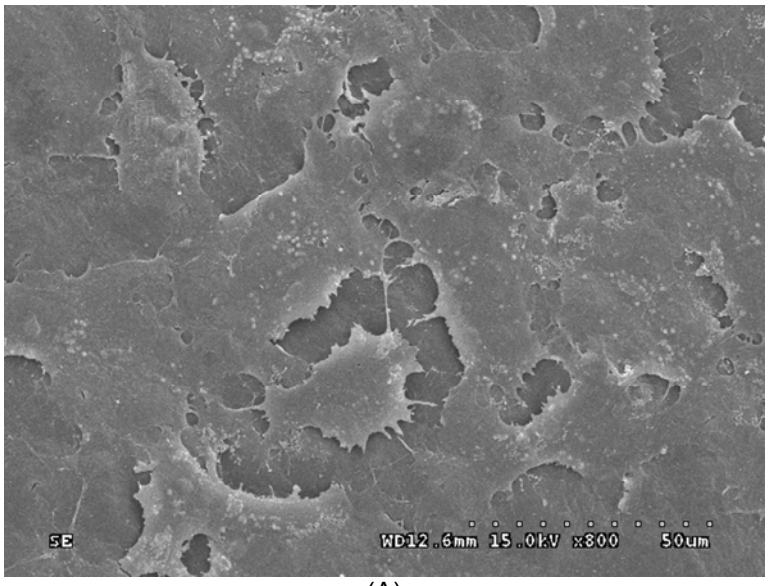

(A)

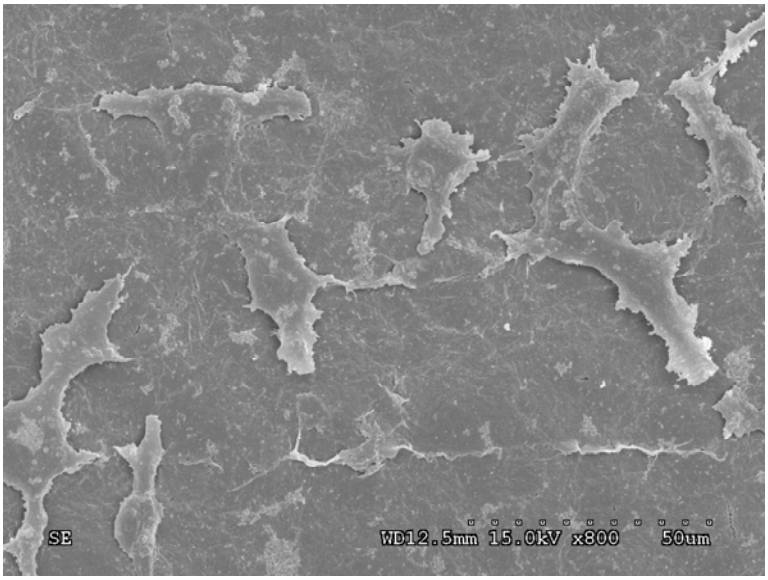

(B)

Figure 3.8 SEM images of (A) KDR-PAE cells grown on PLLA-PVAA-(EDC)-FN-VEGF; (B) PAE cells grown on untreated PLLA.

3.3.6 Cell Retention under Fluidic Shear Stress

Under physiological conditions, vascular endothelial cells are exposed to the shear stress of flowing blood. For this reason, retention of ECs on PLLA and modified PLLA surfaces when exposed to fluid shear stress was examined. In this study, PAE and KDR-PAE cells grown on untreated PLLA or PLLA-PVAA-(EDC)-FN-VEGF films were exposed to 15 dyne/cm² flow, which is within the physiological range of shear stress in arteries. As shown in Table 3.1, PAE and KDR-PAE cells grown on untreated PLLA film had only 27 and 40% cells retained, respectively, after exposed to 30 minutes flow. While on surface-modified PLLA films, both PAE and KDR-PAE cells showed significantly better cell retention, with more than 60% of cells left on the surface after the same flow exposure. In term of cell numbers, PAE or KDR-PAE cells had around 9 times more cells retained on the surface-modified PLLA films than on untreated PLLA films after shear stress exposure (94.6-112 vs. 10.9-19.2 ng/ml).

Table 3.1 PAE or KDR-PAE cells retention on PLLA or surface-modified PLLA [PLLA-PVAA-(EDC)-FN-VEGF] films after exposed to 15 dyn/cm^2 shear stress for 30 minutes.

Cell	Substrate	Before shear stress (ng/ml)	After shear stress (ng/ml)	Retention rate (%)
PAE	PLLA	40.3 $\pm$ 10.5	10.9 $\pm$ 5.4	27
	PLLA-PVAA- (EDC)-FN-VEGF	141.8 $\pm$ 15.8	94.6 $\pm$ 26.7	66.7
KAR-PAE	PLLA	47.9 $\pm$ 10.6	19.2 $\pm$ 7.4	40
	PLLA-PVAA- (EDC)-FN-VEGF	177.1 $\pm$ 11.4	112.0 $\pm$ 39.4	63.2

Endothelial cells grown on the luminal side of vascular stents are continuously exposed to fluid shear stress of the blood when implanted. Retention of ECs on the material surface when exposed to sheer forces is obviously an important consideration. Physiological arterial shear stress is typically 15 dynes/cm^2 and above [107, 108]. In this study, ECs grown on surface- modified PLLA films had significantly higher cell retention than on untreated PLLA films after exposure to a physiological level of shear stress. In fact, the KDR-PAE cell retention on the modified PLLA surfaces was an order of magnitude in excess of that observed on untreated

PLLA surfaces. This result further supports the effectiveness of the surface-modification method employed in this research.

3.4 Conclusion

The surface modification of PLLA involving plasma deposition of PVAA; followed by covalent fibronectin conjugation; followed, in turn, with VEGF adsorption, significantly enhanced endothelialization on biodegradable substrates such as PLLA. The use of KDR-transfected PAE cells, in lieu of unmodified PAE, further increased the rate of endothelialization. This surface-modification technique encourages more enhanced endothelialization on vascular implants under static condition. It also resulted in higher endothelial cell retention under fluid shear stress. However, the incorporation of VEGF on the fibronectin-conjugated PLLA surface is still limited as its release only last for 5 days. For longer periods of growth factor delivery, other techniques need to be used.

CHAPTER 4

ENHANCED ENDOTHELIALIZATION ON PLLA MODIFIED WITH POC/PLGA MICROPARTICLE COMPOSITE AND EPC AUTOSEEDING

4.1 Introduction

In chapter 3, we showed PLLA surfaces modified with PVAA deposition, followed by fibronectin conjugation and VEGF incorporation greatly enhancing endothelialization compared to EC growth on unmodified PLLA surfaces. However, one critical problem is the cell loss from the modified PLLA surfaces once they are exposed fluid shear stress. Thirty minutes of exposure to shear stress of 15 dyn/cm^2, which is in the low range of arterial shear stress, caused 35% cell loss from the modified PLLA substrate. Other limitations of the earlier technique include the difficulty in handling the cell-preseeded vascular graft or stents, the possible damage to the seeded cells on stents when high pressure is employed for stent deploying, and the concern of bacterial or viral contamination during the i*n vitro* cell culture process.

Previous research has shown that autologous EPC has the potential to proliferate and differentiate to functionally mature endothelial cells, thus they can be used for endothelialization on vascular prostheses. In the present study, we immobilized anti-CD34 antibodies on top of the substrate for capturing EPCs. To enable strong adhesion and subsequent EPC growth, fibronectin was conjugated on the material surface, which also provides –COOH groups for subsequent conjugation of anti-CD34 antibodies. Another requirement for EPC growth is that they need certain growth factors, such as VEGF and FGF for their growth. Surface delivery of such growth factors only last for 3- 5 days, as we discussed in the previous chapter. For sustained delivery of growth factors, a controlled drug delivery system has to be used.

In this research approach, biodegradable polymer poly(lactic-co-glycolic acid) (PLGA) microparticles were used as a drug delivery vehicle for controlled release of growth factors. VEGF and FGF were encapsulated in PLGA microparticles using a double emulsion method. The loading efficiency and release of these growth factors were studied. To immobilize the growth factor encapsulated PLGA microparticles on the surface of PLLA, poly(1,8-octanediol-*co*-citrate) (POC), a biodegradable elastomer invented by Dr Yang [109], was used. PLGA microparticles were embedded in POC, making a POC/PLGA microparticle composite, and coated on PLLA films. The rich –COOH groups on the POC surface were used for fibronectin conjugation. Also, as shown in Chapter 3, endothelial cells overexpressing VEGF receptors (VEGFR) had faster proliferation than untransfected cells. Therefore, in this study, VEGFR encoding plasmids were also encapsulated in PLGA microparticles, in order to transfect the EPCs to overexpress VEGFR. The schematic of the design is shown in Figure 4.1.

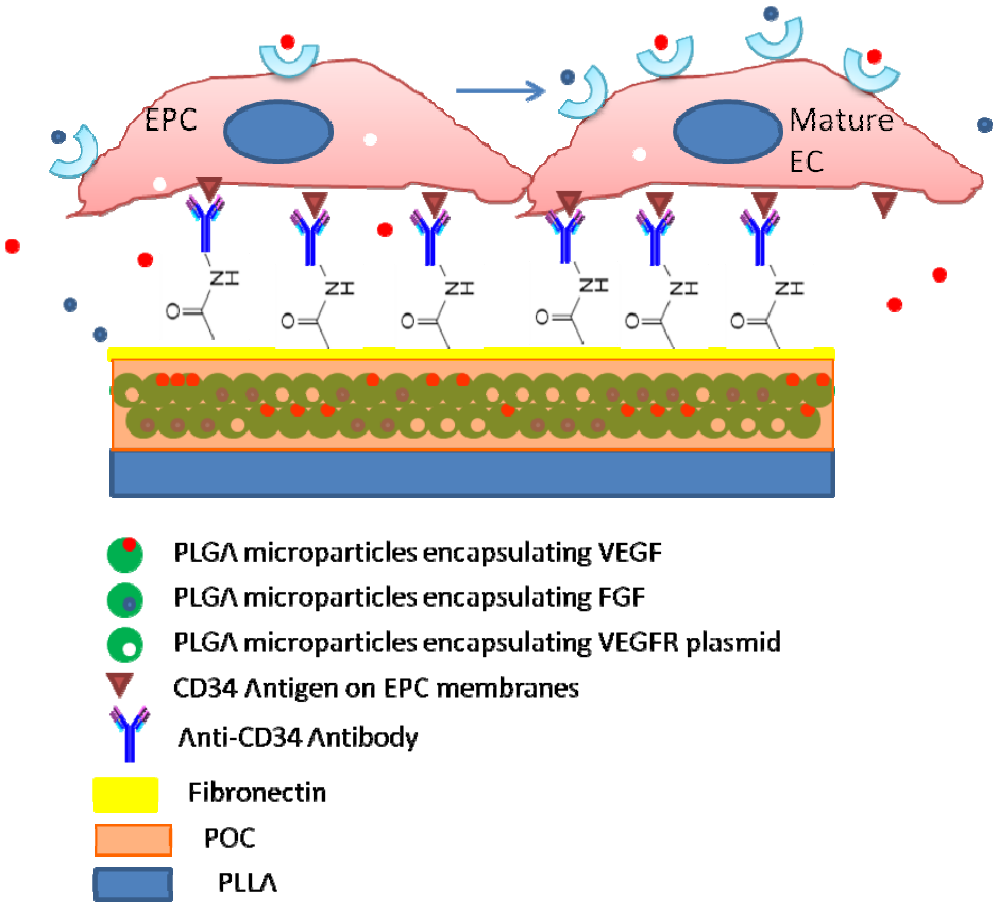

Figure 4.1 Schematic of the surface modification of PLLA and EPC autoseeding for enhancing endothelialization. PLLA is coated with POC/PLGA microparticles composites. Inside the PLGA microparticles, VEGF, bFGF, or VEGFR plasmids are encapsulated for sustained delivery of these factors. The –COOH groups on POC are used to conjugate with fibronectin covalently. Anti-CD34 antibodies conjugated on fibronectin are used to capture EPCs, which grow on fibronectin, and differentiate to mature ECs under released VEGF and bFGF. In addition, EPCs are transfected by VEGFR plasmids, thereby overexpress of VEGFR on their membrane surfaces.

4.2 Materials and Methods

4.2.1 Expansion and Characterization of VEGFR Plasmids

pBLAST9-VEGFR plasmids (InvivoGen Inc., CA) were transformed into competent GC5™ E.coli cells (GENE CHOICE Inc., CA) following the company's instruction [110]. Transformed E.coli cells expressing blasticidin-resistance gene were selected with Fast-Media® Blas blasticidin-containing medium (InvivoGen Inc., CA). Selected E.coli. were expanded, and

the plasmids were extracted and purified using QIAGEN Plasmid Midi Kit (QIAGEN Inc., CA). To characterize whether the extracted plasmids contain VEGFR sequence, the plasmids were digested with endonuclease AgeI and NheI (New England Biolabs Inc., MA), which are located on each end of VEGFR sequence. The digested products were analyzed with electrophoresis.

4.2.2 Synthesis of PLGA Microparticles Encapsulating VEGF, FGF, or VEGFR Plasmids

PLGA (50:50) was purchased from Lakeshore Biomaterials Inc., AL. $VEGF_{165}$ and bFGF were purchased from Invitrogen Inc., CA. PLGA microparticles encapsulating VEGF, bFGF, or VEGFR plasmids were synthesized using the double emulsion method (water/oil/water). In detail, 50 µl aqueous solution containing $VEGF_{165}$ (100 µg/ml), bFGF (100 µg/ml), or VEGFR plasmid (580 µg/ml) were added into 1 ml PLGA solution (25% w/v in dichloromethane), sonicated for 30 seconds at 20 watts to make the primary emulsion (water/oil). The primary emulsion was immediately mixed vigorously with 2 ml polyvinyl alcohol (PVA, 1% w/v) to form the secondary emulsion (water/oil/water). The second emulsion was quickly poured into 200 ml PVA solution (0.1% w/v) and stirred continuously for 4 hours at 400-500 rpm in a chemical hood, to let the dichloromethane (DCM) to evaporate. Synthesized PLGA microparticles were collected by centrifugation, washed twice to remove excess PVA, and freeze-dried. The particles shape and size were observed with SEM.

4.2.3 Characterization of Loading Efficiency and Releasing Profiles of VEGF, bFGF, and VEGFR Plasmids

The loading efficiencies of VEGF, bFGF, and VEGFR plasmids in synthesized PLGA microparticles were studied using a direct measuring method. In detail, 20 mg freeze-dried PLGA microparticles encapsulating VEGF, FGF, or VEGFR plasmids were dissolved in 500 µl DCM, and mixed vigorously with 500 µl DI water. The solution was left undisturbed for 6 hours to separate the water and oil phases. The oil phase was discarded and aqueous phase was collected. The aqueous solution containing VEGF or bFGF was freeze dried and reconstituted

into 50 μl PBS, and their concentration was measured using the BCA protein assay. VEGFR plasmid concentration in the aqueous solution was measured directly with UV spectrometry. The loading efficiency was calculated using the following equation:

$$Loading\ Efficiency = \frac{Amount\ of\ drugs\ existing\ in\ the\ total\ microparticles}{Amount\ of\ drugs\ loaded\ initially} \text{ X } 100\%$$

To characterize the drug release profile, 20 mg PLGA microparticles encapsulating VEGF, bFGF, or VEGFR plasmids were mixed with 1.5 ml releasing media (PBS with 1% BSA, pH 7.4), and incubated with constant gentle shaking at 37° C. The samples were centrifuged, and 0.75 ml supernatant were collected and replaced with the same amount of fresh PBS at predetermined time (1 hour up to 8 weeks). After all the samples were collected, the concentration of VEGF or bFGF in the collected releasing medium was measured using ELISA kits (Invitrogen, Inc., CA) following the manufacturer's instruction. The VEGFR plasmid concentration in the releasing medium was measured at 260/280 nm using UV spectrometry. After measurement, the cumulative release of the growth factors or plasmids was plotted as a function of the incubation time.

4.2.4 Bioactivities of VEGF, FGF, and VEGFR Plasmids Released From PLGA Microparticles

To examine whether the released growth factors still have bioactivity, PAE cells were seeded on 24-well TCP with F-12 medium supplemented with 10% FBS at 5000 cells/cm². The second day, the medium was changed to F-12 medium supplemented with 2% FBS, and the cells were starved overnight (~12 hours). The medium was again replaced with fresh F-12 medium having 2% FBS and 10% (v/v) PLGA microparticle-releasing medium containing either released VEGF or bFGF, and incubate for 5 days. Cells incubated with F-12 medium containing 2% FBS were used as control groups. As comparisons, another group of cells were exposed to known amounts of VEGF or FGF added into the cell culture medium to a final concentration of

1, 5, or 10 ng/ml, and incubated for the same period of time. MTS assays were used to evaluate the cell proliferation in each sample.

To examine the activity of the released VEGFR plasmids, VEGFR plasmids and GFP plasmids (generous gifts from Dr. Victor Lin from University of Texas Southwestern Medical Center) were both encapsulated in PLGA microparticles in the same way as described before. These microparticles were used in the *in vitro* release study for 2 weeks, and the collected releasing medium containing VEGFR and GFP plasmids were freeze-dried, dissolved in 5 µl DI water, and used to transfect PAE cells with Fugene HD transfection reagent (Roche Inc., IN). After incubation for 48 hours, the cells were observed using a fluorescence microscope.

4.2.5 Synthesis of POC

POC was synthesized following a previous method [109]. In brief, 1 mole of each citric acid (Fisher Scientific Inc., PA) and 1,8-octanediol (Sigma Inc., MO) were added to a 250 ml round bottom flask and heated to 160 ºC in oil bath with stirring. After the monomers melted completely, the temperature of the system was lowered to 140 ºC for 2 hours under stirring until the stirrer was not able to move. This synthsized POC prepolymer was dissolved in 1, 4-dioxane, then poured into enough DI water to remove unreacted monomers. The precipitated POC pre-polymer was post-polymerized in freeze dryer under vacuum for 3 weeks to create POC. To make POC/PLGA microparticle composite, 51 mg PLGA microparticles (17 mg containing VEGF, 17 mg containing bFGF, and 17 mg containing VEGFR/GFP plasmids) were mixed with 1.5 g POC pre-polymer. This composite was spread on PLLA films which were coated on glass slides, followed by post-polymerization as described above.

4.2.6 Preparation of Platelet-Rich Plasma

All methods related to collection and handling of whole blood and blood components like plasma and platelets were approved by the Institutional Review Board at the University of

Texas at Arlington. Acid citrate dextrose (ACD) anticoagulant containing tubes were used to collect blood drawn from healthy individuals by venipuncture. Platelet-Rich Plasma (PRP) was prepared as per methods previously described in literature [111]. Briefly, whole blood was centrifuged at 250g for 15 minutes to separate the blood components. Using a sterile transfer pipette, the clear supernatant was collected in clean tubes and used immediately afterwards.

4.2.7 Platelets Adhesion on POC

Two hundred microliters PRP was laid on top of POC or PLLA films in 96-well plates. After 1 hour of incubation at 37 °C, PRP was aspirated and the polymer films were rinsed with PBS 3 times to remove unattached or loosely adhered platelets. Quantitative assessment of the adherent platelets was done using the lactate dehydrogenase (LDH) assay [111, 112]. In brief, the platelets adhering on the polymer films were lysed with100 µl triton-X 100 (1% v/v) for 30 minutes at 37 °C. After lysing the platelets, LDH Assay substrate (100 µl) was added to the lysate and incubated for 30 minutes at 37 °C in darkness. After that, HCl (0.1 N) was added to stop the reaction at the end of the incubation period. Absorbance was measured at 490 nm with a reference wavelength of 650 nm. To observe the morphologies of platelets adhered on POC or PLLA, the platelets were fixed using 2.5% gluteraldehyde/PBS solution, followed by dehydration in a graded series of alcohol (50%, 75%, 90% and 100%) and air dried. The samples were sputter coated with silver and examined by SEM.

4.2.8 Platelets Activation on POC

Platelet activation was assessed by detection of the expression of P-selectin on platelets using flow cytometry [113, 114]. Two hundred microliters PRP was added on top of POC or PLLA films in 96-well plates and incubated for 1 h at 37 °C. After incubation, 5 µl PRP was incubated with 20 µl phycoerythrin (PE)-conjugated mouse anti-human CD42a monoclonal antibody (BD Bioscience Inc. NJ), and 20 µl allophycocyanin (APC)-conjugated mouse anti-

human CD62p monoclonal antibody (BD Bioscience Inc., NJ) at room temperature for 30 minutes in darkness. CD42a, known as platelet glycoprotein IX (GP9), is a small membrane glycoprotein found on the platelet plasma membrane, and is used as a platelet marker. CD62p belongs to the P-selectin family, and is used as an activated platelet marker. After staining, the cells were fixed with 1% paraformaldehyde, and FACSarray bioanalyzer (BD Bioscience Inc., NJ) was used to analyze the amount of the activated platelets (CD62p-positive) among all the platelets (CD42a-positive). In brief, 5000 to 10000 platelets were acquired, and the mean values of red fluorescence intensity of APC which corresponds to CD62p, and the yellow fluorescence density of PE which corresponds to CD42a of the platelets were measured. The percentage of the activated platelets among all the platelets, and the mean APC value of the activated platelets, which were exposed to POC or PLLA, was calculated.

4.2.9 Whole Blood Clotting on POC

Kinetic whole blood clotting time was used to evaluate the thromboresistant properties of POC [115, 116]. Briefly, 850 µl $CaCl_2$ (0.1 M) was added to 8.5 ml ACD blood to initiate the clotting cascade. Immediately after adding the $CaCl_2$, 100 µl re-calcified blood was quickly added on to POC, PLLA, or glass discs which were put in 24-well plates, and incubated at room temperature. At certain time points (10, 20, 30, and 60 minutes), 3 ml of DI water were added into each well and incubated for 5 minutes to lyse the red blood cells which had not formed clots. The amount of hemoglobin released from the lysed red blood was measured of the absorbance at 540 nm using a microplate reader. The absorbance values were plotted versus the blood contacting time.

4.2.10 Hemolysis on POC

Two hundred microliter diluted blood (200 µL ACD blood diluted with 10 ml 0.9% saline) was added on POC or PLLA films, and incubated for 2 hours at 37 °C under gentle agitation.

The diluted blood without polymer contact served as negative controls (NC). Two hundred microliter whole blood diluted with 10 ml DI water served as positive control (PC). After incubation, polymer samples (PS) were removed and the blood samples were centrifuged at 1000 g for 10 min. The supernatant was transferred to a 96-well plate, and the absorbance (Abs) was measured at 545 nm. Percentage of hemolysis was calculated for each polymer using the following equation.

$$\%Hemolysis = \frac{Abs_{PS} - Abs_{NC}}{Abs_{PC}} \text{ x } 100\ \%$$

(PS: Polymer sample; NC: Negative control; PC: Positive control)

4.2.11 Leukocytes Activation on POC

The activation of leukocytes was also measured by flow cytometry. In detail, 100 µl whole blood was added on POC or PLLA films and incubated for one hour at 37 °C. Following incubation, the samples were treated with 10 µl APC-conjugated mouse anti-human CD45 monoclonal antibody (BD Bioscience Inc., NJ) and 20 µl PE-conjugated mouse anti-human CD11b monoclonal antibody (BD Bioscience Inc. NJ) for 30 minutes at room temperature in darkness. CD45 is the leukocyte maker, while CD11b is used as the marker for activated leukocyte. After incubation with antibodies, red blood cells in the samples were lysed using 1× FACS lysing solution (BD Bioscience Inc., NJ), then leukocytes were fixed with 1% paraformaldehyde. For analysis, five thousand to ten thousand leukocytes were acquired and analyzed using FACSarray bioanalyzer. The value of yellow fluorescence density (PE), which corresponds to the expression of CD11b, and red fluorescence density (APC), which corresponds to the expression of CD45 on leukocytes, were measured. The percentage of activated leukocytes (CD11b positive) among all the leukocytes (CD45 positive), as well as the mean value of PE in the activated leukocytes exposed to POC or PLLA were calculated.

4.2.12 Inflammatory Cytokine Release

The inflammatory cytokines, Interleukin 1 beta (IL-1β) and Tumor Necrosis Factor - alpha (TNF- α), were measured using Cytometric Bead Arrays (BD Bioscience Inc., NJ). Briefly, 100 µl whole blood was added on top of POC or PLLA films and incubated for one hour at 37 °C. After incubation, the blood was collected and centrifuged at 2000 g for 10 minutes and the supernatant was collected to obtain the platelet poor plasma (PPP). The concentrations of IL-1β and TNF-α in the PPP were measured using Human TNF Flex Set (BD Inc. NJ) and Human IL-1β Flex Set (BD Bioscience Inc., NJ) following the manufacturer's instructions. In brief, there were two populations of beads, which were coated with antibodies against either IL-1β or TNF-α. These beads also had distinct fluorescence intensity. To use these beads for detection of the cytokine concentration in samples, these beads were incubated with the collected PPP to capture IL-1β or TNF-α. After that, PE-conjugated antibody was used to label the cytokines bound to the beads. Using FACSarray bioanalyzer, the bead population was resolved by their own fluorescence intensities. After separating different groups of beads, the fluorescence intensity of PE, which was in accordance with the amount of IL-1β or TNF-α were analyzed. IL-1β and TNF-α standards of known concentrations were measured for generating the standard curve. The concentration of IL-1β and TNF-α in our experimental samples were calculated against the standard curve, using the software provided with the assay.

4.2.13 Surface Modification of POC with Fibronectin and Anti-CD34 Antibodies

Fibronectin was covalently conjugated on POC using EDC chemistry, since POC has abundant –COOH groups [117]. In detail, POC films were treated with EDC (10 mg/ml, in 0.1 M MES buffer) for 20 minutes to activate the –COOH groups on the film surface, followed by incubation with fibronectin (33 µg/ml) for 4 hours at room temperature with gentle agitation via a two-step method of Bang's Lab [84]. After conjugation with fibronectin, the POC films were rinsed gently with PBS to remove any loosely attached proteins. Following fibronectin

conjugation, mouse anti-human CD34 antibody was subsequently conjugated with fibronectin using the same EDC coupling method.

4.2.14 EPC Isolation, Differentiation, and Characterization

EPCs were isolated from peripheral blood using Ficoll density gradient centrifugation [118]. In brief, peripheral blood diluted with PBS/2% FBS was loaded on top of Ficoll-Paque™ PLUS (GE Healthcare Inc., Sweden) and centrifuged at 400 g for 30 minutes. The mononuclear cells were aspired, seeded on fibronectin-coated TCP, and incubated with EGM-2 Endothelial Cell Growth Medium-2 supplemented with BulletKit (Lonza Inc., MD) containing FBS, bovine brain extract, human epidermal growth factor, hydrocortisone, gentamicin, and amphotericin B. After 3 days culture, the medium was changed and unattached cells were removed. The medium was replaced every 3 days thereafter.

To characterize the EPCs, the cells were seeded on glass cover slips. Uptake of fluorescently-labeled acetylated low-density lipoprotein (Dil-Ac-LDL, Biomedical Technologies, Inc., MA) was used to characterize the EPC-derived cells. In detail, Dil-Ac-LDL was diluted to 10 mg/ml with complete EC growth media and then incubated with the EPCs for 4 hours at 37 ºC. The media was removed and the cells were washed. Fluorescent microscopy was used to observe the cells.

For immunostaining of vWF, rabbit anti-human vWF IgG (1:100) was used as the primary antibody, followed by bovine anti-rabbit IgG-FITC (1:200) antibody to incubate the cells for one hour each. After thorough rinse, the cells were observed with a fluorescent microscope.

4.2.15 EPC Capture on Surface-Modified POC under Shear Stress Influence

POC pre-polymers were smeared on the big glass slides and polymerized as described in section 4.2.5. Similarly, PLLA films were coated on glass slides by smearing PLLA solution (2.5% w/v in chloroform) and allowing it to dry completely. The glass slides with POC or PLLA

coating were soaked in PBS for nine days with 2 times PBS changes per day until the acidity of POC was removed (pH > 7.0). After sterilization with 70% ethanol and UV, the films were treated with fibronectin, followed by conjugation of anti-CD34 antibodies via EDC. An *in vitro* parallel flow system with continuous unidirectional flow (shown in Figure 4.2) was used to study the EPC captured on treated POC or PLLA surface under fluidic shear stress [119]. After rinsing with PBS thoroughly, PLLA or POC films conjugated with fibronectin and anti-CD 34 antibodies were mounted on the flow system using aseptic techniques. EPC suspension (4×10^6 cells in 25 ml complete EGM-2 medium) was loaded in sterile syringes and circulated at 3.5 ml/min (4 dyn/cm^2) for 24 hours. The second day, a sample of cell suspension was examined for the cell viability with 0.4% trypan blue. The cells suspended in medium were found to be still alive. The flow rate was adjusted to 7 ml/min (8 dyn/cm^2) without replacing medium, and the flow was kept another 24 hours. At the third day, the cells in the medium were found to be dead, so the medium was replaced with complete EC medium. The flow rate was increased further to 13 ml/min (15 dyn/cm^2), and the cells were exposed to the complete EC medium flown at 15 dyn/cm^2 for another two days. The flow rate was decided according to the following equation

$$Q = \frac{\tau b h^2}{6\mu}$$

τ: shear stress (dyn/cm^2)
b: slit width (1.8 cm)
h: channel height (0.022 cm)
μ: viscosity of flowing medium (0.01 dyn · sec / cm^2)

At day 1, 2 and 4, the flow chambers were moved out of the incubator, and the cells grown on POC or PLLA films were observed under a microscope and cell images were taken. The cell numbers at 5 randomly picked areas from each sample were counted.

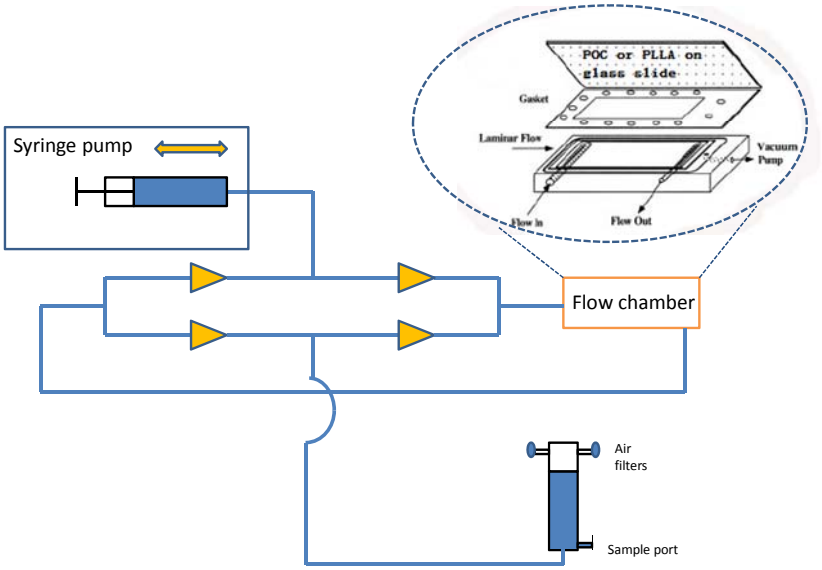

Figure 4.2 Unidirectional continuous parallel flow system. Top: Schematics of the design, four one-way valves are used to enable the continuous flow in only one direction inside the flow chamber, when the syringe is automatically shifted between pushing and withdrawing. Bottom: actual experimental setup. The whole system is put in 37°C incubator filled with 95% air/5% CO_2.

4.2.16 EPC Proliferation on POC/PLGA Microparticle Composite

PLLA thin films were smeared on top of glass coverslips using 2% (w/v) PLLA dissolved in DCM. When completely dried, POC and POC/PLGA microparticle composites were coated on the PLLA films as described in section 4.2.5. PLLA films without POC coating were used as a control. Before cell seeding, POC and POC/PLGA microparticle composite films were soaked in DI water with frequent water change for 9 days until the water became neutral. The films were then conjugated with fibronectin via EDC chemistry as described early. EPC were seeded on these films at 2000 cells/cm^2, and incubated with EGM-2 complete medium at 37 ºC for 7 days. After 1, 3, 5, and 7 days, the MTS assay was used to examine cell proliferation in each sample.

4.3 Results and Discussion

4.3.1 Characterization of VEGFR Plasmids

To characterize the expanded plasmids, the plasmids abstracted from the transformed E.coli, and the original VEGFR plasmid provided by the company were digested with endonuclease AgeI and NheI, which are located on two separate ends of the VEGFR sequence. The digested products were analyzed with electrophoresis. As shown on Figure 4.3, abstracted plasmids (column 2) and original plasmids (column 5) have a similar size at 5-6 kb, which is about the size of the intact VEGFR plasmid (5,598 bp). The digested product showed a size around 2-3 kb (column 3 and 4), which is close to the size of VEGFR insert (2,790bp). The other part of this vector after endonuclease digestion was 2,808bp, similar to that of VEGFR insert, which is why only one thick band was present after digestion. These results proved that the VEGFR plasmid expansion using E.coli was successful.

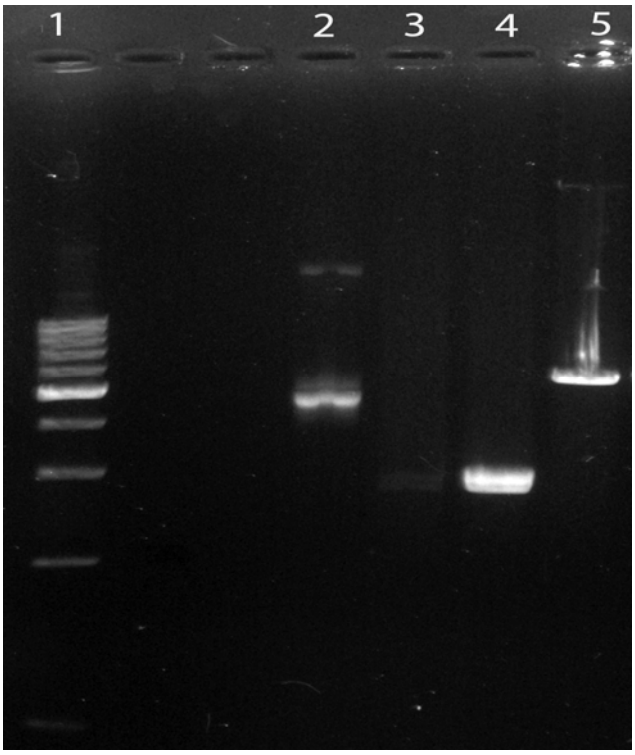

Figure 4.3 Electrophoresis of VEGFR plasmids after endonuclease digestion. (1) 1 kb DNA ladder (1-10kb); (2) Abstracted plasmids without endonuclease digestion; (3) Original VEGFR plasmids digested with endonuclease; (4) Abstracted plasmid digested with endonuclease; (5) Original VEGFR plasmid without endonuclease digestion

4.3.2 Synthesis of PLGA Microparticles Encapsulating VEGF, bFGF, or VEGFR plasmids

PLGA microparticles encapsulating VEGF, FGF, or VEGFR plasmids were synthesized using double-emulsion (water/oil/water) method. As shown in Figure 4.4, most of the synthesized PLGA microparticles are in spherical shape with a diameter of 50-100 μm. The particle surfaces were fairly smooth. From the cross section view, inside the particles there were multiple small pores, representing the spaces where the water-soluble growth factors or plasmids were encapsulated.

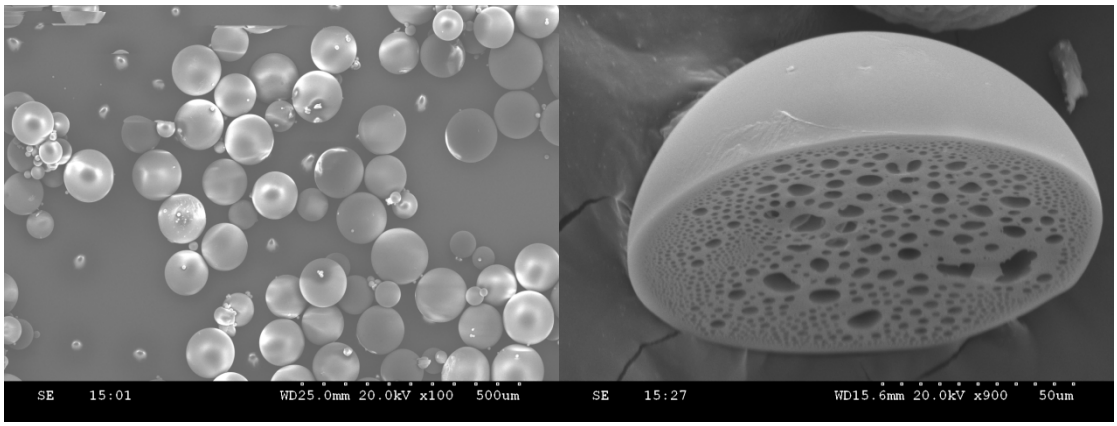

(a) (b)

Figure 4.4 SEM images of PLGA particles encapsulating VEGF, bFGF, or VEGFR plasmids. (a) top view; (b) cross-section view.

4.3.3 Characterization of Loading Efficiencies and Releasing Profiles of VEGF, bFGF, and VEGFR Plasmids

The loading efficiencies of VEGF, bFGF, and VEGFR plasmids in PLGA microparticles were approximately 68%, 61%, and 27%, respectively. The cumulative release curves of these factors were shown in Figure 4.5. Both VEGF and bFGF presented a slow release over 8 weeks, with a total release of 121 ng or 74 ng, respectively, that accounts for 33.5% and 20% of the total VEGF or bFGF loaded in the PLGA microparticles, respectively. Compared to the growth factors, VEGFR plasmids were released much more quickly. It showed a burst release within the first 12 hours, followed by a slower gradual release thereafter up to 2 weeks. After 2 weeks incubation, 713 ng VEGFR plasmids were released, representing 91.4% of the total plasmids loaded in the PLGA microparticles. Previous research showed that PLGA degrades in an erosion fashion [120]. The partial recovery of the growth factors and plasmids is possibly due to the long incubation time at 37 ºC, which might denature and degrade the biomolecules.

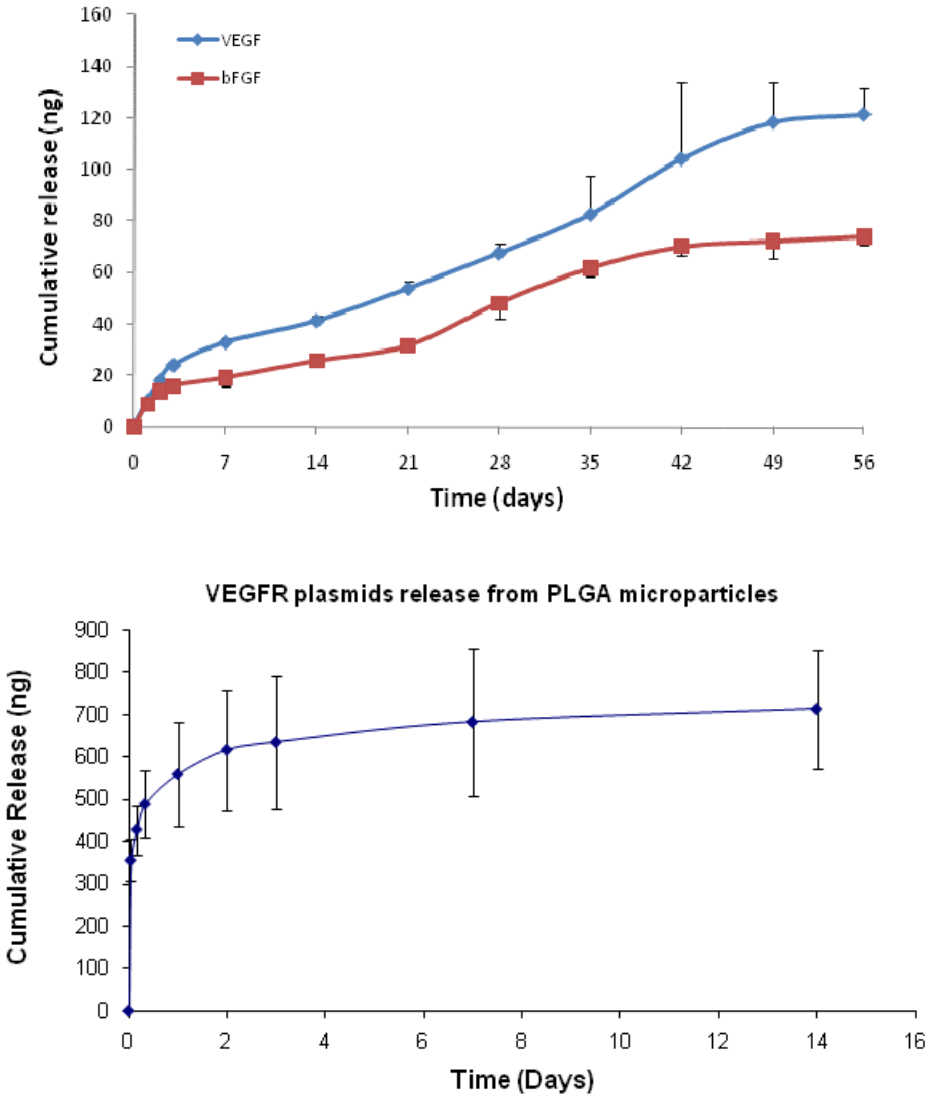

Figure 4.5 *In vitro* release of VEGF, bFGF, and VEGFR plasmid from PLGA microparticles at 37 ºC. (N=4 for VEGF or bFGF; N=3 for VEGFR plasmid)

4.3.4 Bioactivities of VEGF, bFGF, and VEGFR Plasmids Released from PLGA Microparticles

Using the released product of the PLGA microparticles, we tested their mitogenic effects on Pig Aorta Endothelial cells (PAE). We found the releasing media from PLGA microparticles encapsulating VEGF or FGF collected from 2 days to 3 weeks stimulated the PAE proliferation (Figure 4.6). An interesting finding was the releasing media from PLGA microparticles encapsulating VEGF, collected at earlier time points (days 2 and 3) showed

higher mitogenic effects than those collected at later time points (weeks 2 and 3). For all time points, cells exposed to the collected releasing media had significantly better cell proliferation than the controls. For PLGA microparticles encapsulating FGF, their releasing media collected at 3 weeks showed the same effect of stimulating PAE proliferation as that of the releasing media collected at earlier time (days 2 or 3).

By comparing the proliferation of cells exposed to the releasing media from PLGA microparticles with the cell proliferation of cells exposed to media with known concentrations of either VEGF or FGF, we are able to estimate the real concentration of the bioactive VEGF or FGF in the releasing media. As shown in Figure 4.6 and 4.7, the cell proliferation with addition of VEGF was as high as those with addition of 5 ng/ml VEGF. Since the releasing medium was added into the cell culture medium in 1:10 ratio, the bioactive VEGF released during 2 days to 3 weeks should be ~ 50 ng/ml. On the other hand, it is hard to estimate the concentration of bioactive FGF in the releasing medium, since FGF from 1 to 10 ng/ml stimulated a similar level of cell proliferation.

The fact that the estimated concentration of bioactive VEGF in the releasing media (50 ng/ml) was lower than that measured with ELISA (92 ng/ml at day 2) implied that the growth factors released from PLGA microparticles were partially deactivated. Nevertheless, after three weeks, the releasing media of PLGA microparticles containing VEGF or FGF all stimulated endothelial cell proliferation significantly, indicating that using PLGA microparticles for controlled release of growth factors is possible.

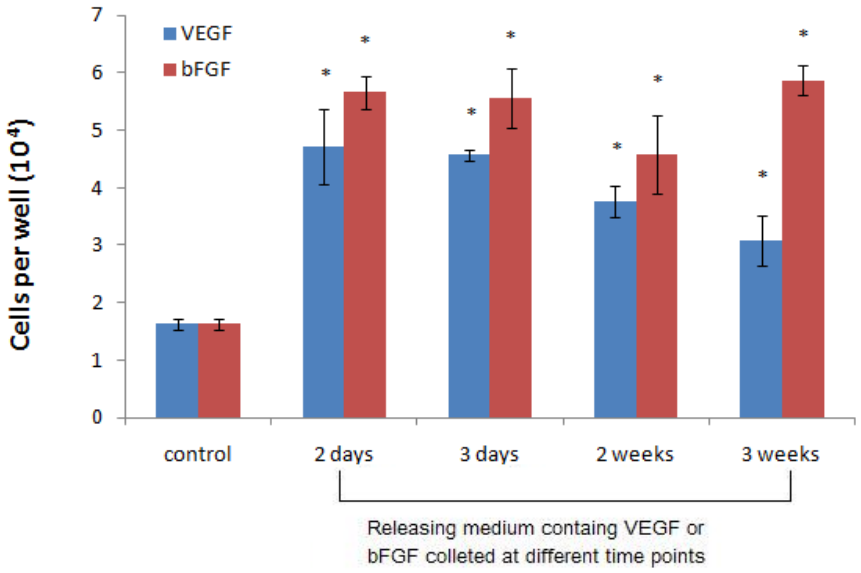

Figure 4.6 Mitogenic effects of VEGF or FGF released from PLGA microparticles at different time points on PAE cells (N=3 *: P<0.05 vs. control)

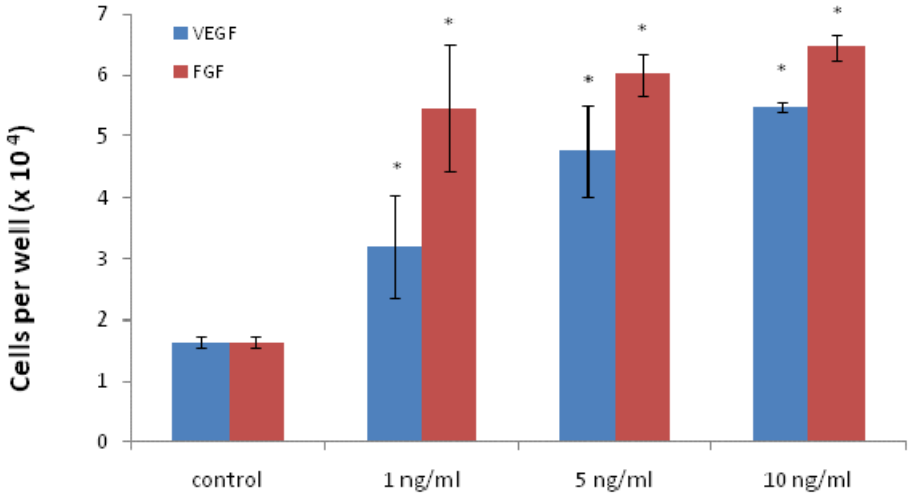

Figure 4.7 Mitogenic effects of VEGF or FGF of known concentrations on PAE cells. N=3, *: p<0.05 vs. control

To examine the functions of the released plasmids, the releasing media containing both VEGFR plasmids and GFP plasmids were used to transfect PAE cells. As shown in Figure 4.8,

part of the cells presented green color, an indication of a successful transfection of GFP plasmids. The transfection rate was about 20-30%. The successful transfection of PAE cells proved that VEGFR plasmids, which were encapsulated and released from PLGA microparticles, preserved their functionality.

sample 1 sample 2

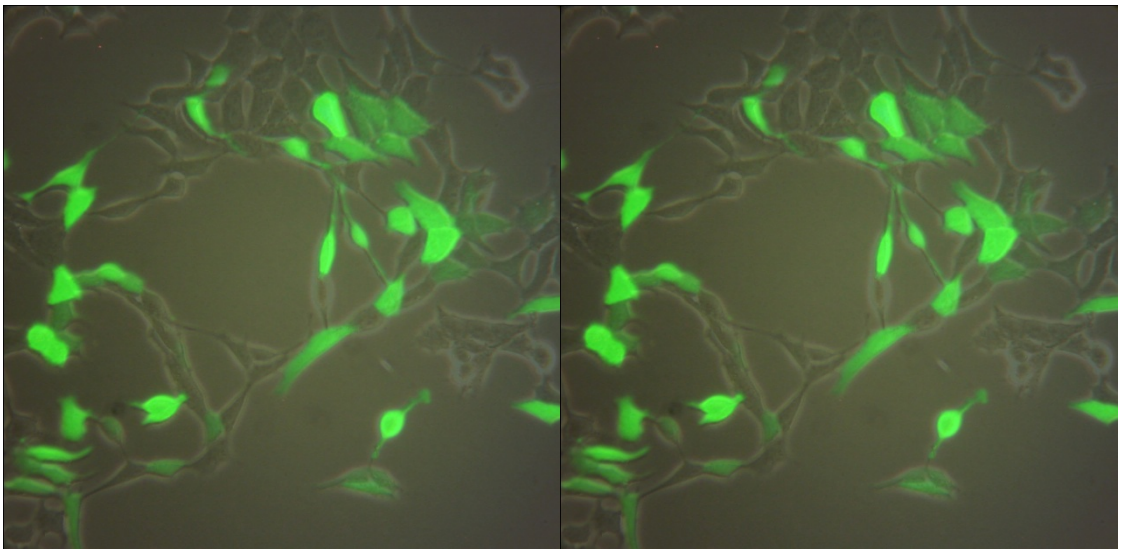

Figure 4.8 PAE cells transfected with KDR and GFP plasmids released from PLGA microparticles *in vitro*. The transfection efficiency is about 20 – 30 %.

4.3.5 Platelets Adhesion on POC

Materials contacting blood should not have adverse effects on blood components, including platelets, red blood cells, and leukocytes. In order to evaluate POC's potential application as a vascular implant material, we tested the platelet adhesion and activation, leukocyte activation, whole blood clotting time and hemolysis on POC. One of the major causes for the failure of blood contacting devices like vascular stents or synthetic vascular grafts is thrombus formation on the material surface [121, 122]. Adhesion and activation of platelets on the material surface is the first step to trigger the thrombotic cascades. In this study, LDH assay was used to quantify the platelets adhered to POC or PLLA (as control). In LDH assay, the absorbance at 490nm was used to measure the number of adhered platelets [123]. In this

study, we found POC and PLLA did not have significant differences in platelet adhesion on their surfaces, as shown in Figure 4.9.

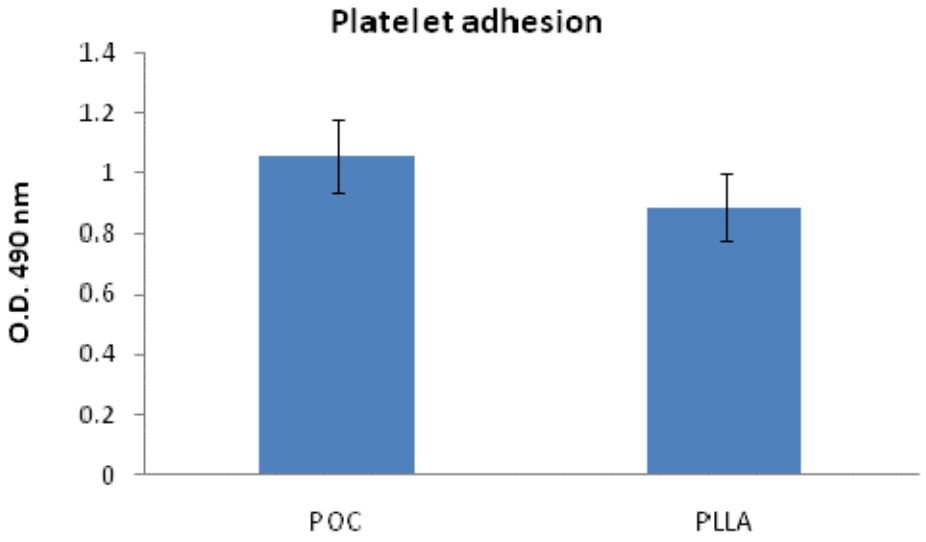

Figure 4.9 Platelet adhesion on POC or PLLA surface. (N=6)

SEM was used to observe the platelet adhesion on POC or PLLA substrates. As shown in Figure 4.10, platelets were found to adhere to both POC and PLLA surfaces. However, there was a distinct difference in the morphology of the adhered platelets. Platelets on POC were mostly round without cytoplasmic extensions (Figures 4.10 A and B). On the other hand, the majority of the platelets on PLLA were flattened with extensive pseudopodial processes (Figures 4.10 C and D), characteristics of the spread dendritic phase, a morphology which has been demonstrated as an indicator of platelet activation [124].

Platelets adhere to materials via either passive adhesion or active binding. Passive adhesion to material surfaces occur without consequent activation, while active binding is accompanied by morphological changes and release of various active pro-coagulant biomolecules [114]. Our results showed that though similar amounts of platelets were attached on POC or PLLA, fewer platelets were activated while attached on POC than on PLLA.

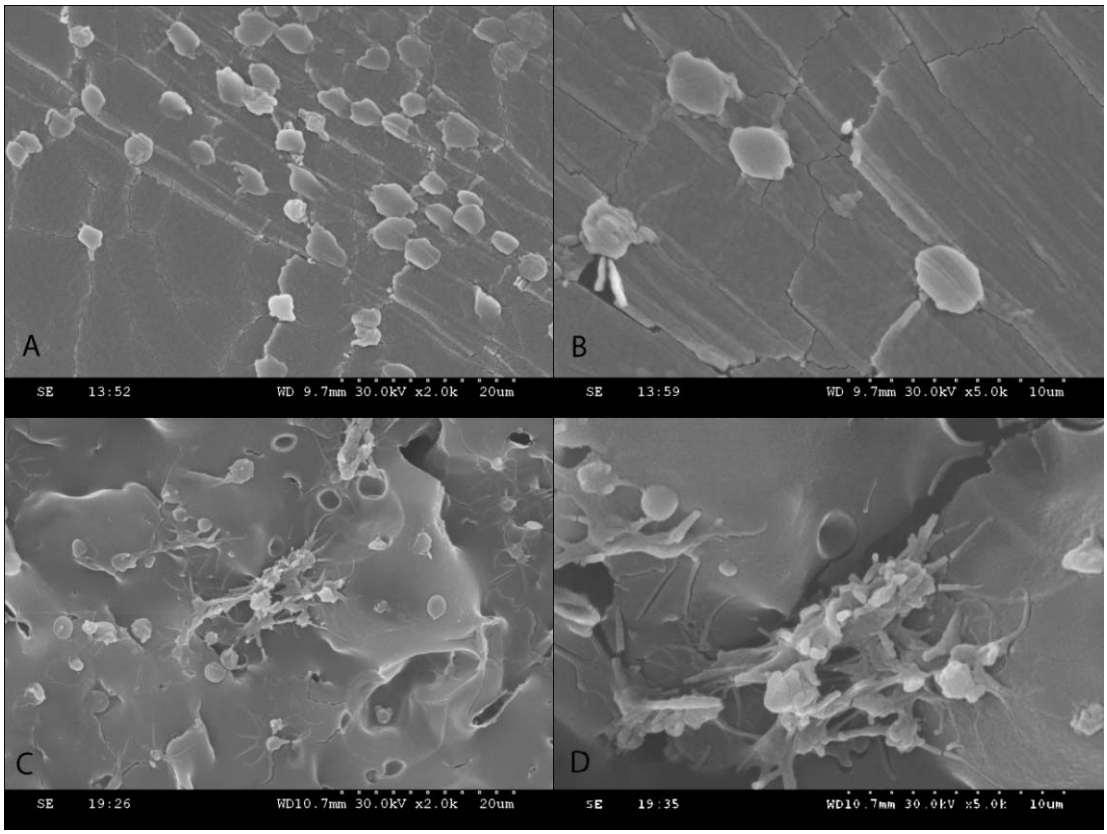

Figure 4.10 SEM images of platelet adhesion on POC (A, B) or PLLA (C, D).
A,C: 2000 x; B,D: 5000x magnification.

4.3.6 Platelets Activation on POC

Although platelets can be activated after adhesion on material surfaces, they may also be activated by not directly contacting materials [125, 126]. Therefore, the activation of the platelets which did not adhere to material surfaces should also be studied. P-selectin is a glycoprotein stored in cytosolic α-granules in resting platelets. Upon activation, the granules release their contents, and P-selectins are translocated to the platelet membrane where they mediate the platelet-platelet and platelet-leukocyte interactions [113, 114]. Since membrane-bound P-selectin is only expressed on activated platelets, it is used as a marker to evaluate the activation of platelets by materials [127, 128]. In this study, the degree of platelet activation was assessed using flow cytometry to measure the expression of P-selectin on activated platelets.

As shown in Figure 4.11, the platelets exposed to POC were much less activated than the platelets exposed to PLLA. The results after analysis revealed that only ~ 0.17% of platelets exposed to POC were activated, while with PLLA, much higher platelet activation was found (~ 0.75%), shown in Figure 4.12. Also, the fluorescence value of P-selectin on the activated platelets exposed to POC was less than those exposed to PLLA (961 vs. 1394). These results together with the SEM results (Figure 4.10) imply that POC is a better material than PLLA, triggering less platelet activation.

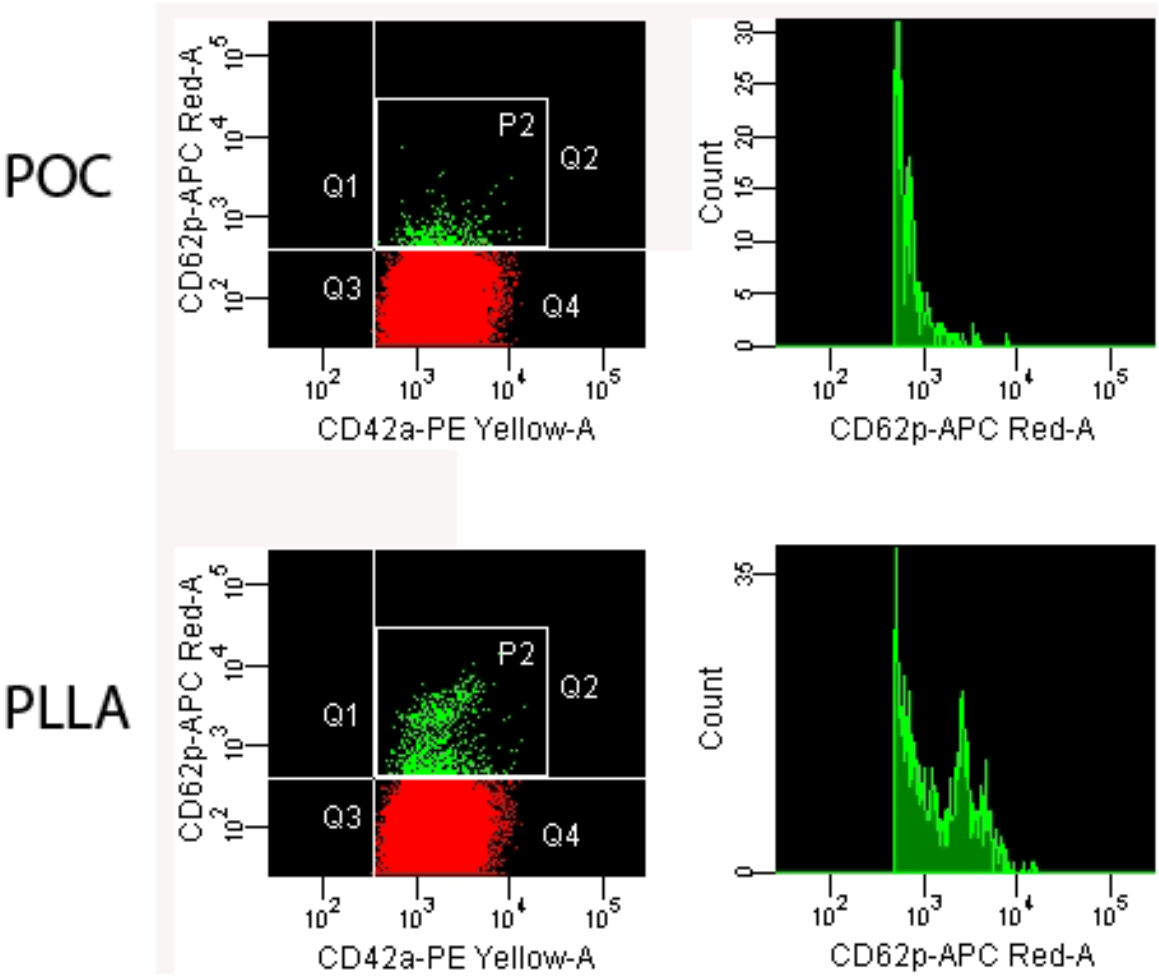

Figure 4.11 Flow cytometry analysis of the platelet activation exposed to POC or PLLA. CD42a: platelet maker; CD62p: activated platelet marker. Red dots were inactivated platelets having low value of CD62p. Green dots were activated platelets having high value of CD62p.

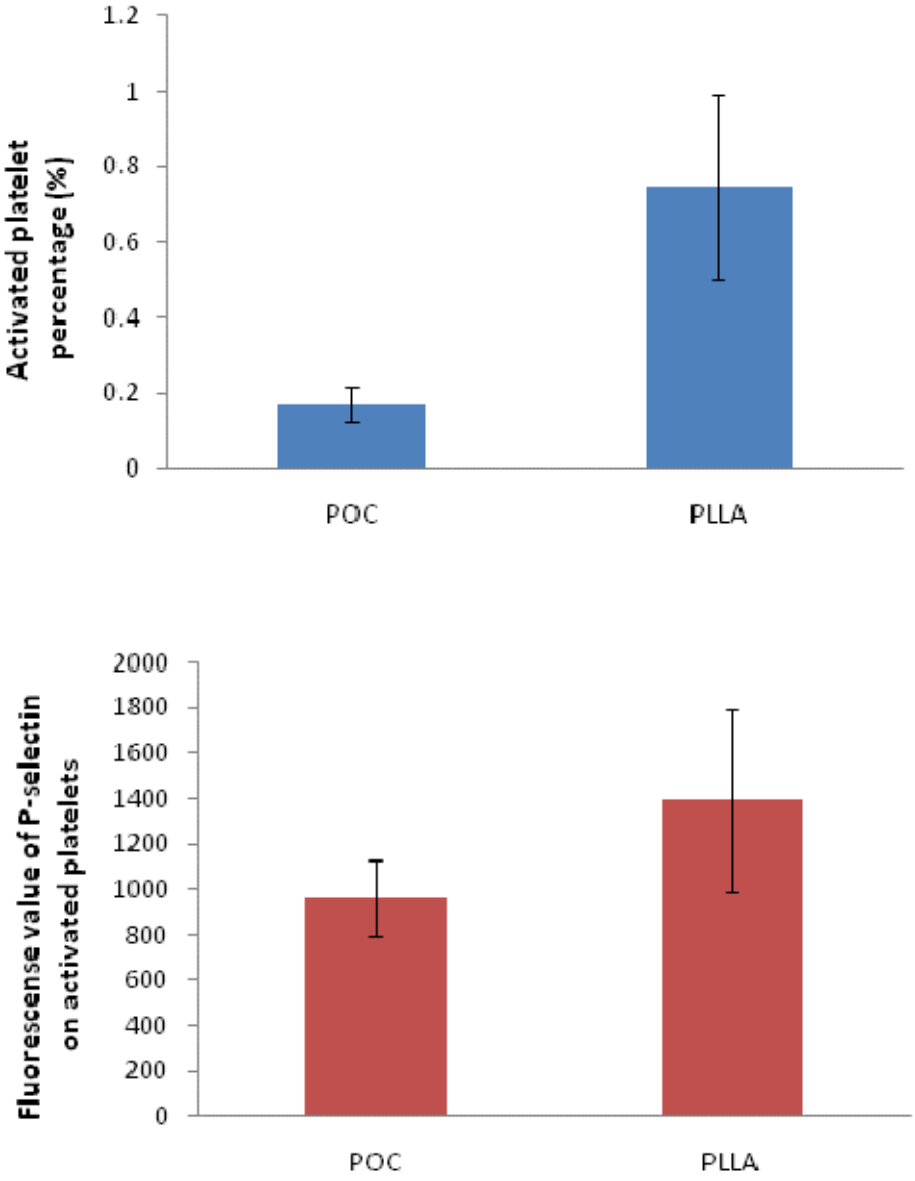

Figure 4.12 Platelets activation by POC or PLLA. Top: Percentage of activated platelets. Bottom: Average fluorescence value of P-selectin on activated platelets. (N=7)

4.3.7 Whole Blood Clotting on POC

Platelet adhesion and activation are the first steps in the blood clotting process, which involves the activation of a cascade of coagulation factors. Contact of blood with materials, for example glass, can activate the intrinsic pathway of coagulation [129]. The clotting process

takes minutes to hours depending on properties of the blood contacting materials. Therefore, measuring the rate of blood clotting enabled us to evaluate the tendency of the material to promote or resist the clot formation. The absorbance value of the hemoglobin measured at 540 nm was inversely correlated to the amount of blood clot formed, since only unclotted red blood cells were lysed in DI water and released their hemoglobins. In other words, lower the absorbance value, more complete the blood clots form. As shown in Figure 4.13, blood formed a clot quickly on glass; while on POC and PLLA, much slower blood clotting was found. No significant difference was found in blood clotting rate between POC and PLLA samples. At 60 minutes, complete blood clotting was found on all three groups. This result indicates that POC is similar to PLLA in resisting blood clot formation on their surfaces.

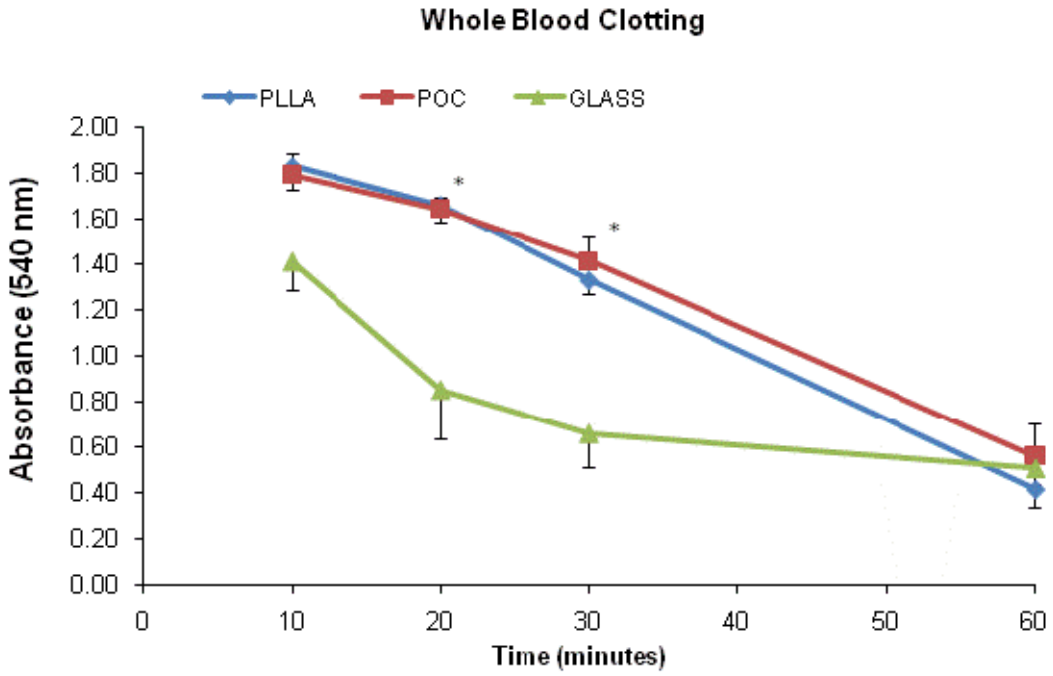

Figure 4.13 Blood clotting kinetics when re-calcified whole blood was exposed to POC, PLLA, or glass. (N=6, *: $p<0.05$ compared to glass at the same time point)

4.3.8 Hemolysis on POC

A hemolysis study was conducted to evaluate the potential of materials, such as POC, to damage red blood cells. The hemoglobin released by the damaged red blood cells was

measured photospectrometrically, and was used as an indicator of the polymer toxicity to the red blood cells [130]. The hemolysis of blood exposed to POC and PLLA was 0.5 ± 0.13 % or 0.27 ± 0.09 % (Mean ± SD), respectively, and no significant difference was found between them. Since the hemolysis level was low enough for both POC and PLLA, it is safe to say POC would not cause apparent hemolysis.

4.3.9 Leukocytes Activation on POC

Implanted biomaterials elicit an acute inflammatory response, leading to the attraction and interaction of inflammatory cells with the implant [131]. Activated leukocytes increase the expression of several distinct membrane protein receptors, which allow them to bind to platelets and endothelial cells during the inflammatory process [132]. CD11b macrophage-1 antigen is a membrane glycoprotein expressed on activated leukocytes, including lymphocytes, monocytes, granulocytes, and a subset of natural killer (NK) cells. CD11b functions in cell-cell and cell-substrate interactions, mediates inflammation by regulating leukocyte adhesion and migration, and plays an important role in immune responses such as phagocytosis, cell-mediated cytotoxicity, chemotaxis and cellular activation [133]. The expression of CD11b are generally used to determine leukocyte activation [134]. Similar to the study of platelet activation, the leukocyte activation was also evaluated using flow cytometry to measure the percentage of leukocytes expressing CD11b (Figure 4.14). As a result, we found both POC and PLLA triggered quite high percentages of leukocyte activation, 54% for POC and 43% for PLLA (Figure 4.15). However, no significant differences were found between them. The fluorescence value of CD11b on the activated leukocytes was also slightly higher when they were activated by POC than by PLLA, although their differences were not statistically significant ($p>0.05$).

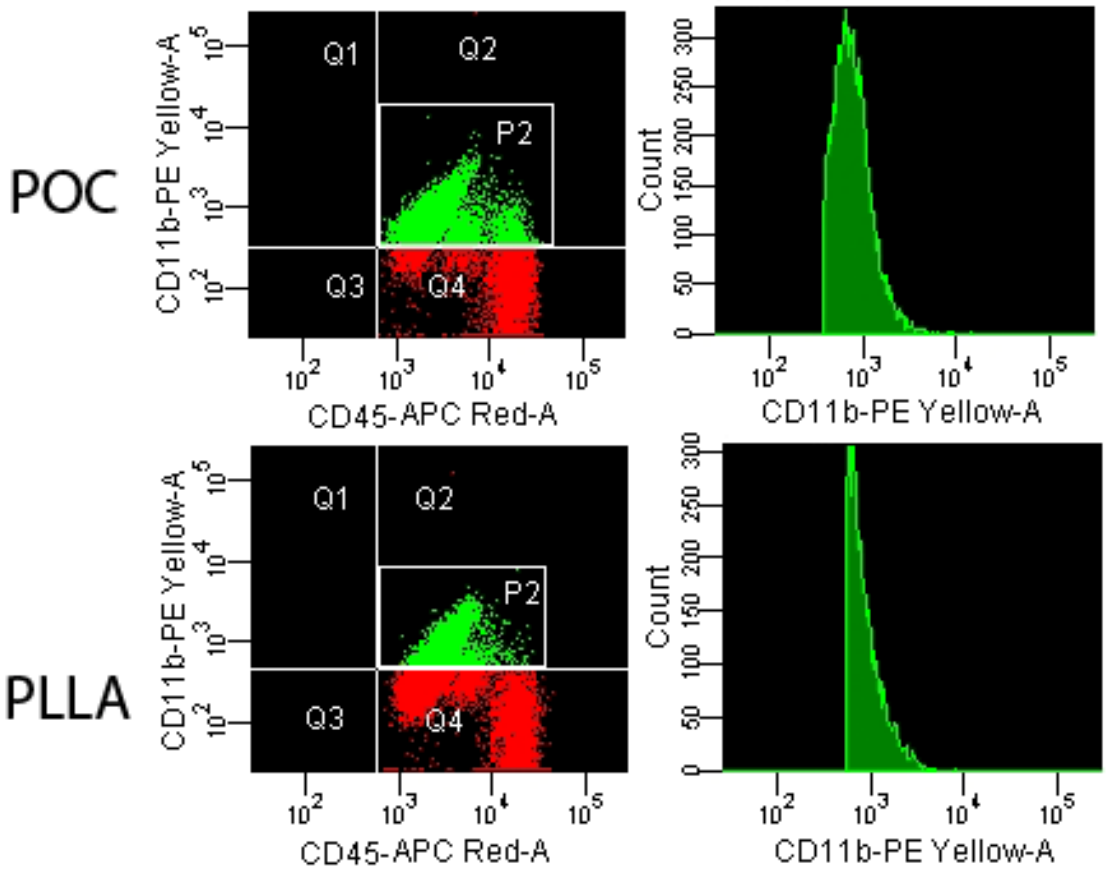

Figure 4.14 Flow cytometry analysis of the leukocyte activation exposed to POC or PLLA. CD45: leukocyte maker; CD11b: activated leukocyte marker. Red dots were inactivated leukocytes having low value of CD11b. Green dots were activated leukocytes having high value of CD11b.

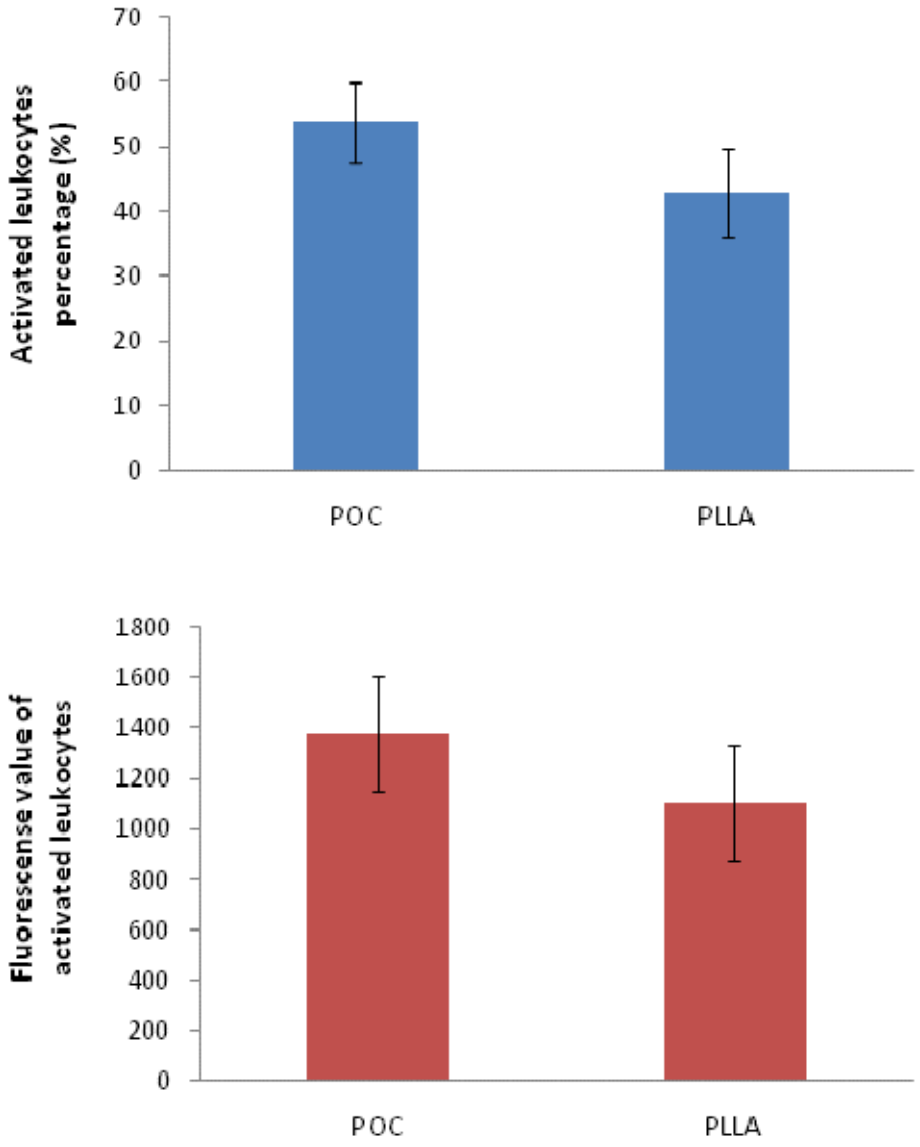

Figure 4.15 Leukocytes activation by POC or PLLA. Top: Percentage of activated leukocytes. Bottom: Average fluorescence value of CD11b on activated leukocytes. (N=9)

4.3.10 Inflammatory Cytokine release

The inflammatory responses of the leukocytes when they are exposed to materials can also be assessed by measuring the inflammatory cytokines that are released by these cells. Cytokines play important roles in inflammation: a higher cytokine concentration correlates to more intense inflammatory responses [135]. TNF-α and IL-1β are two well-known inflammatory

cytokines, which are also associated with the upregulation of complimentary system and play a critical role in inflammation. In the absence of exogenous stimuli, these cytokines are primarily released by activated monocytes and macrophages at low concentrations in the blood. Upon activation of the inflammatory cells, there is an increase in the release of these cytokines from the leukocytes. Release of cytokines can be induced by contact with exogenic materials. Therefore, it has been used to evaluate the hemocompatibility of biomaterials [111, 112, 136]. Using the cytometric bead array, we found blood cells exposed to POC released significantly lower amounts of both TNF-α and IL-1β compared to those exposed to PLLA (6.6 vs 11.8 pg/ml for IL-1β; 6 vs. 10.3 pg/ml for TNF-α) (Fig 4.16), indicating that POC is more biocompatible than PLLA, in terms of less inflammatory cytokine release.

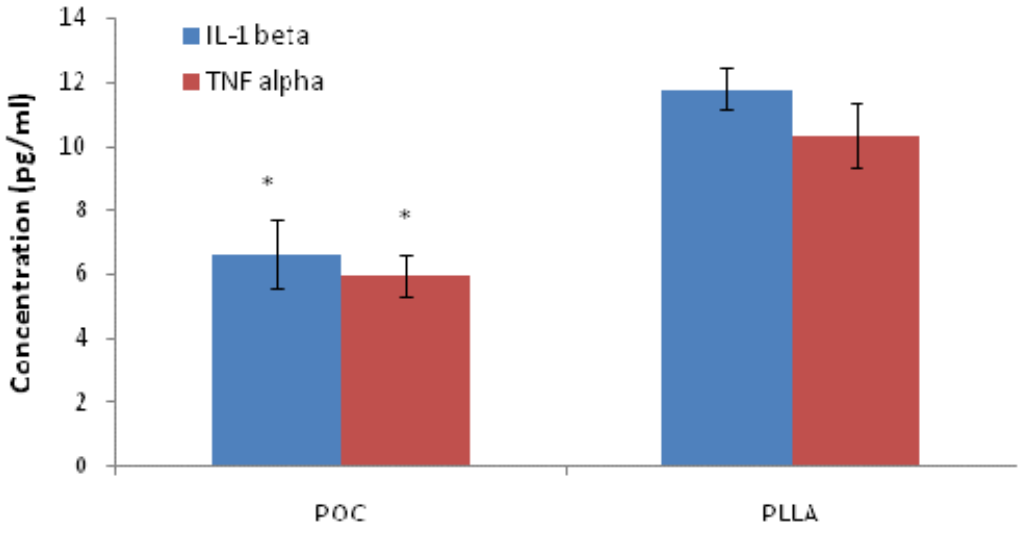

Figure 4.16 Inflammatory cytokine release from blood exposed to POC or PLLA. N=8. *: $p<0.05$ compared to PLLA

In summary, from the above hemocompatibility studies, we found POC is comparable to PLLA in resisting thrombosis. It had similar level of platelet adhesion, less platelet activation, and similar level of resistance to blot clotting compared to PLLA. However, POC triggers higher-level leukocytes activation than PLLA does, though interestingly, less released inflammatory

cytokines (TNF-α and IL-1β) by these cells were observed when they were exposed to POC. Also, POC causes only negligible hemolysis. Overall, it is safe to use POC as a blood contacting material for making vascular prostheses, according to results of these *in vitro* studies.

4.3.11 EPC isolation and characterization

EPCs were isolated from peripheral blood and cultured with complete EGM-2 Endothelial Cell Growth Medium. At day 3, only small numbers of cells were found attached on fibronectin-coated TCP sporadically (Figure 4.17A). After three weeks of cell culture, EPCs were completely confluent and presented the cobblestone-like morphology similar to normal ECs (Figure 4.17B). To character the EPCs, cells were fed with Dil-Ac-LDL (red color). The results showed that red color was found in all the cells, indicating Dil-Ac-LDL was uptaken by these cells (Figure 4.17C). Another EPC characterization method used was immunofluorescence staining of vWF. As shown in Figure 4.17D, the cells expressed vWF very well (green color). These results indicated that EPCs isolated from peripheral blood have good proliferation capacity, and can be induced to differentiate into functionally mature ECs with the use of EC-specific culture medium.

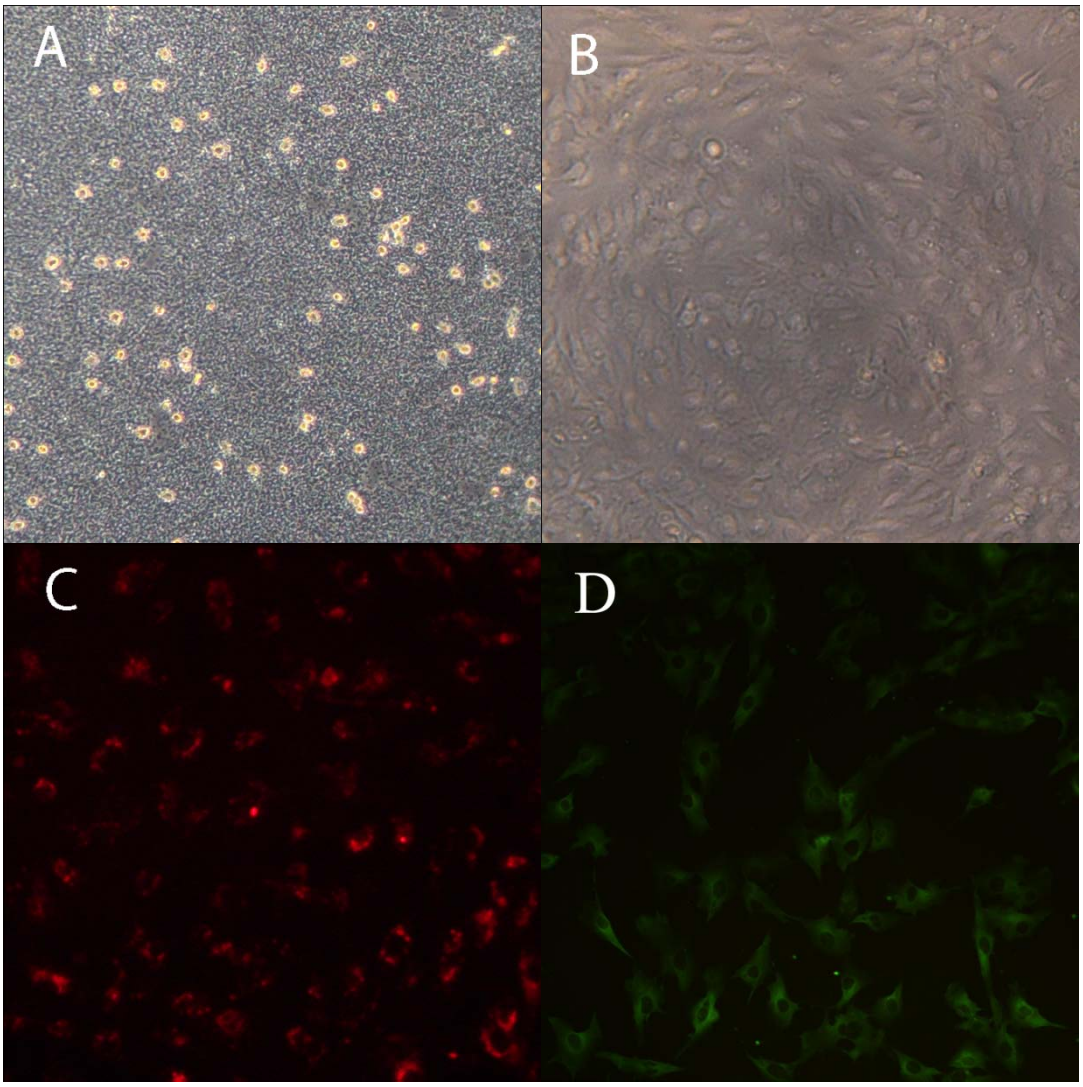

Figure 4.17 Phase contrast image of human EPC isolated from peripheral blood and cultured on fibronectin-coated tissue culture flasks for 3 days (A); or cultured for 3 weeks (B). Fluorescent images of EPC uptaken Dil-ac-LDL in red (C); and EPCs immunofluoresce stained against vWF in green (D)

4.3.12 EPC Capture on Surface-Modified POC under Shear Stress Influence

To immobilize EPC-capturing antibodies on the material surface, an intermediate layer (e.g., polysaccharide or ECM proteins) is normally coated first, on which the anti-CD34 antibodies are immobilized [137]. Besides working as the binding substrate for anti-EPC, this intermediate layer ideally should help EPC adhesion and proliferation. From our lab

experiences, we found fibronectin is the greast ECM protein showing best enhancement of endothelial cell adhesion and proliferation on poly(L-lactic acid) (PLLA) surfaces. Therefore, in this study, POC or PLLA films were first coated with fibronectin covalently via EDC, as described in previous chapters. Following that, anti-CD34 antibodies were bound to fibronectin, using the same method. This combination of anti-CD34 antibody and fibronectin coating provides an ideal substrate for EPC capturing, adhesion, and growth.

For the EPC capturing study, we invented an *in vitro* parallel flow system with continuous unidirectional flow (shown in Figure 4.2) by modifying the flow system developed previously [119]. In our trial experiments, we found the capture of EPCs at high shear stress (15 dyn/cm^2) was limited as the EPC number on the surface after high flow conditions was very low. Therefore, we started the flow at a low shear stress (4 dyn/cm^2) for 1 day, then gradually increased it to 8 dyn/cm^2 for 1 day, then increased to the desired shear stress of 15 dyn/cm^2 for 2 days. As shown in Figure 4.18 and 4.19, there were substantially more EPCs captured on anti-CD34 antibody-conjugated POC film than on PLLA at all time points, especially at day 2 and 4. EPCs grown on PLLA showed a decline in cell numbers, indicating the cells did not grow or started to die after capture on the surface. On the contrary, active cell adhesion/growth was found on POC during the 4 days flow exposure. The cells almost reached confluency after 4 days culture (Figure 4.18F). We also found that exposure of cells to low shear stress (4 dyn/cm^2) for 24 hours did not affect the cell alignments. At higher shear stress (8 and 15 dyn/cm^2), the cells showed very good alignments with the flow direction. The above results suggested that POC is a compatible material for EPC growth. After conjugated with anti-CD34 antibody and fibronectin, it is able to capture EPCs under flow conditions, and support the cell growth.

It is well known that shear stress, a friction force, is always applied on vascular ECs by the flowing flood, and ECs respond to shear stress by changing their morphology and functions. Multiple signal transduction pathways are activated by shear stress through varieties of

membrane mechanical sensors, including ion channels, G proteins, tyrosine kinase receptors, and cytoskeletons. ECs increase their production of growth factors, such as bFGF [138], platelet-derived growth factor (PDGF) [139], transforming growth factor-beta (TGF-β) [140], when exposed to shear stress. Shear stress also plays an important role in the EPC differentiation to mature endothelial cells [141, 142]. Adhesive proteins, such as integrins can also be activated by shear stress [143, 144], and that might be the reason for the enhanced EPC adhesion when they are exposed to shear stress observed in this study.

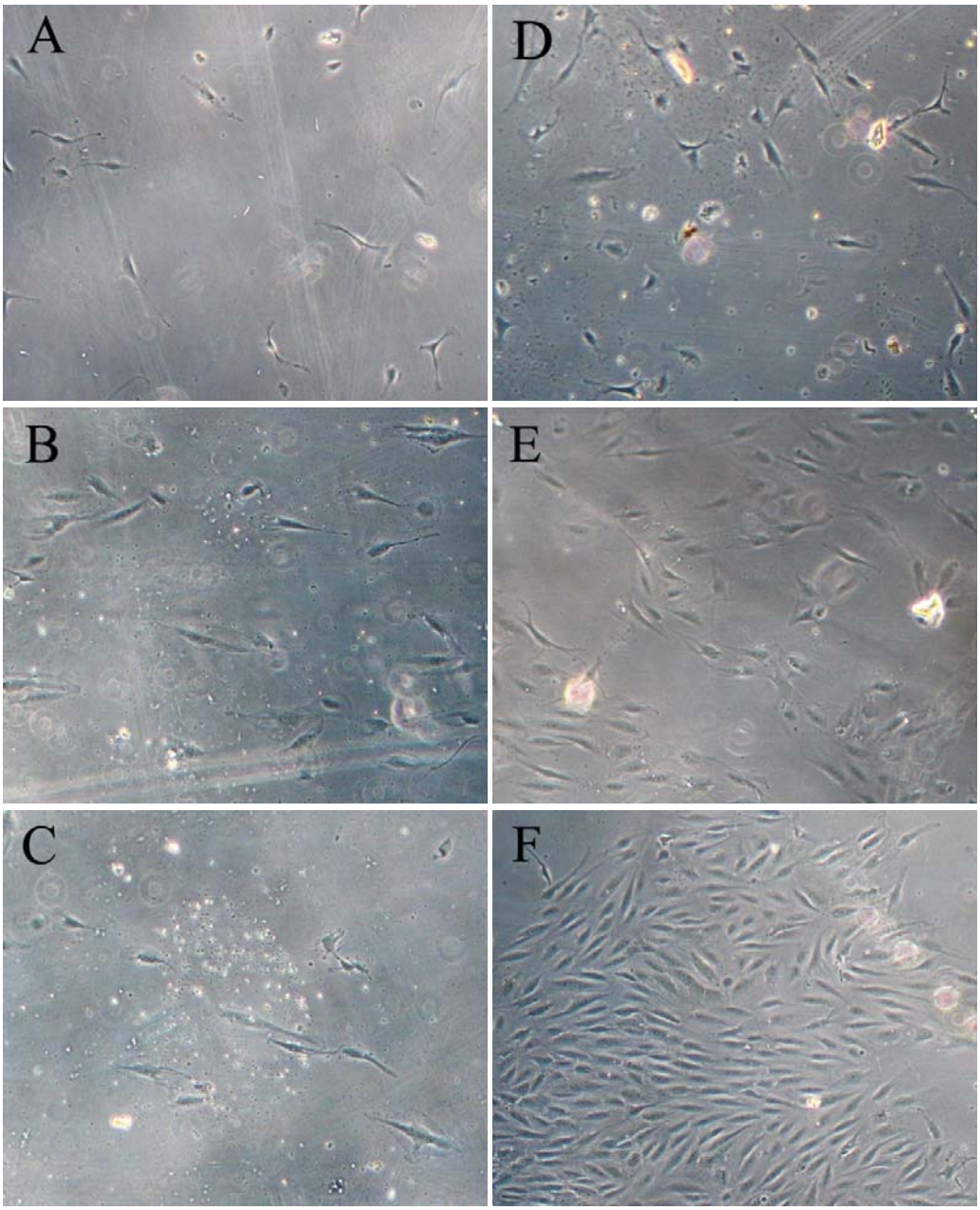

Figure 4.18 Human EPC capturing under continuous flow on surface-modified PLLA films for 1, 2, or 4 days (A-C); or on surface-modified POC films for 1, 2, or 4 days (D-F). Both PLLA and POC films were treated with fibronectin, followed by anti-CD34 antibody to aid the cell capturing.

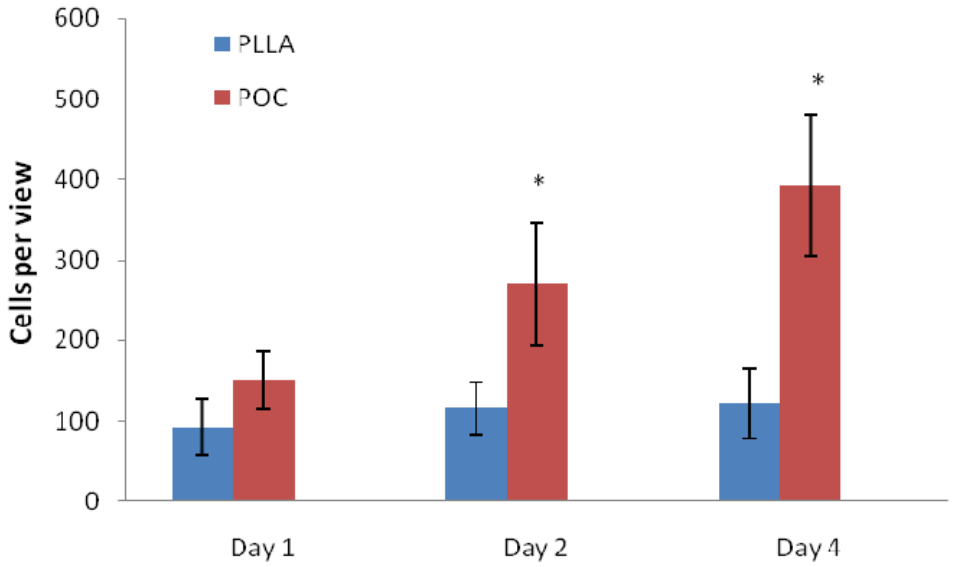

Figure 4.19 Number of EPCs per viewing field in 100x magnification. The EPCs were captured on POC modified PLLA or original PLLA films under continuous flow conditions.

4.3.13 EPC Proliferation on POC/PLGA Microparticle Compostite

Due to the difficult to prevent contamination during long-time cell culture in the flow system, we studied the effects of POC/PLGA microparticle composites, which encapsulate VEGF, FGF, and VEGFR/GFP plasmids on the EPC growth under static conditions. For this purpose, we compared EPC proliferation when the cells grew on PLLA, POC, and POC/PLGA microparticle composites. All the substrates were coated with fibronectin via EDC, and the cells were cultured on the films for up to 7 days. As shown in Figure 4.20, EPCs had rapid proliferation on POC, while they showed negligible cell proliferation on PLLA. When the PLGA microparticles encapsulating VEGF, FGF, and VEGFR/GFP plasmids were incorporated inside POC, a greater cell proliferation was observed, although significant cell proliferation was not shown until day 7. Therefore, it is reasonable to say that the enhanced EPC proliferation on POC/PLGA microparticle composites was due to the growth factors (VEGF and FGF) released from the particles. Different from our previous study which showed that releasing medium from PLGA microparticles at day 2 was able to stimulated EC growth (Figure 4.6), the mitogenic

effects of the PLGA microparticles seemed to be delayed when they were incorporated inside the POC polymer. It took 16 days for the growth factors to show their effects in increasing cell proliferation. This might be due to the 9 days of soaking POC/PLGA microparticle composites in DI water to remove the acidity before cell seeding. It also suggests that the growth factor release is much slower when the PLGA microparticles are embedded inside the POC. Regarding cell transfection, no EPC was found to be transfected by the VEGFR/GFP plasmids when grown on POC/PLGA microparticle composites. It might be that either the cells were not directly in contact with the PLGA microparticles so the plasmid could not get into the cells for transfection, or the plasmids uptaken by the cells were lower than the required amount for an effective transfection.

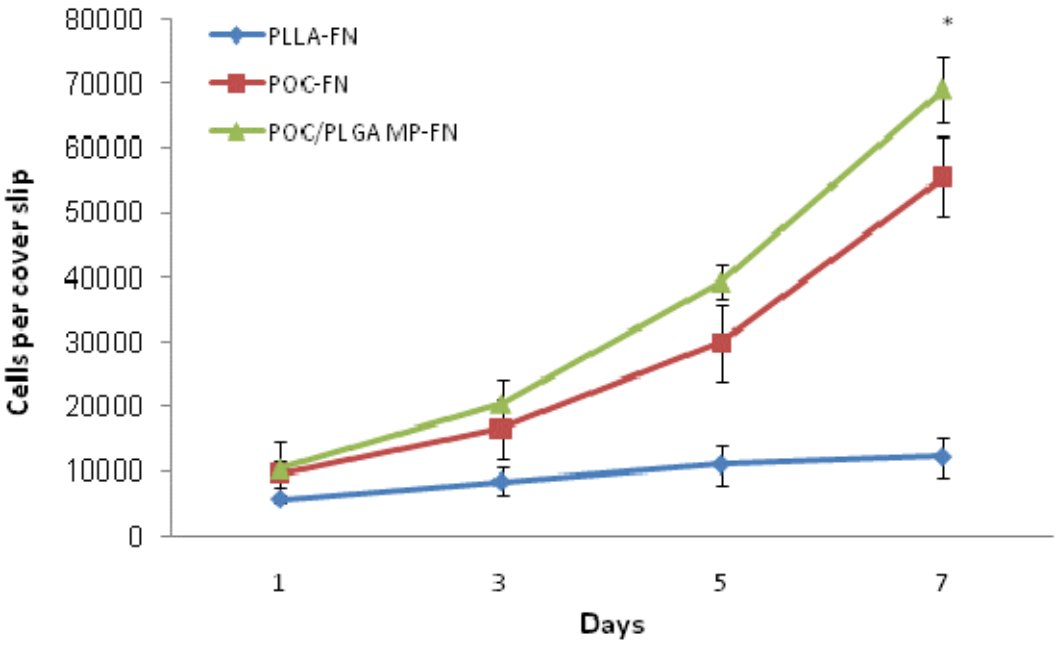

Figure 4.20 EPC proliferation on PLLA, POC, or POC/PLGA microparticles composites (POC/PLGA MP) films. Fibronectin (FN) was conjugated on all the film surfaces. N=4, *: $p<0.05$ compared to POC-FN at day 7.

4.4 Conclusion

The surface modification of PLLA using POC/PLGA microparticle composites coating, followed by fibronectin and anti-CD 34 antibody conjugations successfully captured EPCs under flowing conditions at physiological shear stress. The captured EPCs proliferate actively on the substrates and quick endothlialization was found on the POC/PLGA microparticle composites surface. The higher cell proliferation is possibly attributed from the controlled release of the growth factors from the PLGA microparticles.

CHAPTER 5

CONCLLUSION AND LIMITATIONS

The overall goal of this study was to develop a surface modification technique to enhance the endothelialization on materials, which have good physical and chemical properties to be used for vascular grafts or stents, but lack of affinities for endothelial cells. We started with plasma deposition of PVAA, which carries abundant –COOH groups on its surface. The PVAA depostion showed good effects in enhancing the endothelial cell attaching and growth on material surface. By modify material surface with PVAA, it not only lowers the hydrophobiciy of the polymers, the rich –COOH functional groups also allows conjugation with ECM proteins. After conjugation with fibronectin and VEGF, enhanced endothlelization was found on PLLA. Lastly, autoseeding of EPC was tested. By coating PLLA with POC/PLGA microparticle composite and anti-CD34 antibodies, the EPC in the flowing medium were captured onto PLLA surface, and underwent quick proliferation probably due to influence of the growth factors that were encapsulated and released from the PLGA microparticles. The success of this research provides us a viable technique for modifying the surfaces of materials used in blood-contacting vascular prosthese.

There are a few limitations in this study. First, we found the EPCs can not be captured on anti-CD34 bound materials if the flow shear stress is high (15 dyn/cm^2). Thus a low shear stress (4 dyn/cm^2) was used initially, then the shear stress was gradually increased to a higher level. This might be a problem if a surface-modified vascular graft is implanted into an artery with high blood flow rate. In addition considering the far more complicated situation in vivo, a lot of factors which may favor the EPC capturing cannot be provided via i*n vitro* conditions that were used to capture EPC in this research. An *in vivo* study will give us clearer answers. Another limitation is the acidicity of POC. It needs 7 to 9 days of soaking in DI water to remove

the acidicity before it can be used for cell seeding. The acidicty might came from the incomplete post-polymerization at low temperature which was conducted at freeze-dryer in this study. A longer time post-polymerization of POC or at a higher temperature (not high enough to denature the growth factors) might overcome this problem. Finally, our results show that there was no transfection of the EPC with plasmids delivered from the PLGA microparticles when EPCs were captured onto modified POC/PLGA microparticle composite. It suggests that the no plasmid or not enough plasmids were uptaken by the cells in this condition. A direct contact of the cells to the microparticels which deliver plasmids might enhance the plasmids uptake by the cells, and make the transfection possible.

APPENDIX A

ABBREIVATIONS

ACD	Acid citrate dextrose
APC	Allophycocyanin
AFM	Atomic force microscopy
CABG	Coronary artery bypass graft
CVD	Cardiovascuular Disease
CDC	Centers for Disease Control
CHD	Coronary Heart Disease
DES	Drug eluting stent
DiI-Ac-LDL	1,1′-dioctadecyl-3,3,3′,3′-tetramethylindocarbocyanine perchlorate-acetylated-low density lipoprotein
EC	Endothelial cell
ECM	Extracellular matrix
EDC	1-[3-(Dimethylamino) propyl]-3-ethylcarbodiimide
ELISA	Enzyme-Linked ImmunoSorbent Assay
EPC	Endothelial progenitor cell
FBS	Fetal bovine serum
FDA	Food and Drug Administration
FGF	Fibroblast growth factor
FITC	Fluorescein isothiocyanate
FN	Fibronectin
FTIR	Fourier transform spectroscopy
LDH	Lactate dehydrogenase
MES	2-(N-Morpholino)ethanesulfonic acid
HAEC	Human aorta endothelial cell
IL-1β	Interlukin-1β
KDR	Kinase insert domain receptor

LDL	Low density lipoprotein
PBS	Phosphate buffered saline
PAE	Pig aorta endothelial
PE	Phycoerythrin
PET	Polyethylene terephthalate
PLGA	Poly(lactic-*co*-glycolic acid)
PLLA	Poly(L-lactic acid)
POC	Poly(1,8-octanediol-*co*-citrate)
PPP	Platelet-poor plasma
PRP	Platelet-rich plasma
PTFE	Polytetrafluoroethylene
PU	Polyurethane
PVAA	Poly(vinylacetic acid)
RFGD	Radiofrequency glow discharge
TCP	Tissue culture plate
TNF-α	Tumor necrosis factor-α
VAA	Vinylacetic acid
VCAM-1	Vascular cell adhesion molecule
VEGF	Vascular endothelial growth factor
VEGFR	Vascular endothelial growth factor receptor
VSMC	Vascular smooth muscle cell
vWF	von Willbrand Factor
XPS	X-ray photoelectron spectroscopy

REFERENCES

1. Lloyd-Jones, D., et al., *Heart disease and stroke statistics--2010 update: a report from the American Heart Association.* Circulation. **121**(7): p. e46-e215.
2. Leitinger, N., *Oxidized phospholipids as modulators of inflammation in atherosclerosis.* Curr Opin Lipidol, 2003. **14**(5): p. 421-30.
3. Hansson, G.K., *Inflammation, atherosclerosis, and coronary artery disease.* N Engl J Med, 2005. **352**(16): p. 1685-95.
4. Garcia de Tena, J., *Inflammation, atherosclerosis, and coronary artery disease.* N Engl J Med, 2005. **353**(4): p. 429-30; author reply 429-30.
5. Ravi, S., Z. Qu, and E.L. Chaikof, *Polymeric materials for tissue engineering of arterial substitutes.* Vascular, 2009. **17 Suppl 1**: p. S45-54.
6. Chlupac, J., E. Filova, and L. Bacakova, *Blood vessel replacement: 50 years of development and tissue engineering paradigms in vascular surgery.* Physiol Res, 2009. **58 Suppl 2**: p. S119-39.
7. Rose, B. and C.J. Pepine, *Restenosis following coronary artery angioplasty: patterns, recognition, and results of repeat angioplasty.* Cardiovasc Clin, 1988. **19**(2): p. 233-51.
8. Fischman, D.L., et al., *A randomized comparison of coronary-stent placement and balloon angioplasty in the treatment of coronary artery disease. Stent Restenosis Study Investigators.* N Engl J Med, 1994. **331**(8): p. 496-501.
9. Garcia-Garcia, H.M., et al., *Drug-eluting stents.* Arch Cardiol Mex, 2006. **76**(3): p. 297-319.
10. Daemen, J., et al., *Early and late coronary stent thrombosis of sirolimus-eluting and paclitaxel-eluting stents in routine clinical practice: data from a large two-institutional cohort study.* Lancet, 2007. **369**(9562): p. 667-78.

11. Joner, M., et al., *Pathology of drug-eluting stents in humans: delayed healing and late thrombotic risk.* J Am Coll Cardiol, 2006. **48**(1): p. 193-202.

12. Lagerqvist, B., et al., *Long-term outcomes with drug-eluting stents versus bare-metal stents in Sweden.* N Engl J Med, 2007. **356**(10): p. 1009-19.

13. Stone, G.W., et al., *Safety and efficacy of sirolimus- and paclitaxel-eluting coronary stents.* N Engl J Med, 2007. **356**(10): p. 998-1008.

14. Kotani, J., et al., *Incomplete neointimal coverage of sirolimus-eluting stents: angioscopic findings.* J Am Coll Cardiol, 2006. **47**(10): p. 2108-11.

15. Woodhouse, K.A., J.I. Weitz, and J.L. Brash, *Lysis of surface-localized fibrin clots by adsorbed plasminogen in the presence of tissue plasminogen activator.* Biomaterials, 1996. **17**(1): p. 75-7.

16. Esmon, C.T., *The roles of protein C and thrombomodulin in the regulation of blood coagulation.* J Biol Chem, 1989. **264**(9): p. 4743-6.

17. Ajani, A.E., et al., *Late thrombosis: a problem solved?* J Interv Cardiol, 2003. **16**(1): p. 9-13.

18. Mao, X., et al., *Enhanced human bone marrow stromal cell affinity for modified poly(L-lactide) surfaces by the upregulation of adhesion molecular genes.* Biomaterials, 2009. **30**(36): p. 6903-11.

19. Bear, M.M., et al., *Polystereoisomers of 2-butyl and 3,3-dimethyl-2-butyl malic acid esters: configurational structures/properties relationship.* Polymer, 2000. **41**(10): p. 3705-3712.

20. He, B., J.Z. Bei, and S.G. Wang, *Synthesis and characterization of a functionalized biodegradable copolymer: poly((L)-lactide-co-RS-beta-malic acid).* Polymer, 2003. **44**(4): p. 989-994.

21. Cai, Q., et al., *A novel porous cells scaffold made of polylactide-dextran blend by combining phase-separation and particle-leaching techniques.* Biomaterials, 2002. **23**(23): p. 4483-92.

22. Woo, K.M., et al., *Suppression of apoptosis by enhanced protein adsorption on polymer/hydroxyapatite composite scaffolds.* Biomaterials, 2007. **28**(16): p. 2622-30.

23. Qu, X., A. Wirsen, and A.C. Albertsson, *Synthesis and characterization of pH-sensitive hydrogels based on chitosan and D,L-lactic acid.* Journal of Applied Polymer Science, 1999. **74**(13): p. 3193-3202.

24. Perego, G., et al., *Functionalization of poly-(L-lactic-co-epsilon-caprolactone): effects of surface modification on endothelial cell proliferation and hemocompatibility [corrected].* J Biomater Sci Polym Ed, 2003. **14**(10): p. 1057-75.

25. Bamford, C.H. and K.G. Allamee, *Studies in Polymer Surface Functionalization and Grafting for Biomedical and Other Applications.* Polymer, 1994. **35**(13): p. 2844-2852.

26. Fang, Y.E., et al., *Study of radiation-induced graft copolymerization of vinyl acetate onto ethylene-co-propylene rubber.* Journal of Applied Polymer Science, 1996. **62**(13): p. 2209-2213.

27. Bearinger, J.P., D.G. Castner, and K.E. Healy, *Biomolecular modification of p(AAm-co-EG/AA) IPNs supports osteoblast adhesion and phenotypic expression.* J Biomater Sci Polym Ed, 1998. **9**(7): p. 629-52.

28. Liu, Y., et al., *Layer-by-layer assembly of biomacromolecules on poly(ethylene terephthalate) films and fiber fabrics to promote endothelial cell growth.* J Biomed Mater Res A, 2007. **81**(3): p. 692-704.

29. Calderon, J.G. and R.B. Timmons, *Surface molecular tailoring via pulsed plasma-generated acryloyl chloride polymers: Synthesis and reactivity.* Macromolecules, 1998. **31**(10): p. 3216-3224.

30. Wan, Y., et al., *Cell adhesion on gaseous plasma modified poly-(L-lactide) surface under shear stress field.* Biomaterials, 2003. **24**(21): p. 3757-64.

31. Gumpenberger, T., et al., *Adhesion and proliferation of human endothelial cells on photochemically modified polytetrafluoroethylene.* Biomaterials, 2003. **24**(28): p. 5139-44.

32. Lakard, S., et al., *Adhesion and proliferation of cells on new polymers modified biomaterials.* Bioelectrochemistry, 2004. **62**(1): p. 19-27.

33. Mitchell, S.A., et al., *Isopropyl alcohol plasma modification of polystyrene surfaces to influence cell attachment behavior.* Surface science, 2004. **561**: p. 110-120.

34. France, R.M., et al., *Plasma copolymerization of allyl alcohol/1,7-octadiene: surface characterization and attachment of human keratinocytes.* Chem Mater, 1998. **10**: p. 1176-83.

35. Zhang, Z., et al., *Surface plasmon resonance studies of protein binding on plasma polymerized di(ethylene glycol) monovinyl ether films.* Langmuir, 2003. **19**: p. 4765-70.

36. Ziegelaar, B.W., et al., *The modulation of corneal keratocyte and epithelial cell responses to poly(2-hydroxyethyl methacrylate) hydrogel surfaces: phosphorylation decreases collagenase production in vitro.* Biomaterials, 1999. **20**(21): p. 1979-88.

37. El Khadali, F., et al., *Modulating fibroblast cell proliferation with functionalized poly(methyl methacrylate) based copolymers: chemical composition and monomer distribution effect.* Biomacromolecules, 2002. **3**(1): p. 51-6.

38. Haddow, D.B., et al., *Comparison of proliferation and growth of human keratinocytes on plasma copolymers of acrylic acid/1,7-octadiene and self-assembled monolayers.* J Biomed Mater Res, 1999. **47**(3): p. 379-87.

39. Gupta, B., et al., *Plasma-induced graft polymerization of acrylic acid onto poly(ethylene terephthalate) films: characterization and human smooth muscle cell growth on grafted films.* Biomaterials, 2002. **23**(3): p. 863-71.

40. Bisson, I., et al., *Acrylic acid grafting and collagen immobilization on poly(ethylene terephthalate) surfaces for adherence and growth of human bladder smooth muscle cells.* Biomaterials, 2002. **23**(15): p. 3149-58.

41. Elliott, J.T., et al., *The effect of surface chemistry on the formation of thin films of native fibrillar collagen.* Biomaterials, 2007. **28**(4): p. 576-85.

42. Barbosa, J.N., M.A. Barbosa, and A.P. Aguas, *Adhesion of human leukocytes to biomaterials: An in vitro study using alkanethiolate monolayers with different chemically functionalized surfaces.* J Biomed mater Res, 2003. **65A**: p. 429-34.

43. Arima, Y. and H. Iwata, *Effect of wettability and surface functional groups on protein adsorption and cell adhesion using well-defined mixed self-assembled monolayers.* Biomaterials, 2007. **28**(20): p. 3074-82.

44. LaDisa, J.F., Jr., et al., *Stent implantation alters coronary artery hemodynamics and wall shear stress during maximal vasodilation.* J Appl Physiol, 2002. **93**(6): p. 1939-46.

45. Nelken, N. and P.A. Schneider, *Advances in stent technology and drug-eluting stents.* Surg Clin North Am, 2004. **84**(5): p. 1203-36, v.

46. Lam, K.H., et al., *Reinforced poly(L-lactic acid) fibres as suture material.* J Appl Biomater, 1995. **6**(3): p. 191-7.

47. Harada, K. and S. Enomoto, *Stability after surgical correction of mandibular prognathism using the sagittal split ramus osteotomy and fixation with poly-L-lactic acid (PLLA) screws.* J Oral Maxillofac Surg, 1997. **55**(5): p. 464-8; discussion 468-9.

48. Matsusue, Y., et al., *In vitro and in vivo studies on bioabsorbable ultra-high-strength poly(L-lactide) rods.* J Biomed Mater Res, 1992. **26**(12): p. 1553-67.

49. Partio, E.K., et al., *Talocrural arthrodesis with absorbable screws, 12 cases followed for 1 year.* Acta Orthop Scand, 1992. **63**(2): p. 170-2.

50. Tamai, H., et al., *Initial and 6-month results of biodegradable poly-l-lactic acid coronary stents in humans.* Circulation, 2000. **102**(4): p. 399-404.

51. Ormiston, J.A., et al., *A bioabsorbable everolimus-eluting coronary stent system for patients with single de-novo coronary artery lesions (ABSORB): a prospective open-label trial.* Lancet, 2008. **371**(9616): p. 899-907.

52. Liu, X. and P.X. Ma, *The nanofibrous architecture of poly(L-lactic acid)-based functional copolymers.* Biomaterials, 2010. **31**(2): p. 259-69.

53. Mosquera, D.A. and M. Goldman, *Endothelial cell seeding.* Br J Surg, 1991. **78**(6): p. 656-60.

54. Gulati, R., et al., *Diverse origin and function of cells with endothelial phenotype obtained from adult human blood.* Circ Res, 2003. **93**(11): p. 1023-5.

55. Heeschen, C., et al., *Profoundly reduced neovascularization capacity of bone marrow mononuclear cells derived from patients with chronic ischemic heart disease.* Circulation, 2004. **109**(13): p. 1615-22.

56. Murohara, T., et al., *Transplanted cord blood-derived endothelial precursor cells augment postnatal neovascularization.* The Journal of clinical investigation, 2000. **105**: p. 1527-36.

57. He, T., et al., *Transplantation of circulating endothelial progenitor cells restores endothelial function of denuded rabbit carotid arteries.* Stroke, 2004. **35**(10): p. 2378-84.

58. Schatteman, G.C., M. Dunnwald, and C. Jiao, *Biology of bone marrow-derived endothelial cell precursors.* Am J Physiol Heart Circ Physiol, 2007. **292**(1): p. H1-18.

59. Rohde, E., et al., *Blood monocytes mimic endothelial progenitor cells.* Stem Cells, 2006. **24**(2): p. 357-67.

60. Harraz, M., et al., *CD34- blood-derived human endothelial cell progenitors.* Stem Cells, 2001. **19**(4): p. 304-12.

61. Ferrari, N., et al., *Bone marrow-derived, endothelial progenitor-like cells as angiogenesis-selective gene-targeting vectors.* Gene Ther, 2003. **10**(8): p. 647-56.

62. Peichev, M., et al., *Expression of VEGFR-2 and AC133 by circulating human CD34(+) cells identifies a population of functional endothelial precursors.* Blood, 2000. **95**(3): p. 952-8.

63. Shirota, T., H. Yasui, and T. Matsuda, *Intralumenal tissue-engineered therapeutic stent using endothelial progenitor cell-inoculated hybrid tissue and in vitro performance.* Tissue Eng, 2003. **9**(3): p. 473-85.

64. Shirota, T., et al., *Fabrication of endothelial progenitor cell (EPC)-seeded intravascular stent devices and in vitro endothelialization on hybrid vascular tissue.* Biomaterials, 2003. **24**(13): p. 2295-302.

65. Bhattacharya, V., et al., *Enhanced endothelialization and microvessel formation in polyester grafts seeded with CD34(+) bone marrow cells.* Blood, 2000. **95**(2): p. 581-5.

66. Schmidt, D., et al., *Umbilical cord blood derived endothelial progenitor cells for tissue engineering of vascular grafts.* Ann Thorac Surg, 2004. **78**(6): p. 2094-8.

67. Schmidt, D., et al., *Living patches engineered from human umbilical cord derived fibroblasts and endothelial progenitor cells.* Eur J Cardiothorac Surg, 2005. **27**(5): p. 795-800.

68. Conklin, B.S., et al., *Basic fibroblast growth factor coating and endothelial cell seeding of a decellularized heparin-coated vascular graft.* Artif Organs, 2004. **28**(7): p. 668-75.

69. Hristov, M., W. Erl, and P.C. Weber, *Endothelial progenitor cells: mobilization, differentiation, and homing.* Arterioscler Thromb Vasc Biol, 2003. **23**(7): p. 1185-9.

70. Fontaine, V., et al., *Essential role of bone marrow fibroblast growth factor-2 in the effect of estradiol on reendothelialization and endothelial progenitor cell mobilization.* Am J Pathol, 2006. **169**(5): p. 1855-62.

71. Asahara, T., et al., *VEGF contributes to postnatal neovascularization by mobilizing bone marrow-derived endothelial progenitor cells.* Embo J, 1999. **18**(14): p. 3964-72.

72. Bhattacharyya, D., et al., *A New Class of Thin Film Hydrogels Produced by Plasma Polymerization.* Chem Mater, 2007. **19**: p. 2222-8.

73. Beamson, G. and D. Briggs, *High-Resolution XPS of Organic Polymers.* The Scienta ESCA300 Database, 1992.

74. Xu, C., et al., *In vitro study of human vascular endothelial cell function on materials with various surface roughness.* J Biomed Mater Res A, 2004. **71**: p. 154-61.

75. Miller, D.C., et al., *Endothelial and vascular smooth muscle cell function on poly(lactic-co-glycolic acid) with nano-structured surface features.* Biomaterials, 2004. **25**(1): p. 53-61.

76. Kunzler, T.P., et al., *Systematic study of osteoblast and fibroblast response to roughness by means of surface-morphology gradients.* Biomaterials, 2007. **28**(13): p. 2175-82.

77. Lee, J.H., et al., *Interaction of cells on chargeable functional group gradient surfaces.* Biomaterials, 1997. **18**(4): p. 351-8.

78. Tidwell, C.D., S.I. Ertel, and R.B. D., *Endothelial cell growth and protein adsorption on terminally functionalized, self-assembled monolayers of alkanethiolates on gold.* Langmuir, 1997. **13**: p. 3404-13.

79. Cooper, E., et al., *Rates of attachment of fibroblasts to self-assembled monolayers formed by the adsorption of alkylthiols onto gold surfaces.* J. Mater. Chem., 1997. **7**: p. 435-41.

80. Vischer, U.M., *von Willebrand factor, endothelial dysfunction, and cardiovascular disease.* J Thromb Haemost, 2006. **4**(6): p. 1186-93.

81. Massia, S.P. and J.A. Hubbell, *Vascular endothelial cell adhesion and spreading promoted by the peptide REDV of the IIICS region of plasma fibronectin is mediated by integrin alpha 4 beta 1.* J Biol Chem, 1992. **267**(20): p. 14019-26.

82. Connolly, D.T., et al., *Tumor vascular permeability factor stimulates endothelial cell growth and angiogenesis.* J Clin Invest, 1989. **84**(5): p. 1470-8.

83. Waltenberger, J., et al., *Different signal transduction properties of KDR and Flt1, two receptors for vascular endothelial growth factor.* J Biol Chem, 1994. **269**(43): p. 26988-95.

84. http://www.bangslabs.com/technotes/205.pdf.

85. Nguyen, K.T., et al., *Shear stress reduces protease activated receptor-1 expression in human endothelial cells.* Ann Biomed Eng, 2001. **29**(2): p. 145-52.

86. Socrates, G., *Infrared Characteristic Group Frequencies*. second ed. 1994: John Wiley & Sons.

87. Beamson, G. and D. Briggs, *High-Resolution XPS of Organic PolymersThe Scienta ESCA300 Database*. 1992: John Wiley & Sons

88. Timmons, R.B. and A.J. Griggs, eds. *Pulsed Plasma Polymerizations*. Plasma Polymer Films, ed. H. Biederman. 2004, Imperial College Press: London. 217-246.

89. Wijelath, E.S., et al., *Novel vascular endothelial growth factor binding domains of fibronectin enhance vascular endothelial growth factor biological activity.* Circ Res, 2002. **91**(1): p. 25-31.

90. Goerges, A.L. and M.A. Nugent, *pH regulates vascular endothelial growth factor binding to fibronectin: a mechanism for control of extracellular matrix storage and release.* J Biol Chem, 2004. **279**(3): p. 2307-15.

91. Sahni, A. and C.W. Francis, *Vascular endothelial growth factor binds to fibrinogen and fibrin and stimulates endothelial cell proliferation.* Blood, 2000. **96**(12): p. 3772-8.

92. Schoppet, M., et al., *Molecular interactions and functional interference between vitronectin and transforming growth factor-beta.* Lab Invest, 2002. **82**(1): p. 37-46.

93. Ikuta, T., H. Ariga, and K. Matsumoto, *Extracellular matrix tenascin-X in combination with vascular endothelial growth factor B enhances endothelial cell proliferation.* Genes Cells, 2000. **5**(11): p. 913-927.

94. Ferrara, N., et al., *Molecular and biological properties of the vascular endothelial growth factor family of proteins.* Endocr Rev, 1992. **13**(1): p. 18-32.

95. Dvorak, H.F., et al., *Vascular permeability factor/vascular endothelial growth factor and the significance of microvascular hyperpermeability in angiogenesis.* Curr Top Microbiol Immunol, 1999. **237**: p. 97-132.

96. Nagy, J.A., et al., *Vascular permeability, vascular hyperpermeability and angiogenesis.* Angiogenesis, 2008. **11**(2): p. 109-19.

97. Ehrbar, M., et al., *The role of actively released fibrin-conjugated VEGF for VEGF receptor 2 gene activation and the enhancement of angiogenesis.* Biomaterials, 2008. **29**(11): p. 1720-9.

98. Wilcke, I., et al., *VEGF(165) and bFGF protein-based therapy in a slow release system to improve angiogenesis in a bioartificial dermal substitute in vitro and in vivo.* Langenbecks Arch Surg, 2007. **392**(3): p. 305-14.

99. Kanczler, J.M., et al., *The effect of the delivery of vascular endothelial growth factor and bone morphogenic protein-2 to osteoprogenitor cell populations on bone formation.* Biomaterials, 2009.

100. Jay, S.M. and W.M. Saltzman, *Controlled delivery of VEGF via modulation of alginate microparticle ionic crosslinking.* J Control Release, 2009. **134**(1): p. 26-34.

101. Emerich, D.F., et al., *Injectable hydrogels providing sustained delivery of vascular endothelial growth factor are neuroprotective in a rat model of Huntington's disease.* Neurotox Res. **17**(1): p. 66-74.

102. Neufeld, G., et al., *Vascular endothelial growth factor and its receptors.* Prog Growth Factor Res, 1994. **5**(1): p. 89-97.

103. Fujita, Y., et al., *Transactivation of fetal liver kinase-1/kinase-insert domain-containing receptor by lysophosphatidylcholine induces vascular endothelial cell proliferation.* Endocrinology, 2006. **147**(3): p. 1377-85.

104. Waltenberger, J., et al., *Functional upregulation of the vascular endothelial growth factor receptor KDR by hypoxia.* Circulation, 1996. **94**(7): p. 1647-54.

105. Fukino, K., et al., *Genetic background influences therapeutic effectiveness of VEGF.* Biochem Biophys Res Commun, 2003. **310**(1): p. 143-7.

106. Murota, S.I., M. Onodera, and I. Morita, *Regulation of angiogenesis by controlling VEGF receptor.* Ann N Y Acad Sci, 2000. **902**: p. 208-12; discussion 212-3.

107. Nerem, R.M. and W.A. Seed, *Coronary artery geometry and its fluid mechanical implications.*, in *Fluid Dynamics as a Localizaing Factor for Atherosclerosis*, G. Schettler, Editor. 1983, Springer-Verlag: Heidelberg. p. 51-59.

108. Malek, A.M., S.L. Alper, and S. Izumo, *Hemodynamic shear stress and its role in atherosclerosis.* JAMA, 1999. **282**(21): p. 2035-42.

109. Yang, J., A.R. Webb, and G.A. Ameer, Novel citric acid-based biodegradable elastomers for tissue engineering. Adv Mater, 2004. 16: p. 511-6.

110. Rehman, J., et al., *Exercise acutely increases circulating endothelial progenitor cells and monocyte-/macrophage-derived angiogenic cells.* J Am Coll Cardiol, 2004. **43**(12): p. 2314-8.

111. Motlagh, D., et al., *Hemocompatibility evaluation of poly(glycerol-sebacate) in vitro for vascular tissue engineering.* Biomaterials, 2006. **27**(24): p. 4315-24.

112. Motlagh, D., et al., *Hemocompatibility evaluation of poly(diol citrate) in vitro for vascular tissue engineering.* J Biomed Mater Res A, 2007. **82**(4): p. 907-16.

113. Berman, C.L., et al., *A platelet alpha granule membrane protein that is associated with the plasma membrane after activation. Characterization and subcellular localization of*

platelet activation-dependent granule-external membrane protein. J Clin Invest, 1986. **78**(1): p. 130-7.

114. Gorbet, M.B. and M.V. Sefton, *Biomaterial-associated thrombosis: roles of coagulation factors, complement, platelets and leukocytes.* Biomaterials, 2004. **25**(26): p. 5681-703.

115. Imai, Y. and Y. Nose, *A new method for evalution of antithrombogenicity of materials.* J Biomed Mater Res, 1972. **6**(3): p. 165-72.

116. Huang, N., et al., *Hemocompatibility of titanium oxide films.* Biomaterials, 2003. **24**(13): p. 2177-87.

117. Yang, J., et al., *Synthesis and evaluation of poly(diol citrate) biodegradable elastomers.* Biomaterials, 2006. **27**(9): p. 1889-98.

118. Banerjee, S., et al., *Endothelial progenitor cell mobilization after percutaneous coronary intervention.* Atherosclerosis, 2006. **189**(1): p. 70-5.

119. Shiu, Y.T., M.M. Udden, and L.V. McIntire, *Perfusion with sickle erythrocytes up-regulates ICAM-1 and VCAM-1 gene expression in cultured human endothelial cells.* Blood, 2000. **95**(10): p. 3232-41.

120. Husmann, M., et al., *Polymer erosion in PLGA microparticles produced by phase separation method.* Int J Pharm, 2002. **242**(1-2): p. 277-80.

121. Kannan, R.Y., et al., *Current status of prosthetic bypass grafts: a review.* J Biomed Mater Res B Appl Biomater, 2005. **74**(1): p. 570-81.

122. Kuchulakanti, P.K., et al., *Correlates and long-term outcomes of angiographically proven stent thrombosis with sirolimus- and paclitaxel-eluting stents.* Circulation, 2006. **113**(8): p. 1108-13.

123. Tamada, Y., E.A. Kulik, and Y. Ikada, *Simple method for platelet counting.* Biomaterials, 1995. **16**(3): p. 259-61.

124. Allen, R.D., et al., *Transformation and motility of human platelets: details of the shape change and release reaction observed by optical and electron microscopy.* J Cell Biol, 1979. **83**(1): p. 126-42.

125. Cholakis, C.H., W. Zingg, and M.V. Sefton, *Effect of heparin-PVA hydrogel on platelets in a chronic canine arterio-venous shunt.* J Biomed Mater Res, 1989. **23**(4): p. 417-41.

126. Gemmell, C.H., et al., *Platelet activation in whole blood by artificial surfaces: identification of platelet-derived microparticles and activated platelet binding to leukocytes as material-induced activation events.* J Lab Clin Med, 1995. **125**(2): p. 276-87.

127. Murakami, T., et al., *Flow cytometric analysis of platelet activation markers CD62P and CD63 in patients with coronary artery disease.* Eur J Clin Invest, 1996. **26**(11): p. 996-1003.

128. Michelson, A.D., *Flow cytometry: a clinical test of platelet function.* Blood, 1996. **87**(12): p. 4925-36.

129. Ratner, B.D., et al., eds. *Biomaterials Science: An Introduction to Materials in Medicine*. 2004, Academic Press.

130. Fischer, D., et al., *In vitro cytotoxicity testing of polycations: influence of polymer structure on cell viability and hemolysis.* Biomaterials, 2003. **24**(7): p. 1121-31.

131. Tang, L., et al., *Molecular determinants of acute inflammatory responses to biomaterials.* J Clin Invest, 1996. **97**(5): p. 1329-34.

132. Muller, W.A., *Leukocyte-endothelial-cell interactions in leukocyte transmigration and the inflammatory response.* Trends Immunol, 2003. **24**(6): p. 327-34.

133. Solovjov, D.A., E. Pluskota, and E.F. Plow, *Distinct roles for the alpha and beta subunits in the functions of integrin alphaMbeta2.* J Biol Chem, 2005. **280**(2): p. 1336-45.

134. Nguyen, K.T., et al., *In vitro hemocompatibility studies of drug-loaded poly-(L-lactic acid) fibers.* Biomaterials, 2003. **24**(28): p. 5191-201.

135. Suska, F., et al., *IL-1alpha, IL-1beta and TNF-alpha secretion during in vivo/ex vivo cellular interactions with titanium and copper.* Biomaterials, 2003. **24**(3): p. 461-8.

136. DeFife, K.M., et al., *Adhesion and cytokine production by monocytes on poly(2-methacryloyloxyethyl phosphorylcholine-co-alkyl methacrylate)-coated polymers.* J Biomed Mater Res, 1995. **29**(4): p. 431-9.

137. Aoki, J., et al., *Endothelial progenitor cell capture by stents coated with antibody against CD34: the HEALING-FIM (Healthy Endothelial Accelerated Lining Inhibits Neointimal Growth-First In Man) Registry.* J Am Coll Cardiol, 2005. **45**(10): p. 1574-9.

138. Malek, A.M., et al., *Fluid shear stress differentially modulates expression of genes encoding basic fibroblast growth factor and platelet-derived growth factor B chain in vascular endothelium.* J Clin Invest, 1993. **92**(4): p. 2013-21.

139. Mitsumata, M., et al., *Fluid shear stress stimulates platelet-derived growth factor expression in endothelial cells.* Am J Physiol, 1993. **265**(1 Pt 2): p. H3-8.

140. Ohno, M., et al., *Fluid shear stress induces endothelial transforming growth factor beta-1 transcription and production. Modulation by potassium channel blockade.* J Clin Invest, 1995. **95**(3): p. 1363-9.

141. Yamashita, J., et al., *Flk1-positive cells derived from embryonic stem cells serve as vascular progenitors.* Nature, 2000. **408**(6808): p. 92-6.

142. Obi, S., et al., *Fluid shear stress induces arterial differentiation of endothelial progenitor cells.* J Appl Physiol, 2009. **106**(1): p. 203-11.

143. Li, S., et al., *Fluid shear stress activation of focal adhesion kinase. Linking to mitogen-activated protein kinases.* J Biol Chem, 1997. **272**(48): p. 30455-62.

144. Chen, J., et al., *Twisting integrin receptors increases endothelin-1 gene expression in endothelial cells.* Am J Physiol Cell Physiol, 2001. **280**(6): p. C1475-84.

145. Takada, Y., et al., *Fluid shear stress increases the expression of thrombomodulin by cultured human endothelial cells.* Biochem Biophys Res Commun, 1994. **205**(2): p. 1345-52.

BIOGRAPHICAL INFORMATION

Hao Xu was born in Wuxi, China in February 1975. He earned his M.D. in 1998, and Master of Engineering in Biomedical Engineering in 2002, both in China. He came to the United States to pursue his Ph.D degree in 2005. He joined the Bioengineering Department in the University of Texas at Arlington, a joint program with the University of Texas Southwestern Medical Center at Dallas in 2006. He plans to complete his Ph.D education in the spring of 2010. He will continue his career as a researcher in the biomedical engineering field.